

1. Report No. NASA CR-2548		2. Government Accession No.		3. Recipient's Catalog No.	
4. Title and Subtitle STEADY-STATE AND TRANSIENT ANALYSIS OF A SQUEEZE FILM DAMPER BEARING FOR ROTOR STABILITY				5. Report Date May 1975	
				6. Performing Organization Code	
7. Author(s) L. E. Barrett and E. J. Gunter				8. Performing Organization Report No. ME-4040-114-73U	
9. Performing Organization Name and Address University of Virginia Charlottesville, Virginia 22902				10. Work Unit No.	
				11. Contract or Grant No. NGL 47-005-050	
12. Sponsoring Agency Name and Address National Aeronautics and Space Administration Washington, D. C. 20546				13. Type of Report and Period Covered Contractor Report	
				14. Sponsoring Agency Code	
15. Supplementary Notes Final Report. Project Manager, Robert E. Cunningham, Fluid System Components Division, NASA Lewis Research Center, Cleveland, Ohio					
16. Abstract <p>This report presents a study of the steady-state and transient response of the squeeze film damper bearing. Both the steady-state and transient equations for the hydrodynamic bearing forces are derived. The steady-state equations are used to determine the bearing equivalent stiffness and damping coefficients. These coefficients are used to find the bearing configuration which will provide the optimum support characteristics based on a stability analysis of the rotor-bearing system. The effects of end seals and cavitated fluid film are included. The transient analysis of rotor-bearing systems is performed by coupling the bearing and journal equations and integrating forward in time. The effects of unbalance, cavitation, and retainer springs are included in the analysis. Methods of determining the stability of a rotor-bearing system under the influence of aerodynamic forces and internal shaft friction are discussed. Particular emphasis is placed on solving the system characteristic frequency equation, and stability maps produced by using this method are presented. The study shows that for optimum stability and low force transmissibility the squeeze bearing should operate at an eccentricity ratio $\epsilon < 0.4$.</p>					
17. Key Words (Suggested by Author(s)) Damper bearing; Oil squeeze film; Steady-state analysis; Transient analysis; Rotor stability; Rotor dynamics			18. Distribution Statement Unclassified - unlimited STAR category 07 (rev.)		
19. Security Classif. (of this report) Unclassified		20. Security Classif. (of this page) Unclassified		21. No. of Pages 107	22. Price* \$5.25

* For sale by the National Technical Information Service, Springfield, Virginia 22151

TABLE OF CONTENTS

CHAPTER 1	INTRODUCTION	1
CHAPTER 2	THEORETICAL ANALYSIS	
	2.1 Reynolds Equation	4
	2.2 Bearing Forces in Fixed Coordinates	6
	2.3 Bearing Cavitation	10
	2.4 Bearing Forces in Rotating Coordinates	12
CHAPTER 3	ROTOR-BEARING STABILITY AND STEADY-STATE ANALYSIS	
	3.1 Rotor-Bearing Stability	23
	3.2 Steady-State Analysis	33
CHAPTER 4	TRANSIENT ANALYSIS	
	4.1 Introduction	42
	4.2 Analysis	44
CHAPTER 5	CONCLUSIONS AND RECOMMENDATIONS	
	5.1 Predicting Rotor Instability	71
	5.2 Determining the Stiffness and Damping Coefficients of the Squeeze Film Damper Bearing	72
	5.3 Transient Analysis	73
	5.4 Advantages of Bearing Simulation	74
	5.5 Limitations of Analytical Investigations	74
	5.6 Recommendations for Future Research	75
	BIBLIOGRAPHY	77
	APPENDIX A DESCRIPTION OF PROGRAM SQFDAMP	79

LIST OF FIGURES

FIGURE		PAGE
2-1	Squeeze Film Damper Bearing Configuration in Fixed and Rotating Coordinate Systems	5
2-2	Comparison of Finite Length and Short Bearing Solutions	7
2-3	Uncavitated Pressure Profile Showing Region of Negative Hydrodynamic Pressure	11
2-4	Cavitated Pressure Profile With Negative Hydrodynamic Pressure Equated to Zero	13
2-5	a. Axial Pressure Distribution of Bearing With Circumferential Oil Groove	19
	b. Axial Pressure Distribution of Bearing With End Seals and Circumferential Oil Groove	
3-1	Three-Mass Flexible Rotor Mounted On Flexible, Damped Supports	26
3-2	Characteristic Matrix For Three-Mass Model Including Aerodynamic Cross-Coupling, Internal Shaft Friction and Absolute Shaft Damping	27
3-3	Stability of a Flexible Rotor With Aerodynamic Cross Coupling ($Q = 20,000 \text{ lb/in}$, $N = 10,000 \text{ RPM}$)	30
3-4	Stability of a Flexible Rotor With Aerodynamic Cross Coupling ($Q = 100,000 \text{ lb/in}$, $N = 10,000 \text{ RPM}$)	31
3-5	Damping Coefficient For Squeeze Film Bearing With Cavitated Film - End Seals And Oil Supply Groove Included	35
3-6	Stiffness Coefficient For Squeeze Film Bearing With Cavitated Film - End Seals And Oil Supply Groove Included	36
3-7	Maximum Pressure For Squeeze Film Bearing With Cavitated Film - End Seals And Oil Supply Groove Included	37
3-8	Damping Coefficient For Squeeze Film Bearing With Uncavitated Film - End Seals And Oil Supply Groove Included	39

FIGURE		PAGE
3-9	Maximum Pressure For Squeeze Film Bearing With Uncavitated Film - End Seals And Oil Supply Groove Included	40
4-1	Unbalanced Rotor In Cavitated Squeeze Film Bearing - L = 0.45 IN. - Unbalance Eccentricity = 0.002 IN. - No Retainer Spring	46
4-2	Stiffness Coefficient For Squeeze Film Bearing Of Figure (4-1)	49
4-3	Damping Coefficient For Squeeze Film Bearing Of Figure (4-1)	50
4-4	Unbalanced Rotor In Cavitated Squeeze Film Bear- ing L = 0.90 IN. - Unbalance Eccentricity = 0.002 IN. - No Retainer Spring	51
4-5	Stiffness Coefficient For Squeeze Film Bearing Of Figure (4-4)	52
4-6	Damping Coefficient For Squeeze Film Bearing Of Figure (4-4)	53
4-7	Unbalanced Rotor In Cavitated Squeeze Film Bear- ing - L = 0.45 IN. - Unbalance Eccentricity = 0.002 IN. - Retainer Spring Stiffness, KR = 123,000 LB/IN.	55
4-8	Unbalanced Rotor In Cavitated Squeeze Film Bear- ing - L = 0.90 IN. - Unbalance Eccentricity = 0.001 IN. - No Retainer Spring	56
4-9	Unbalanced Rotor In Cavitated Squeeze Film Bear- ing - L = 0.90 IN - Unbalance Eccentricity = 0.001 IN. - Retainer Spring Stiffness, KR = 123,000 LB/IN	57
4-10	Unbalanced Rotor In Cavitated Squeeze Film Bear- ing - L = 0.90 IN. - Unbalance Eccentricity = 0.002 IN. - Retainer Spring Stiffness, KR = 123,000 LB/IN	59
4-11	Unbalanced Rotor in Uncavitated Squeeze Film Bear- ing - L = 0.90 IN. - Unbalance Eccentricity = 0.002 IN. - Retainer Spring Stiffness, KR = 123,000 LB/IN	60

FIGURE		PAGE
4-12	Vertical Unbalanced Rotor In Squeeze Film Bearing - Effect Of Unbalance Magnitude - Unbalance Eccentricity = 1.75 Mils	61
4-13	Vertical Unbalanced Rotor In Squeeze Film Bearing - Effect Of Unbalance Magnitude - Unbalance Eccentricity = 2.10 Mils	62
4-14	Vertical Unbalanced Rotor In Squeeze Film Bearing - Effect of Unbalance Magnitude - Unbalance Eccentricity = 2.45 Mils	63
4-15	Vertical Unbalanced Rotor In Squeeze Film Bearing - Effect of Unbalance Magnitude - Unbalance Eccentricity = 3.50 Mils	64
4-16	Horizontal Unbalanced Rotor In Squeeze Film Bearing - Effect Of Retainer Springs - Retainer Spring Stiffness, KR = 0 LB/IN	66
4-17	Horizontal Unbalanced Rotor In Squeeze Film Bearing - Effect Of Retainer Springs - Retainer Spring Stiffness, KR = 50,000 LB/IN	67
4-18	Horizontal Unbalanced Rotor In Squeeze Film Bearing - Effect Of Retainer Springs - Retainer Spring Stiffness, KR = 100,000 LB/IN	68
4-19	Horizontal Unbalanced Rotor In Squeeze Film Bearing - Effect of Retainer Springs - Retainer Spring Stiffness, KR = 200,000 LB/IN	69

NOMENCLATURE

SYMBOL	DESCRIPTION	UNITS
C	Bearing Clearance	in.
C_o	Equivalent bearing damping	lb-sec/in
C_{xx}, C_{xy} C_{yy}, C_{yx}	Bearing damping	lb-sec/in
e	Journal Eccentricity	in.
EMU	Ratio of unbalance eccentricity to bearing clearance	---
F_x	Force component in x-direction	lbf
F_y	Force component in y-direction	lbf
F_r	Force component in radial direction	lbf
F_θ	Force component in tangential direction	lbf
FMAX	Maximum hydrodynamic force	lbf
FU	Force due to rotating unbalance	lbf
FURATIO	Ratio of FMAX to FU	---
h	Fluid film thickness	in.
$\vec{i}, \vec{j}, \vec{k}$	Unit vectors in fixed coordinate system	---
k_o	Equivalent bearing stiffness	lb/in
KR	Retainer Spring Stiffness	lb/in
k_{xx}, k_{xy} k_{yy}, k_{yx}	Bearing Stiffness	lb/in
L	Bearing length	in.
N	Rotor speed	RPM
$\vec{n}_r, \vec{n}_\theta$	Unit vecotors in rotating coordinate system	---

SYMBOL	DESCRIPTION	UNITS
P	Pressure	lb/in ²
P _{MAX}	Maximum hydrodynamic pressure	lb/in ²
Q	Aerodynamic cross coupling	lb/in
R	Bearing radius	in
t	Time	sec
W	Weight	lbf
x,y,z	Displacements	in.
μ	Viscosity	lb-sec/in ²
θ,θ'	Angular measure	---
φ̇	Journal precession rate	sec ⁻¹
ω	Angular velocity	sec ⁻¹

CHAPTER 1

INTRODUCTION

Modern turbomachines are highly complex systems. Current design trends are producing machines that consist of several process stages joined together. The rotors in these machines are highly flexible shafts, often mounted in more than two bearings, that rotate at very high speeds. It is not uncommon to see machines that operate above the second critical speed. As a result the system dynamics are very complicated.

One of the major problems encountered in these machines is instability produced by aerodynamic forces on impeller wheels, friction in the stressed rotor and hydrodynamic forces in the bearings. The instability is characterized by large amplitude whirl orbits and often results in bearing or total machine failure. It is often aggravated by unbalance and other external forces transmitted to the machine. Production losses from failed machines are very high and it may take many months to repair or replace the failed unit. In addition operator safety is jeopardized when machines fail and occasional loss of life occurs.

From the earliest investigations of rotor instability, it has been known that the use of flexible, damped supports has an effect on instability and can eliminate it or alter the speed at which it occurs. Recent research has produced a large body of knowledge on the use of these supports and their effect on instability.

The squeeze film damper bearing is one type of flexible

support that is currently being investigated. This study examines the squeeze bearing and through computer simulation shows its effects on several rotor-bearing systems. The equations for the hydrodynamic bearing forces are developed in both fixed and rotating coordinate systems. The use of two coordinate systems allows for both steady-state and transient analysis of bearing performance. This results in more efficient bearing analysis and a savings in time and money when experimental testing of the bearings is conducted.

The steady-state behavior of the bearing results in the formulation of bearing stiffness and damping coefficients which can be used to set the bearing configuration. This is accomplished by comparing the coefficients with required values obtained from a stability analysis of the rotor-bearing system. Several methods of determining the system stability are discussed. The effects of end seals and cavitation of the fluid film are also included in the steady-state coefficients.

The transient analysis is very useful in determining the bearing response to particular forms of external and internal forces as noted previously. Also the effect of bearing retainer springs and fluid film cavitation can be found. The transient response is found by tracking the journal motion forward in time by integrating the equations of motion under the influence of the system forces.

The limitations of and assumptions used in deriving the steady-state and transient equations are discussed in order to

obtain meaningful interpretation of the results and to establish useful design criteria.

Dr. R. Gordon Kirk developed the computer programs used to perform the transient analysis in this report.

CHAPTER 2
THEORETICAL ANALYSIS

2.1 REYNOLDS EQUATION

The configuration of the squeeze film damper bearing is shown in Figure (2-1) where the clearance has been exaggerated. Both fixed and rotating coordinate systems are shown, and the bearing equations are derived for both systems. The definitions of the various parameters are listed in the nomenclature section of this report.

The basic bearing equation is the Reynolds equation which is derived from the Navier-Stokes equations for incompressible flow. With the proper bearing parameters the equation for the fluid film forces are derived. [1]

The Reynolds equation for the short, plain journal bearing is given in both fixed and rotating coordinates by:

Fixed coordinates:

$$\frac{\partial}{\partial Z} \left[\frac{h^3}{6\mu} \frac{\partial P}{\partial Z} \right] = (\omega_b + \omega_j) \frac{\partial h}{\partial \theta} + 2 \frac{\partial h}{\partial t} \quad (2-1)$$

Rotating coordinates:

$$\frac{\partial}{\partial Z} \left[\frac{h^3}{6\mu} \frac{\partial P}{\partial Z} \right] = (\omega_b + \omega_j - 2\dot{\phi}) \frac{\partial h}{\partial \theta'} + 2 \frac{\partial h}{\partial t} \quad (2-2)$$

As shown in Figure (2-1), the angle θ in the fixed coordinate expression is measured from the positive x-axis in the direction of rotation whereas the angle θ' in the rotating coordinate expression is measured from the line of centers in the

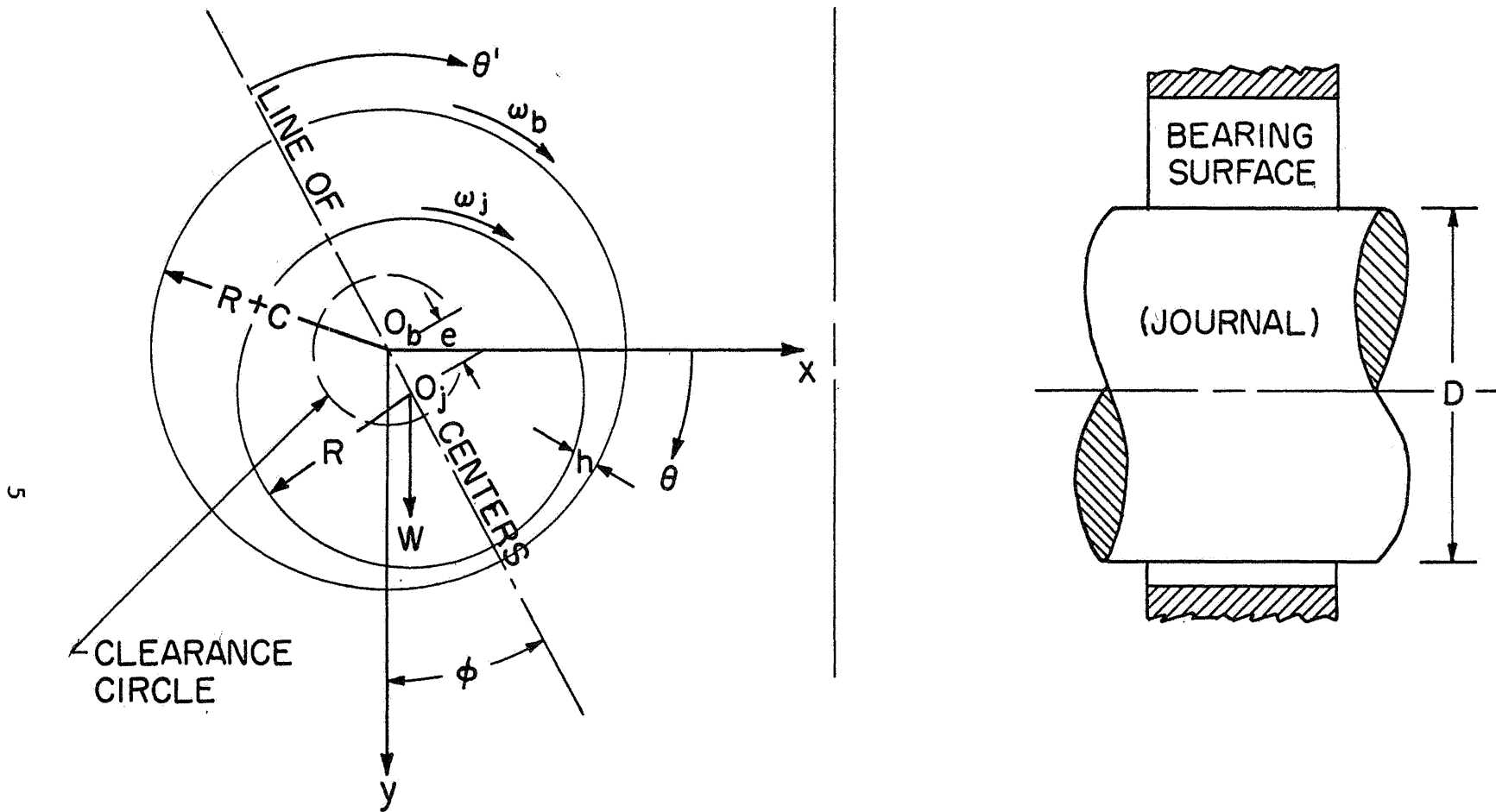


Figure 2-1 Squeeze Film Damper Bearing Configuration in Fixed and Rotating Coordinate Systems

direction of rotation. The assumptions used in the derivation of equations (1) and (2) include:

1. The fluid inertia terms in the Navier-Stokes equations have been neglected due to their small magnitude.
2. Body forces in the fluid film have been neglected.
3. The fluid viscosity is constant.
4. The flow in the radial direction has been neglected, that is, the short bearing approximation has been used.

Figure (2.2) shows a comparison of the short bearing solution and the general solution of the Reynolds equation solved by a finite difference technique for the plain journal bearing under steady state conditions. It can be seen that the short bearing solution is highly accurate for a wide range of eccentricities for $L/D < 1/4$ and is acceptable for L/D values up to 1 if the eccentricity ratio is low. The normal design range of the squeeze film bearings will be $L/D < 1/2$ and eccentricity ratios < 0.4 .

By assuming the bearing is perfectly aligned (h not a function of Z) equations (1) and (2) are integrated directly to yield expressions for the fluid film forces.

2.2 BEARING FORCES IN FIXED COORDINATES

For the plain bearing with full end leakage the appropriate boundary conditions are:

$$P(\theta, 0) = P(\theta, L) = 0$$

(2-3)

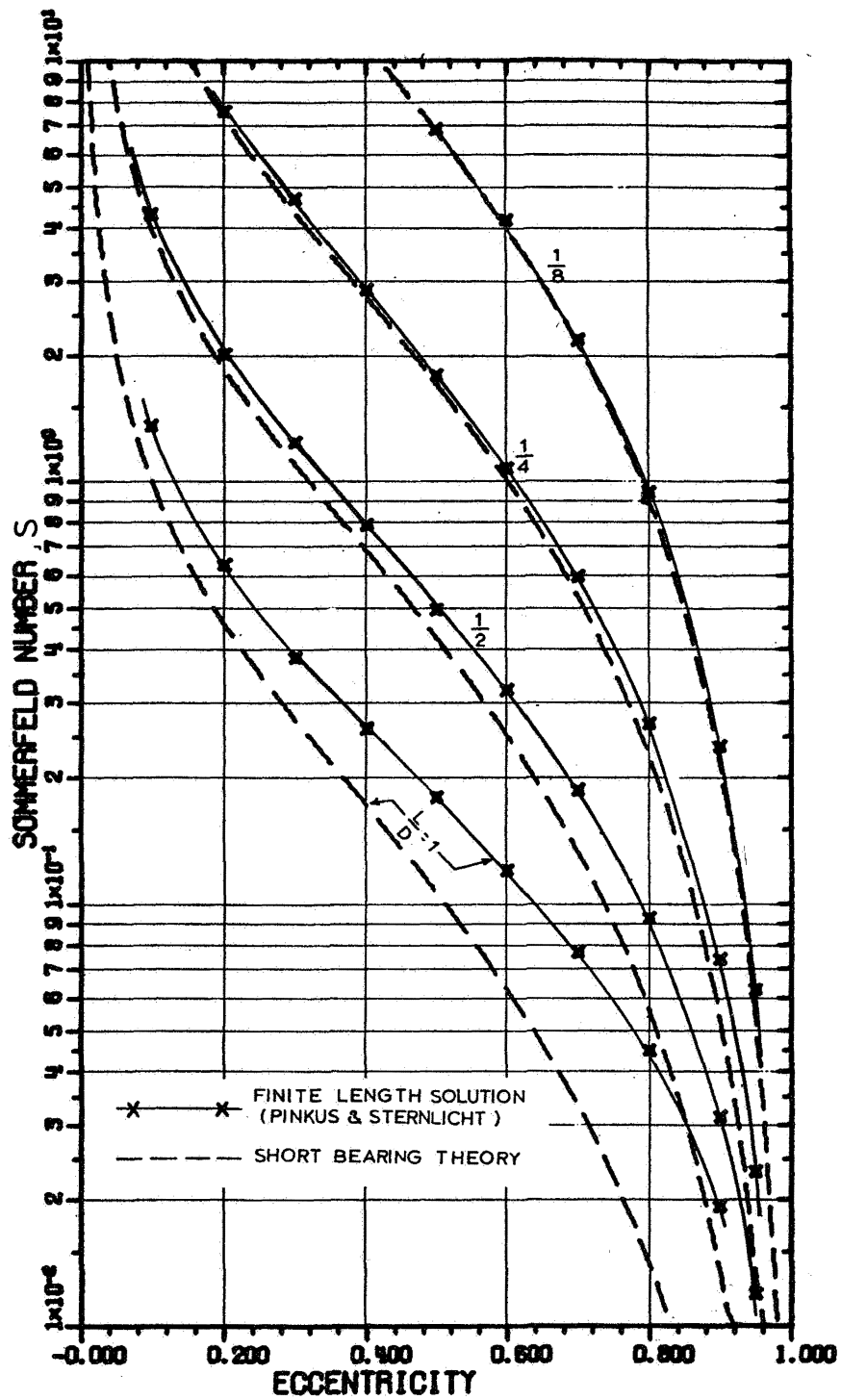


Figure 2-2 Comparison of Finite Length and Short Bearing Solutions

In the fixed coordinate system the film thickness, h , is given by:

$$h = c - x \cos \theta - y \sin \theta \quad (2-4)$$

Substituting into equation (2-1) and integrating yields:

$$P(\theta, Z) = \frac{3\mu}{h^3} \left[Z^2 - LZ \right] \left[(\omega_b + \omega_j) \frac{\partial h}{\partial \theta} + 2 \frac{\partial h}{\partial t} \right] \quad (2-5)$$

Differentiation of equation (2-4) yields:

$$\frac{\partial h}{\partial \theta} = x \sin \theta - y \cos \theta \quad (2-6)$$

$$\frac{\partial h}{\partial t} = -\dot{x} \cos \theta - \dot{y} \sin \theta \quad (2-7)$$

The incremental force acting on the journal is:

$$\vec{\Delta F} = -P(\theta, Z) R d\theta dZ \vec{n}_r \quad (2-8)$$

The relationship between the unit vectors in the fixed and rotating reference frames is:

$$\vec{i} = \cos \theta \vec{n}_r - \sin \theta \vec{n}_\theta \quad (2-9)$$

$$\vec{j} = \sin \theta \vec{n}_r + \cos \theta \vec{n}_\theta \quad (2-10)$$

$$\vec{n}_r = \cos \theta \vec{i} + \sin \theta \vec{j} \quad (2-11)$$

$$\vec{n}_\theta = -\sin \theta \vec{i} + \cos \theta \vec{j} \quad (2-12)$$

Substituting equation (2-11) into equation (2-8) yields:

$$\Delta \vec{F} = -P(\theta, Z) R d\theta dZ (\cos \theta \vec{i} - \sin \theta \vec{j}) \quad (2-13)$$

The elemental x and y force components may be found by taking the dot product of equation (2-13) with unit vectors in the x and y directions.

$$\Delta \vec{F}_x = (\Delta \vec{F} \cdot \vec{i}) \vec{i} = -(P(\theta, Z) R d\theta dZ \cos \theta) \vec{i} \quad (2-14)$$

$$\Delta \vec{F}_y = (\Delta \vec{F} \cdot \vec{j}) \vec{j} = -(P(\theta, Z) R d\theta dZ \sin \theta) \vec{j} \quad (2-15)$$

The total force components in the x and y directions are found by integrating equations (2-14) and (2-15) over the entire journal surface.

$$F_x = - \int_0^{2\pi} \int_0^L P(\theta, Z) R \cos \theta dZ d\theta \quad (2-16)$$

$$F_y = - \int_0^{2\pi} \int_0^L P(\theta, Z) R \sin \theta dZ d\theta \quad (2-17)$$

Substituting the expressions for $\frac{\partial h}{\partial \theta}$ and $\frac{\partial h}{\partial t}$ into the pressure equation and integrating around the bearing circumference gives:

$$\begin{Bmatrix} F_x \\ F_y \end{Bmatrix} = \frac{-\mu R L^3}{2} \int_0^{2\pi} \frac{(\omega_b + \omega_j)(x \sin \theta - y \cos \theta) - 2(\dot{x} \cos \theta + \dot{y} \sin \theta)}{(c - x \cos \theta - y \sin \theta)^3} \begin{Bmatrix} \cos \theta \\ \sin \theta \end{Bmatrix} d\theta \quad (2-18)$$

The above equation is applicable to the evaluation of the forces developed in the plain journal bearing as well as the squeeze film damper bearing for arbitrary values of journal displacement, velocity, and shaft and bearing housing angular velocities. Hence the analysis can also be used for the general floating bush bearing with rotation.

For the case of the squeeze film damper where the journal and housing are constrained from rotating, ($\omega_b = \omega_j = 0$), the force expressions become

$$\begin{Bmatrix} F_x \\ F_y \end{Bmatrix} = \frac{-\mu RL^3}{2} \int_0^{2\pi} \frac{-2(\dot{x} \cos \theta + \dot{y} \sin \theta)}{(c - x \cos \theta - y \sin \theta)^3} \begin{Bmatrix} \cos \theta \\ \sin \theta \end{Bmatrix} d\theta \quad (2-19)$$

These non-linear fluid film forces are easily combined with the rotor-bearing system dynamical equations providing a complete non-linear dynamical analysis of the system. Because the bearing force equations are written in fixed Cartesian coordinates a transformation from one coordinate system to another is not required. This is very important for conservation of computation time since the bearing pressure profile must be integrated at each time step of the system motion.

2.3 BEARING CAVITATION

If the complete pressure profile is calculated without regard to cavitation or rupture of the film, then the bearing pressure will be similar to Figure (2.3). This figure represents the three dimensional pressure generated in the bearing.

The exact mechanism causing cavitation in fluids is not

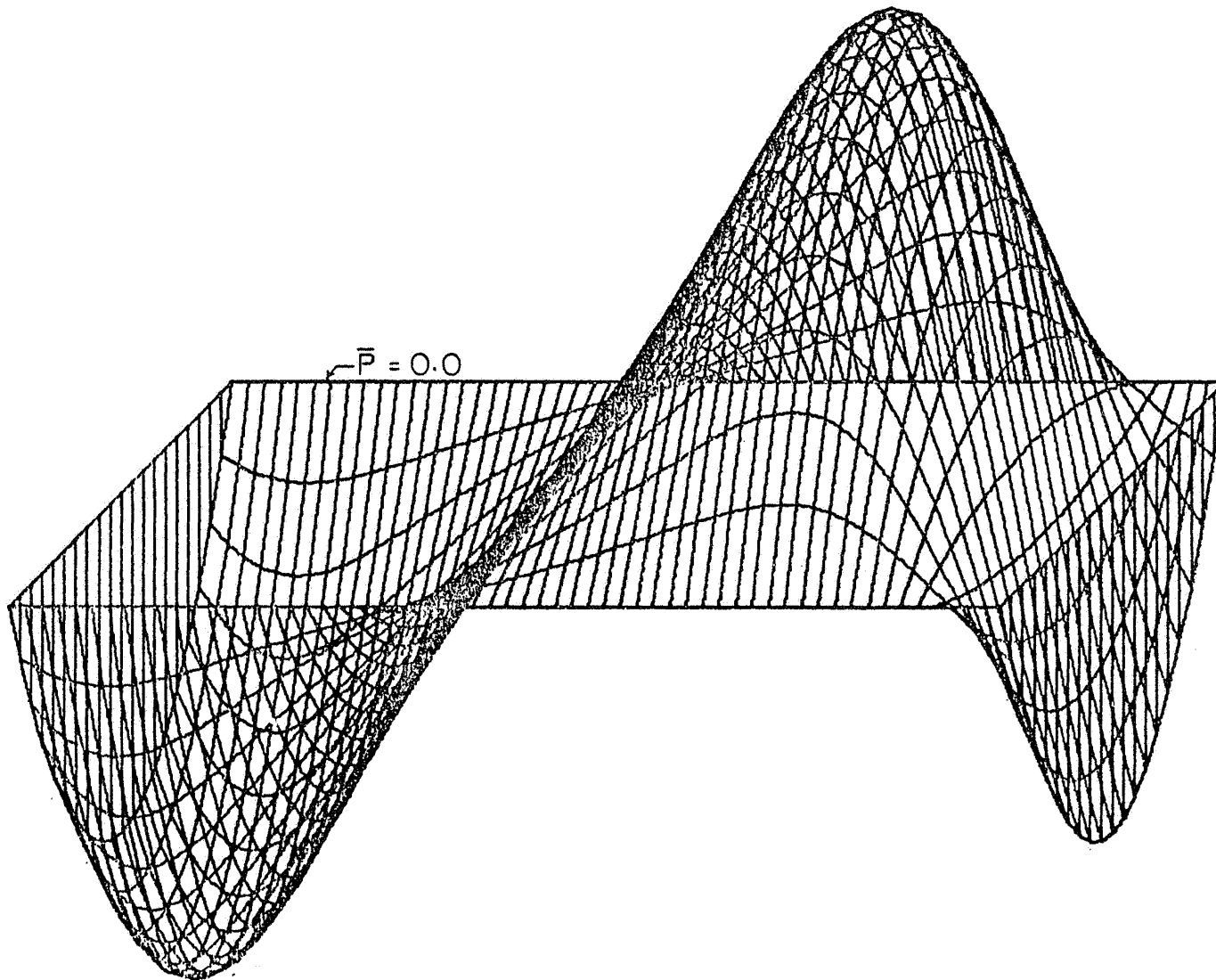


Figure 2-3 Uncavitated Pressure Profile Showing Region of Negative Hydrodynamic Pressure

fully known. It is known that film rupture is influenced by gas and solid content of the fluid. Recent investigations have shown that a fluid may stand large tensile stresses [2], and its ability to withstand rupture is dependent on its past history. In this investigation it is assumed that cavitation occurs when the pressure in the film drops below ambient pressure. The cavitated film then extends over only a section of the bearing circumference as shown in Figure (2-4). Recent experimental research has shown that cavitation in the squeeze bearing occurs in streamers of bubbles which extend around the entire bearing [3]. These streamers initially appear at the center of the bearing and extend outward as the rotor speed increases. It is beyond the scope of this present research to analyze this type of cavitation effect. Therefore the conventional cavitated film is assumed to occur when $P < P_c$ where P_c is the assumed cavitation pressure.

When evaluating the integral of equation (2-19), negative pressures are equated to zero if the film is assumed to cavitate. If the oil supply pressure is sufficiently high and suitable operating conditions exist the film does not cavitate.

2.4 BEARING FORCES IN ROTATING COORDINATES

The Reynolds equation in rotating coordinates was given by equation (2-2). Assuming steady-state circular synchronous precession of the journal about the bearing center and no axial misalignment, equation (2-2) can be integrated in closed form. The resulting equations for the bearing forces give the equivalent stiffness and damping of the bearing.

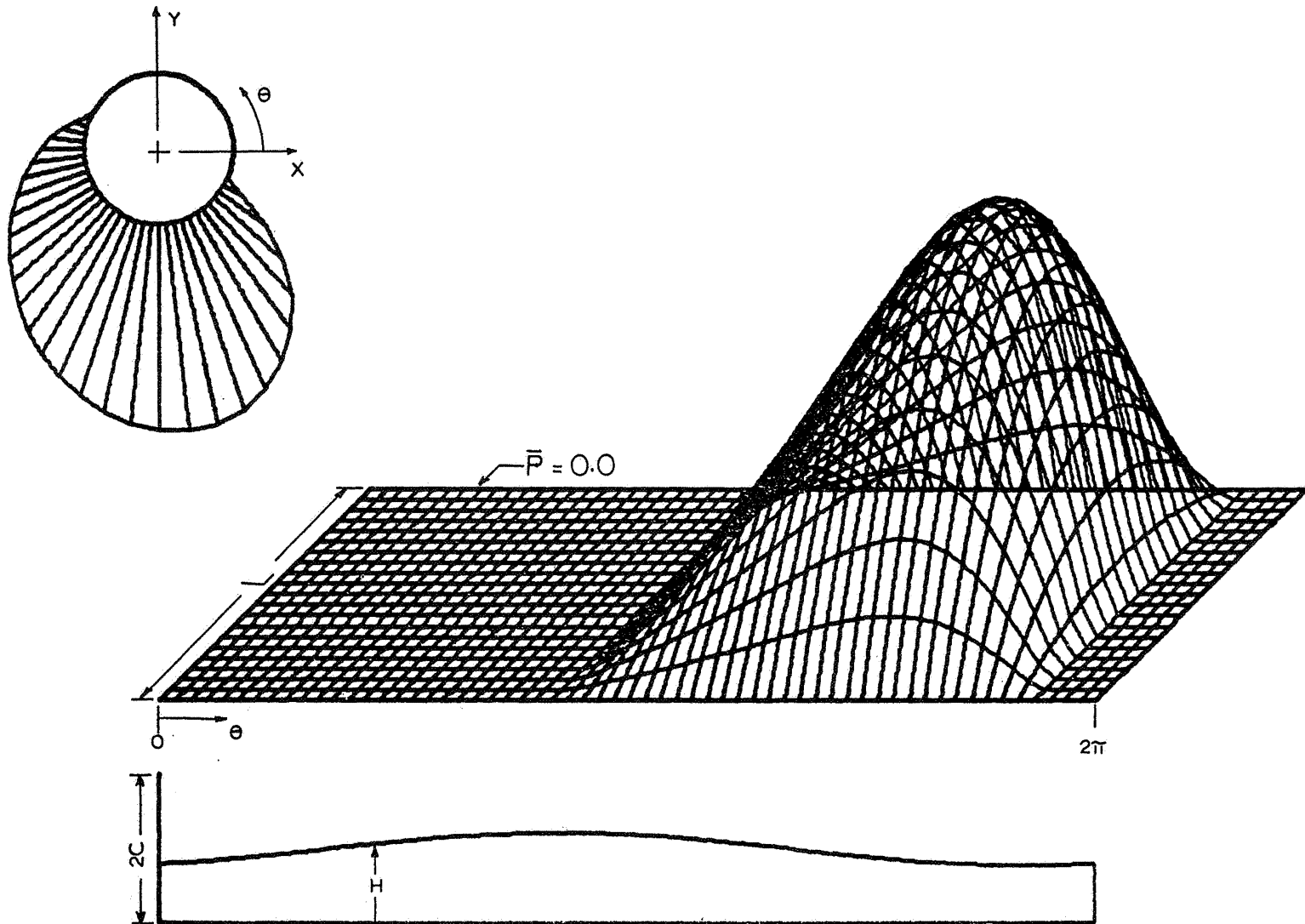


Figure 2-4 Cavitated Pressure Profile With Negative Hydrodynamic Pressure Equated to Zero

Applying the boundary conditions:

$$P(\theta, 0) = P(\theta, L) = 0 \quad (2-20)$$

and integrating equation (2-2) yields:

$$P(\theta, Z) = \frac{3\mu}{h^3} \left[-2\dot{\phi} \frac{\partial h}{\partial \theta'} + 2 \frac{\partial h}{\partial t} \right] [Z^2 - LZ] \quad (2-21)$$

where θ' is measured from the line of centers in the direction of rotation as shown in Figure (2-1).

In rotating coordinates the film thickness, h , is given by:

$$h = c(1 + \epsilon \cos \theta') \quad (2-22)$$

where the eccentricity ratio, ϵ , is defined as:

$$\epsilon = \frac{e}{c} \quad (2-23)$$

Differentiation of equation (2-22) gives:

$$\frac{\partial h}{\partial \theta'} = -c \epsilon \sin \theta' \quad (2-24)$$

and

$$\frac{\partial h}{\partial t} = c\dot{\epsilon} \cos \theta' \quad (2-25)$$

Substituting the expressions for h and its derivatives into equation (2-21) and integrating gives the fluid film force:

$$\vec{F} = \frac{\mu RL^3}{c^2} \int_{\theta_1'}^{\theta_2'} \frac{(\dot{\phi} \epsilon \sin \theta' + \dot{\epsilon} \cos \theta')}{(1 + \epsilon \cos \theta')^3} d\theta' \vec{n}_r \quad (2-26)$$

The transformation into the $\vec{n}_r, \vec{n}_\theta$ coordinates is

$$\vec{n}_r = -\cos \theta' \vec{n}_r - \sin \theta' \vec{n}_\theta \quad (2-27)$$

The components of the fluid film force in the radial and tangential directions, \vec{n}_r and \vec{n}_θ are found by taking the dot product of the force with unit vectors in the radial and tangential directions. Thus:

$$\vec{F}_r = (\vec{F} \cdot \vec{n}_r) \vec{n}_r \quad (2-28)$$

and

$$\vec{F}_\theta = (\vec{F} \cdot \vec{n}_\theta) \vec{n}_\theta \quad (2-29)$$

and the force components are:

$$\begin{pmatrix} F_r \\ F_\theta \end{pmatrix} = \frac{-\mu RL^3}{c^2} \int_{\theta_1'}^{\theta_2'} \frac{(\dot{\phi} \epsilon \sin \theta' + \dot{\epsilon} \cos \theta')}{(1 + \epsilon \cos \theta')^3} \begin{pmatrix} \cos \theta' \\ \sin \theta' \end{pmatrix} d\theta' \quad (2-30)$$

The limits of integration, θ_1' and θ_2' , define the area over which a positive pressure profile exists and are dependent on the type of journal motion and whether or not cavitation occurs.

It is assumed that the journal is precessing in steady-state circular motion about the origin. Therefore $\dot{\epsilon} = 0$ and the pressure expression, equation (2-21) becomes:

$$P(\theta', z) = \frac{6\mu\omega\epsilon \sin \theta'}{c^2 (1 + \epsilon \cos \theta')^3} \left[z^2 - zL \right] \quad (2-31)$$

The maximum pressure in the axial direction occurs at $Z = L/2$ and equation (2-31) is rewritten as:

$$P(\theta', L/2) = \frac{-3\mu L^2 \omega \epsilon \sin \theta'}{2c^2 (1 + \epsilon \cos \theta')^3} \quad (2-32)$$

By differentiating equation (2-32) with respect to θ' and equating to zero, the tangential location of the maximum pressure may be found. The angle, θ'_{\max} , where the pressure is maximum is given by:

$$(1 + \epsilon \cos \theta'_{\max}) \cos \theta'_{\max} + 3 \epsilon \sin^2 \theta'_{\max} = 0 \quad (2-33)$$

The angle θ'_{\max} varies with ϵ and shifts from

$$\theta'_{\max} = \frac{3\pi}{2} \quad \text{when } \epsilon = 0$$

to

$$\theta'_{\max} = \pi \quad \text{when } \epsilon = 1$$

and the maximum pressure is given by:

$$P_{\max} = \frac{-3\mu L^2 \omega \epsilon \sin \theta'_{\max}}{2c^2 (1 + \epsilon \cos \theta'_{\max})^3} \quad (2-34)$$

The pressure expressed by equation (2-32) is positive over the region $\theta' = \pi$ to $\theta' = 2\pi$ and for the cavitated fluid film the limits of integration in equation (2-30) are:

$$\theta'_1 = \pi, \quad \theta'_2 = 2\pi \quad (2-35)$$

The radial and tangential components of the fluid film force are given by:

$$\begin{pmatrix} F_r \\ F_\theta \end{pmatrix} = \frac{-\mu RL^3 \epsilon \omega}{c^2} \int_{\pi}^{2\pi} \frac{\sin \theta'}{(1 + \epsilon \cos \theta')^3} \begin{pmatrix} \cos \theta' \\ \sin \theta' \end{pmatrix} d\theta' \quad (2-36)$$

The integrals in equation (2-36) were integrated using Booker's method [4]. The resulting force components are:

$$F_r = \frac{-2\mu RL^3 \epsilon \omega e}{c^3 (1 - \epsilon^2)^2} \quad (2-37)$$

and

$$F_\theta = \frac{-\mu RL^3 \pi e \omega}{2c^3 (1 - \epsilon^2)^{3/2}} \quad (2-38)$$

The force in equation (2-37) appears as a stiffness coefficient times a displacement acting in line of the displacement towards the bearing center. The equivalent bearing stiffness is:

$$K_0 = \frac{2\mu RL^3 \epsilon \omega}{c^3 (1 - \epsilon^2)^2} \quad (2-39)$$

Since the journal is precessing and not rotating, every point in the journal has a velocity equal to $e\omega$. The force in equation (2-38) therefore appears as a damping coefficient times a velocity acting in the direction opposite the journal motion.

The equivalent bearing damping is:

$$C_0 = \frac{\mu RL^3 \pi}{2c^3 (1 - \epsilon^2)^{3/2}} \quad (2-40)$$

For the uncavitated film the limits of integration in equation (2-36) become:

$$\theta'_1 = 0, \theta'_2 = 2\pi \quad (2-41)$$

Integrating and evaluating at those limits yields force components given by:

$$F_r = 0 \quad (2-42)$$

$$F_\theta = \frac{-\mu RL^3 \pi e \omega}{c^3 (1 - \epsilon^2)^{3/2}} \quad (2-43)$$

It is therefore evident that a complete fluid film does not produce an equivalent bearing stiffness but doubles the damping of the cavitated film.

Although the equations for the bearing characteristics were derived for a plain bearing with no circumferential oil groove they are applicable to other bearing configurations. For example Figure (2-5a) represents a plain bearing with circumferential oil groove and full end leakage.

The total length of the bearing, L, corresponds to the length of the plain bearing with no oil groove. The bearing in Figure (2.5a) consists of two plain bearings without an oil groove whose length is L/2. Thus the bearing parameter L in the equations may be replaced by L/2 and the equations multiplied by 2 to obtain the total effect of the two half bearings. The net effect is to decrease the maximum pressure by a factor of 2:

$$\frac{2\left(\frac{L}{2}\right)^2}{L^2} = \frac{1}{2} \quad (2-44)$$

Similarly the damping and stiffness values are decreased by a factor of 4:

$$\frac{2\left(\frac{L}{2}\right)^3}{L^3} = \frac{1}{4} \quad (2-45)$$

The bearing represented in Figure (2.5b) is a plain bearing with circumferential oil groove and end seals to prevent end leakage. If there is no end leakage the boundary conditions are:

$$\left. \frac{\partial P}{\partial Z} \right|_{Z=0,L} = 0 \quad (2-46)$$

and the net effect leaves the pressure and bearing characteristic equations unchanged.

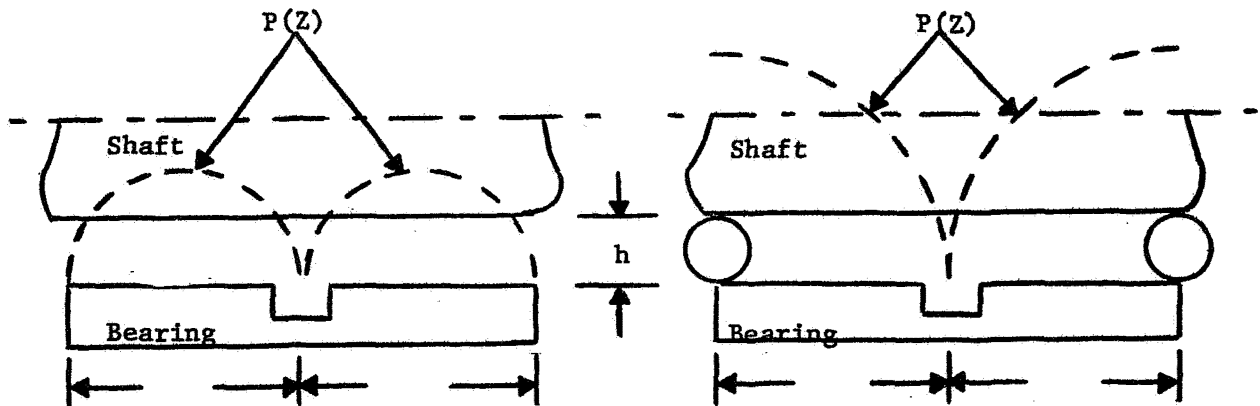


Figure 2-5 a. Axial Pressure Distribution of Bearing With Circumferential Oil Groove
 b. Axial Pressure Distribution of Bearing With End Seals and Circumferential Oil Groove

The bearing equations derived in this section are summarized in Table (2-1). Also included in the table are the equations for pure radial squeeze motion. For this type of operation $\dot{\phi} = 0$ and results from a purely unidirectional load on the journal. The radial and tangential force components are derived from equation (2-30) where only the term containing $\dot{\epsilon}$ in the integral is retained. The pressure equation is also modified to include only the $\dot{\epsilon}$ term. The maximum pressure occurs at $\theta = \pi$ for all values of journal eccentricity. Examination of the pressure equation reveals that the hydrodynamic pressure is positive only in the region $\theta' = \frac{\pi}{2}$ to $\frac{3\pi}{2}$. These values of θ' are the limits of integration in equation (2-30) for the cavitated film.

The table also shows that for purely radial motion no bearing stiffness is obtained in either the cavitated or uncavitated bearing. Thus if this type of motion exists retainer springs must be included to provide support flexibility.

For the case of circular journal precession, the table shows the stiffness and damping of the cavitated film and damping of the uncavitated film remain essentially constant for low eccentricity ratios. As the eccentricity ratio increases above 0.4 there is a rapid increase in these properties and they approach infinity as ϵ approaches 1. This variation of stiffness in the cavitated film is very important. As the eccentricity becomes large the support becomes more rigid with a corresponding increase in the rotor critical speed. If the rotor critical speed is increased above the operating speed, the phase angle between the

TYPE OF MOTION	MAXIMUM PRESSURE	EQUIVALENT DAMPING Ko (lb/in)	EQUIVALENT DAMPING Co (lb-sec/in)
CIRCULAR SYNCHRONOUS PRECESSION $\dot{\phi} = \omega, \dot{\epsilon} = 0$	$\frac{-3\mu L^2 \omega \epsilon \sin \theta_m}{2c^2 (1 + \epsilon \cos \theta_m)^3}$	$\frac{2\mu RL^3 \epsilon \omega}{c^3 (1 - \epsilon^2)^2}$	$\frac{\mu RL^3 \pi}{2c^3 (1 - \epsilon^2)^{3/2}}$
CAVITATED FILM	where θ_m is given by:		
UNCAVITATED FILM	$(1 + \epsilon \cos \theta_m) \cos \theta_m + 3\epsilon \sin^2 \theta_m = 0$	0	$\frac{\mu RL^3 \pi}{c^3 (1 - \epsilon^2)^{3/2}}$
PURE RADIAL SQUEEZE MOTION $\dot{\phi} = 0, \dot{\epsilon} \neq 0$	$\frac{-3\mu L^2 \dot{\epsilon} \cos \theta_m}{2c^2 (1 + \epsilon \cos \theta_m)^3}$	0	$\frac{\mu RL^3 [\pi - \cos^{-1}(\epsilon)] (2\epsilon^2 + 1)}{c^3 (1 - \epsilon^2)^{5/2}}$
CAVITATED FILM	$\theta_m = \pi$		
UNCAVITATED FILM		0	$\frac{\mu RL^3 \pi (2\epsilon^2 + 1)}{c^3 (1 - \epsilon^2)^{5/2}}$

Table 2-1. Summary of Equivalent Stiffness and Damping Coefficients for Squeeze Film Damper Bearings.

rotor unbalance vector and amplitude vector becomes less than 90°. When this condition occurs the force transmitted through the support structure will always be greater than the unbalance load. With an uncavitated film this problem does not occur because no bearing stiffness is generated. To obtain the stiffness required to stabilize a rotor (see Chapter 3) it is necessary to use retainer springs in the support bearings.

One of the most significant parameters affecting damper performance is the length to clearance ratio. The stiffness and damping coefficients vary as $(L/C)^3$ and therefore either doubling the bearing length or decreasing the clearance by 1/2 will increase the coefficients by a factor of 8.

CHAPTER 3

ROTOR-BEARING STABILITY AND STEADY-STATE ANALYSIS

3.1 ROTOR-BEARING STABILITY

After Jeffcott's [5] analysis in 1919 of the single mass flexible rotor on rigid bearings, manufacturers began producing light, flexible rotors operating above the first critical speed. However, some manufacturers encountered severe operating difficulties with some of their designs. These machines underwent violent whirling while running above the critical speed and often failed.

Experimental and analytical investigations by Newkirk and Kimball [6] [7] revealed that the whirl instability was not caused by unbalance in the rotor, but by internal shaft effects such as internal friction. Kimball theorized that forces normal to the plane of the deflected rotor could be produced by alternating stresses in the metal fibers of the shaft. In light of this theory, Newkirk concluded also that the same normal forces could be produced by shrink fits on the rotor shaft. By incorporating these forces in Jeffcott's model Newkirk showed that the rotor was unstable above twice the rotor critical speed.

Further investigation by Newkirk showed cases of rotor instability which were not produced by shaft effects but by effects in the journal bearings. [8] One cause of journal bearing instability was later shown to be due to lack of radial stiffness in the bearing and the instability occurred at twice the rotor

critical speed. These instabilities were especially common in lightly loaded rotors and larger bearing loads tended to promote stability. The effect of the larger loads is to cause cavitation of the fluid film which results in a radial stiffness component of the bearing forces being produced. [9], [10], [11]

In 1965 Alford reported on the effects of aerodynamic forces on rotors [12]. He showed that these forces couple the rotor equations of motion and can produce instability. He also noted that labyrinth seals and balance pistons also produce forces that can promote instability.

Recent investigators including Gunter, Kirk and Choudhury [13] [14][15] have analyzed the effects of support flexibility and damping on reducing rotor instability produced by the forces just described. As a result they have derived stability criteria for determining the necessary support characteristics.

One of the most general methods for determining rotor stability is to derive the characteristic frequency equation of the system. The stability is given by the roots of this equation. The real part of the root corresponds to an exponentially increasing or decreasing function of time. Thus a positive real part indicates instability whereas a negative real part indicates a stable system. This type of stability analysis of a rotor-bearing system therefore requires that the characteristic equation be known. This equation is not always easy to obtain.

The characteristic equation is derived from the homogeneous second order differential equations of motion of the system [15].

By assuming solutions of the form

$$x_i = A_i e^{\lambda t} \quad i = 1, 2, \dots, n$$

and differentiating, the equations are substituted back into the equations of motion. This produces a matrix known as the characteristic matrix. The determinant of this matrix gives the characteristic equation, a polynomial of degree $2n$ in λ , where n is the number of degrees of freedom of the system.

The computer program SDSTB [16] was used to produce the stability maps shown in this chapter. The program calculates the characteristic equation for a three-mass symmetric flexible rotor mounted in journal bearings and supported in squeeze film damper bearings. The rotor-bearing model is shown in Figure (3-1). The rotor is assumed to remain stationary in the axial direction so the rotor has six degrees of freedom and the characteristic equation is therefore of degree twelve. The characteristic matrix is shown in Figure (3-2). The determinant of this matrix gives the characteristic equation. The unknown variable in this equation is λ , the natural frequency of the system. An examination of the characteristic matrix shows that the coefficients of λ are functions of the rotor and bearing properties as well as internal shaft friction, absolute rotor damping and aerodynamic cross coupling. The natural frequencies and stability of the system are found by finding the roots of this equation.

The journal and support bearing characteristics can either be inserted directly as linear coefficients or they may be calculated

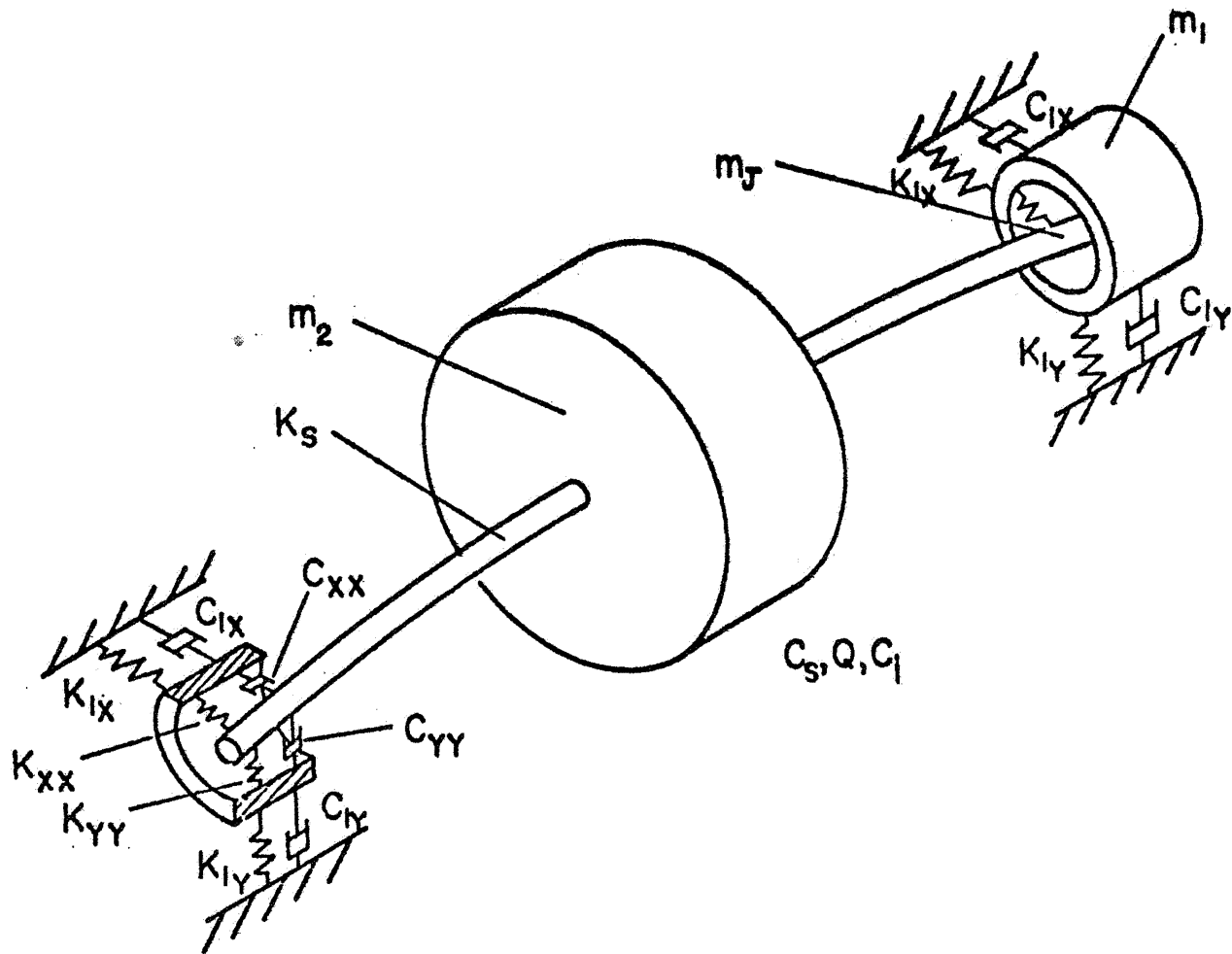


Figure 3-1 Three-Mass Flexible Rotor Mounted in Flexible, Damped Supports

$$\begin{array}{l}
 x_2: \\
 y_2: \\
 x_J: \\
 y_J: \\
 x_b: \\
 y_b:
 \end{array}
 \left[\begin{array}{cccccc}
 m_2 \lambda^2 & & -\lambda IC & & & \\
 +(IC+cs)\lambda & Q+\omega IC & -k_s & -\omega IC & 0 & 0 \\
 +k_s & & & & & \\
 & m_2 \lambda^2 & & -\lambda IC & & \\
 -Q-\omega IC & +(IC+cs)\lambda & \omega IC & -k_s & 0 & 0 \\
 +k_s & & & & & \\
 & & m_J \lambda^2 & c_{xy} \lambda & -c_{xx} \lambda & -c_{xy} \lambda \\
 -\lambda IC/2 & 0 & +(c_{xx}+IC/2)\lambda & +k_{xy} & -k_{xx} & -k_{xy} \\
 -(k_s+\omega IC)/2 & & +(k_s+\omega IC)/2 & & & \\
 +k_{xx} & & & & & \\
 & -\lambda IC/2 & c_{yx} \lambda & m_J \lambda^2 & -c_{yx} \lambda & -c_{yy} \lambda \\
 0 & -(k_s-\omega IC)/2 & +k_{yx} & +(c_{yy}+IC/2)\lambda & -k_{yx} & -k_{yy} \\
 & & & +(k_s-\omega IC)/2 & & \\
 & & & +k_{yy} & & \\
 & & -c_{xx} \lambda & -c_{xy} \lambda & m_b \lambda^2 & (c_{xy}+c_{1xy})\lambda \\
 0 & 0 & -k_{xx} & -k_{xy} & +(c_{xx}+c_{1xx})\lambda & +(k_{xy}+k_{1xy}) \\
 & & & & +(k_{xx}+k_{1xx}) & \\
 & & -c_{yx} \lambda & -c_{yy} \lambda & (c_{yx}+c_{1yx})\lambda & m_b \lambda^2 \\
 0 & 0 & -k_{yx} & -k_{yy} & +(k_{yx}+k_{1yx}) & +(c_{yy}+c_{1yy})\lambda \\
 & & & & & +(k_{yy}+k_{1yy})
 \end{array} \right]
 \begin{array}{l}
 A_1 \\
 A_2 \\
 A_3 \\
 A_4 \\
 A_5 \\
 A_6
 \end{array}
 =
 \begin{array}{l}
 0 \\
 0 \\
 0 \\
 0 \\
 0 \\
 0
 \end{array}$$

Figure 3-2 Characteristic Matrix For Three-Mass Model
Including Aerodynamic Cross-Coupling Internal
Shaft Friction and Absolute Shaft Damping

in the program from the bearing parameters by solving for the equilibrium positions of the journal and support. These characteristics are non-linear functions of the journal eccentricity. The stability maps in this chapter were produced with the linearized journal and support bearing characteristics given as input data to the program. The assumption of linear bearing characteristics is useful because for low eccentricity the characteristics do not vary greatly with changes in eccentricity. This assumption allows a large savings in computer time. If the non-linear characteristics are calculated, the amount of computer time increases because an iterative procedure is used to find the equilibrium position.

As an example of how a stability map is produced, consider the following system:

ROTOR CHARACTERISTICS

ROTOR WEIGHT	675 lbs
JOURNAL WEIGHT	312 lbs (each)
SUPPORT WEIGHT	15 lbs (each)
SHAFT STIFFNESS	280000 lb/in
SHAFT DAMPING	.10 lb-sec/in
INTERNAL DAMPING	0.0 lb-sec/in
ROTOR SPEED	10000 RPM

BEARING CHARACTERISTICS

k_{xx}	1.287×10^6 lb/in
k_{yy}	1.428×10^6 lb/in
C_{xx}	1200 lb-sec/in

c_{yy}	1290 lb-sec/in
$k_{xy} = k_{yx}$	0.0 lb/in
$c_{xy} = c_{yx}$	0.0 lb-sec/in

Two values of aerodynamic cross coupling were selected, $Q = 20000$ lb/in and $Q = 100,000$ lb/in. For each value of Q , several values of support stiffness were selected ranging from 50,000 lb/in to 500,000 lb/in. For each value of support stiffness a range of support damping values from 0 to 10000 lb-sec/in was used. Using this method a stability contour was found for a given value of aerodynamic cross coupling and support stiffness. The rotor and bearing characteristics remained unchanged.

Figures (3-3) and (3-4) show the stability maps for the above system for the two values of aerodynamic cross coupling. There is an intermediate range of support damping values for which the system is stable for a given value of the support stiffness. As the stiffness is increased the system becomes less stable. With $Q = 20000$ lb/in the optimum amount of damping ranges from 500 to 2500 lb-sec/in as the stiffness increases from 50000 to 500000 lb/in. For damping less than 100 lb-sec/in the system is unstable for all values of stiffness. The same is true if the damping exceeds 10000 lb-sec/in.

For $Q = 100000$ lb/in the optimum damping is 1000 lb-sec/in and does not shift over the stiffness range selected. When the stiffness reaches 250000 lb/in the system is unstable for all values of damping.

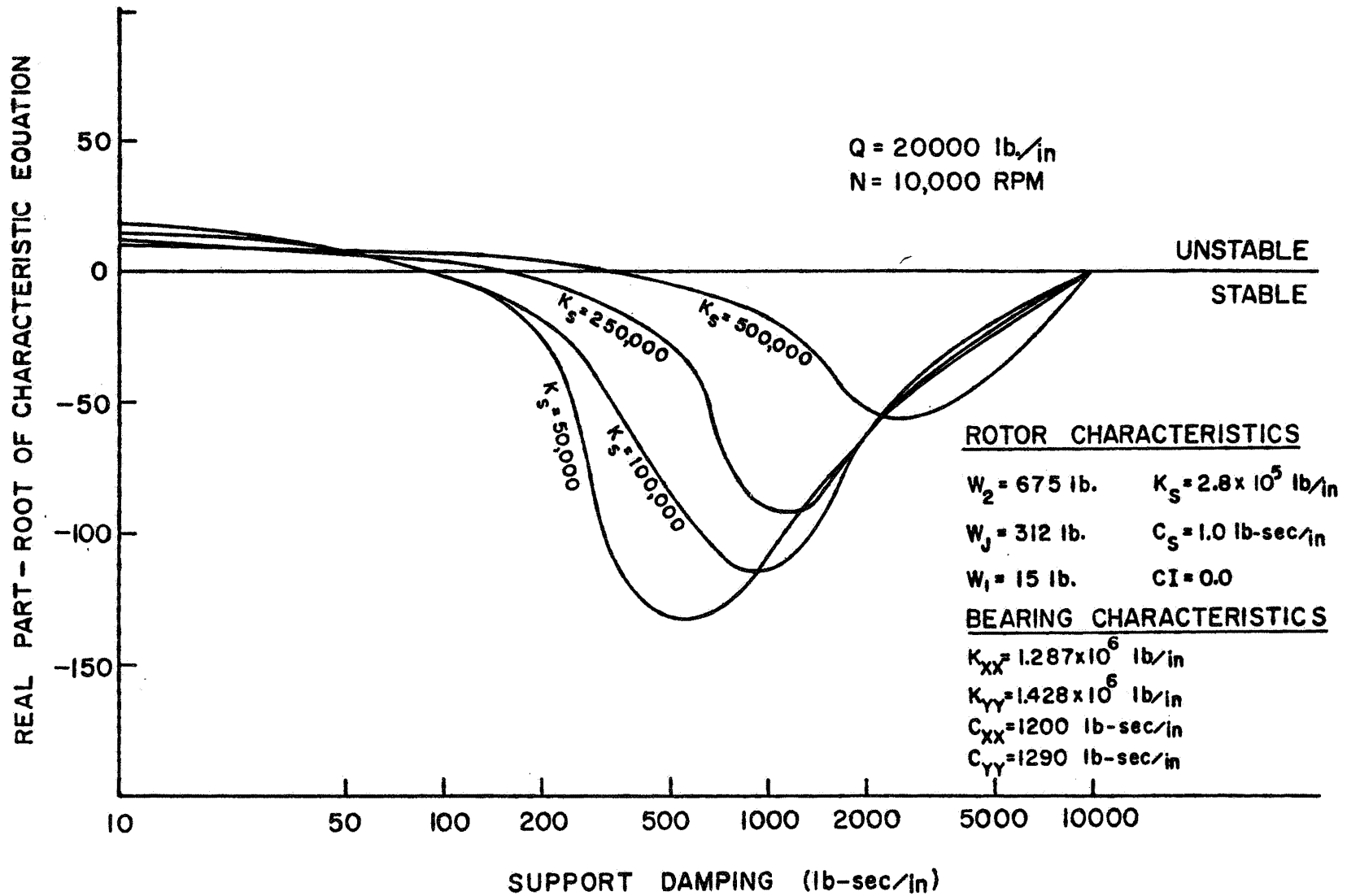


Figure 3-3 Stability of a Flexible Rotor With Aerodynamic Cross Coupling ($Q = 20,000 \text{ lb/in.}$, $N = 10,000 \text{ RPM}$)

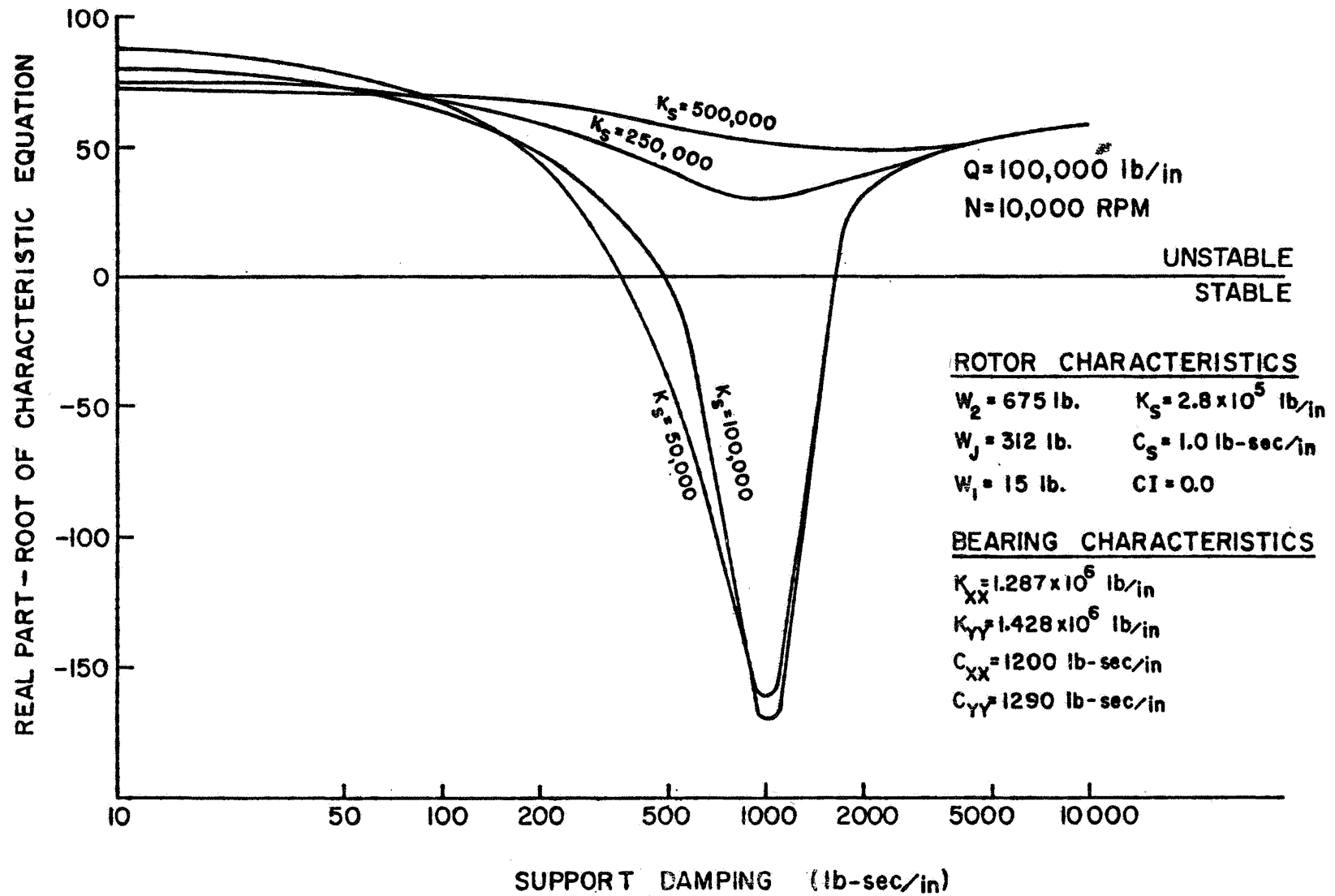


Figure 3-4 Stability of a Flexible Rotor With Aerodynamic Cross Coupling ($Q = 100,000$ lb/in., $N = 10,000$ RPM)

The stability calculation depends upon the accuracy of the root solving technique applied to the characteristic equation. For symmetric bearing and support characteristics repeated roots of the equation occur and many root solving routines break down under this condition. Although no cases have been encountered where the root solving routine has failed, it is possible that some combinations of rotor-bearing properties might cause this to happen. However because root solving routines are generally easy to obtain it would be easy to replace the one currently in SDSTB if such a situation arose.

The amount of computer time required to solve the characteristic equation depends upon the root solving technique and the order of the characteristic equation. Many studies do not require extensive stability maps and it is only necessary to determine whether the system is stable and not how stable. In these cases application of the Routh stability criteria [15] gives the required information without solving for the roots of the characteristic equation. This results in a savings of computer time. The option of using only the Routh stability criteria is available in SDSTB.

The method of determining the stability of the system from the characteristic equation becomes less practical when the order of the system is large. The elements of the characteristic matrix must be found from the equations of motion and unless the determinant is found by a computer routine, the characteristic equation must be expanded by hand. Therefore complicated systems may re-

quire a prohibitive amount of formulation time.

Recent research in transfer matrix and finite element techniques for determining the stability and natural frequencies of rotor bearing systems has been directed toward overcoming these difficulties [17] [18]. However, because iterative procedures are required in the solution, higher order modes may be expensive to obtain from the standpoint of computer time. The type of method used will depend on the amount of computer funds available and the availability of programs using the various techniques.

3.2 STEADY-STATE ANALYSIS

The steady-state stability maps just discussed provide information on the support characteristics needed to promote stability in a given rotor-bearing system. There remains the problem of relating these characteristics to the actual support bearing. The squeeze bearing equations derived in Chapter 2 in rotating coordinates are used to determine the preliminary bearing design. As noted in Chapter 2, these equations were derived assuming steady-state circular, synchronous precession of the journal.

The bearing characteristics, stiffness, damping and pressure are functions of the amplitude of the journal orbit, fluid viscosity and bearing geometry. The addition of oil supply grooves, end seals and cavitation affect the bearing characteristics.

The steady-state equations have been programmed on a digital

computer. This program, SQFDAMP, analyzes three basic bearing configurations:

1. Plain bearing, no oil supply groove or end seals.
2. Bearing with oil supply groove but without end seals.
3. Bearing with both oil supply groove and end seals.

Both cavitated and uncavitated fluid films can be analyzed. A listing of the program with a description of the input data requirements and sample output are contained in Appendix A.

The program calculates the bearing characteristics and plots them as functions of the journal eccentricity ratio, ϵ . By varying the bearing parameters the designer is able to determine the bearing characteristics and select a bearing configuration that will provide the stability requirements of the system under consideration.

Figures (3-5) - (3-7) show the characteristics for a bearing being considered for the 675 lb rotor system described earlier. The bearing has an oil supply groove and end seals, and the fluid film is assumed to be cavitated. The bearing parameters are, length, 1.0 inches, radius, 1.2 inches and fluid viscosity 10 microreyns. For the case where $Q = 20000$ lb/in it was determined that the optimum support damping is about 500 lb-sec/in and the support stiffness should be less than 100000 lb/in. Because it is desirable to keep the eccentricity ratio of the journal low, Figures (3-5) and (3-6) reveal that this bearing will provide the necessary stiffness and damping characteristics with a clearance of about 4 mils at an eccentricity ratio of $\epsilon = .10$ to $.20$.

SQUEEZE FILM DAMPER
OIL SUPPLY GROOVE AND SEALS
CAVITATION

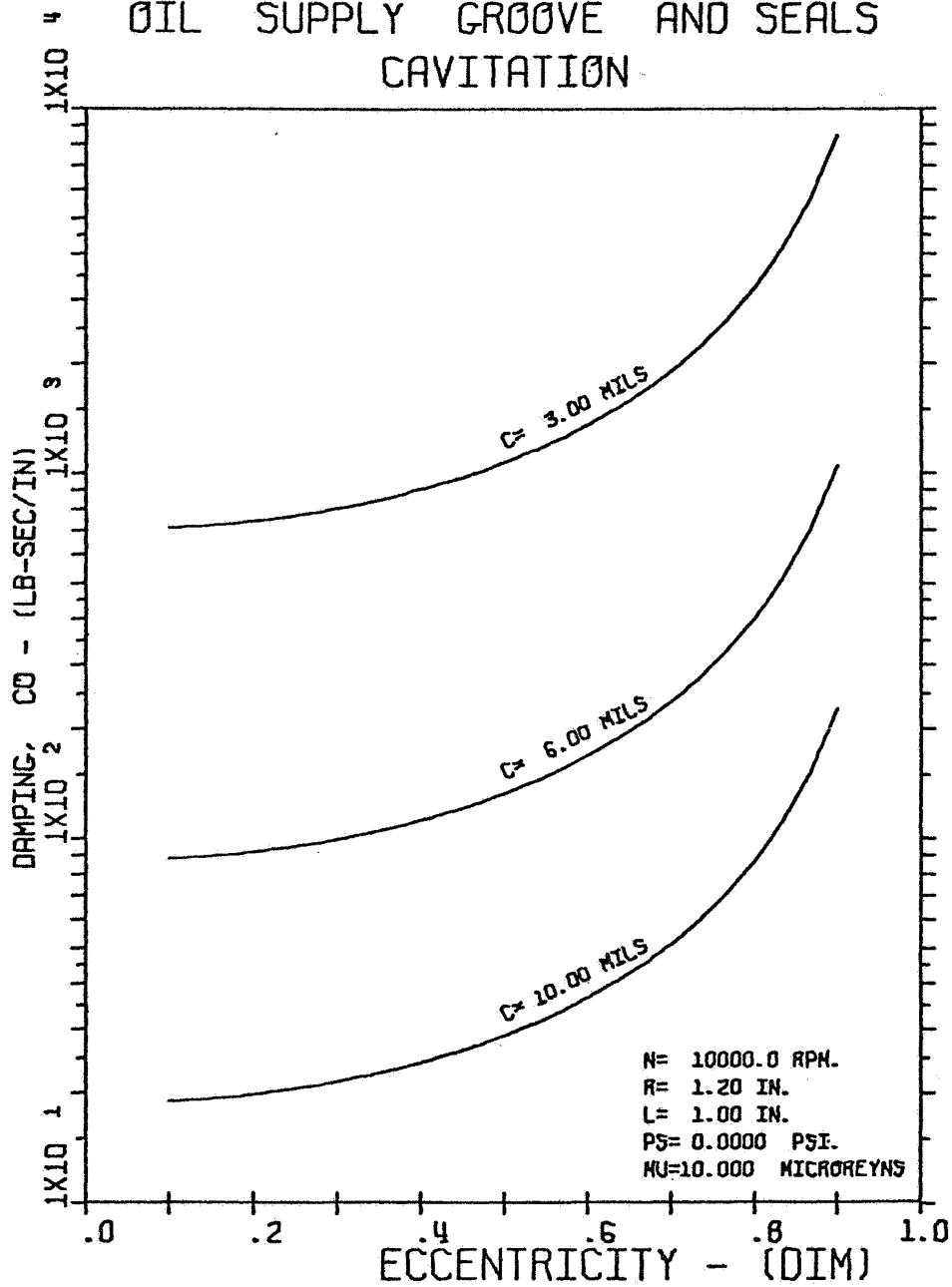


Figure 3-5. Damping Coefficient for Squeeze Film Bearing With Cavitated Film - End Seals and Oil Supply Groove Included.

SQUEEZE FILM DAMPER
OIL SUPPLY GROOVE AND SEALS
CAVITATION

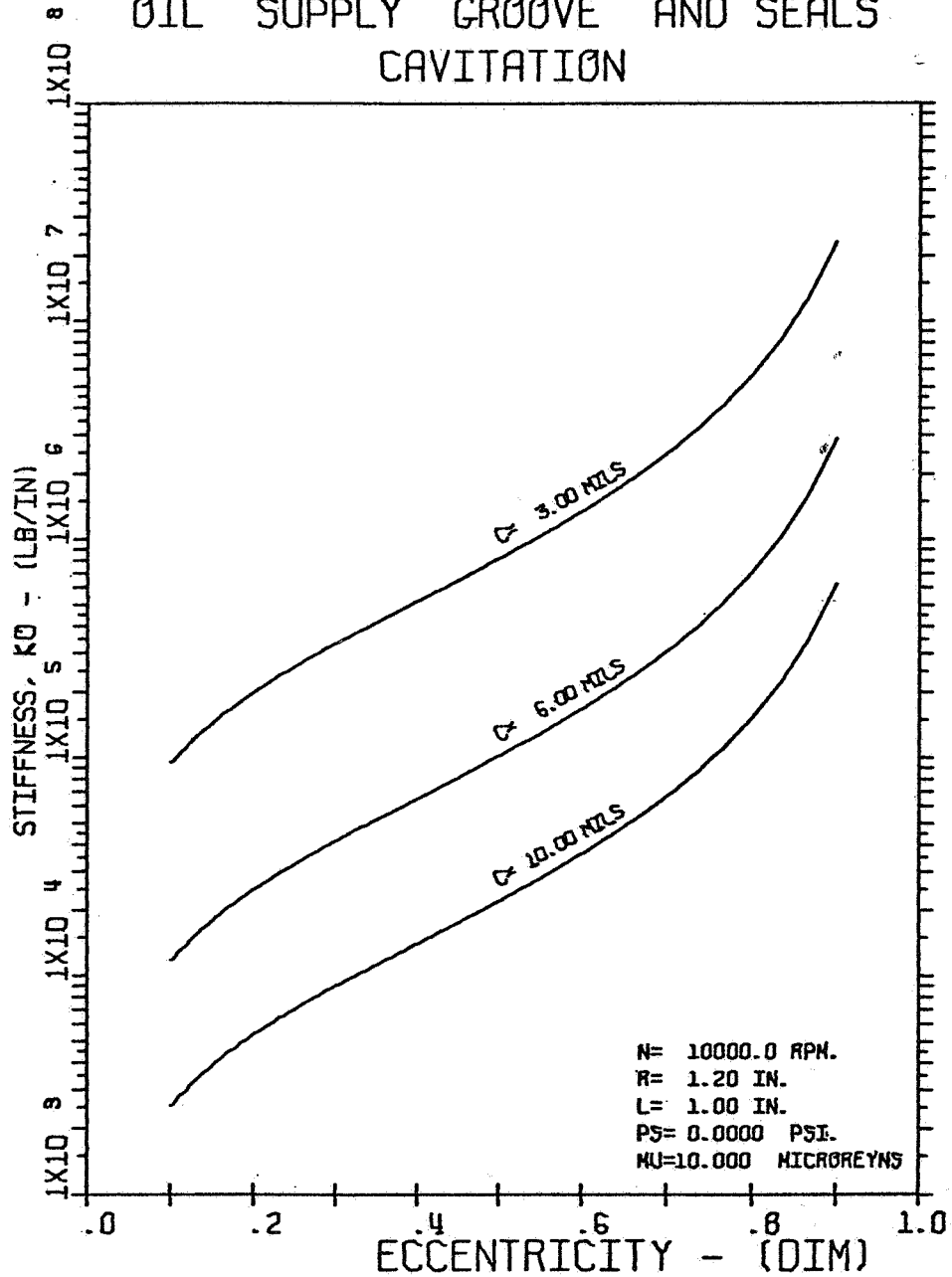


Figure 3-6. Stiffness Coefficient for Squeeze Film Bearing With Cavitated Film - End Seals and Oil Supply Groove Included.

SQUEEZE FILM DAMPER
OIL SUPPLY GROOVE AND SEALS
CAVITATION

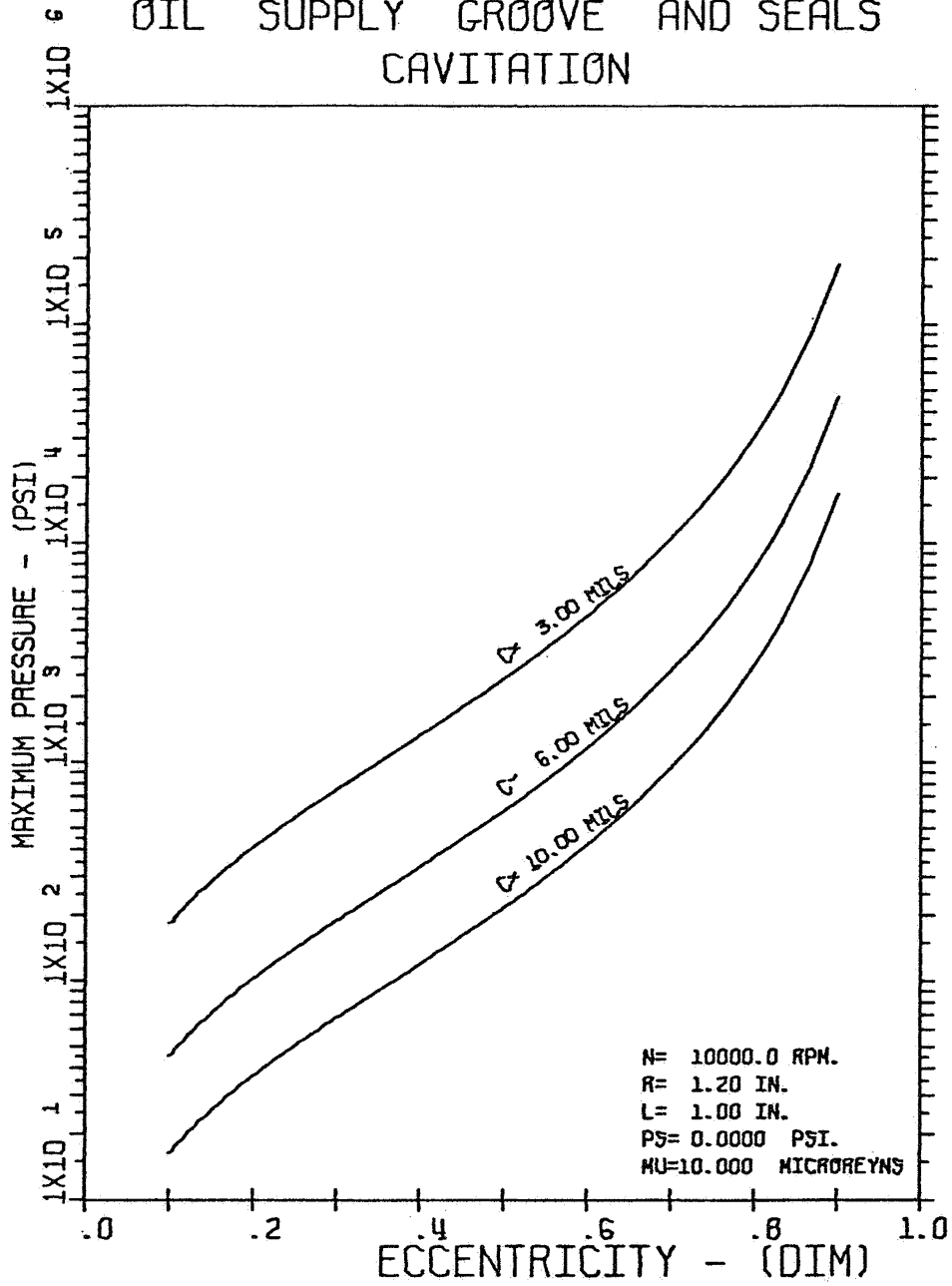


Figure 3-7. Maximum Pressure for Squeeze Film Bearing with Cavitated Film - End Seals and Oil Supply Groove Included.

This corresponds to a journal orbit of 0.4 to 0.8 mils amplitude. The maximum hydrodynamic pressure in the bearing is about 100 psi for this clearance. If the fluid film cavitates, the resulting characteristics are shown in Figures (3-8) and (3-9). A slightly larger clearance, 5.0 mils, will produce the optimum damping. However, because the uncavitated film does not produce an equivalent stiffness, retainer springs must be incorporated in the bearing. If the end seals are flexible the required spring rate may be obtained from them.

One advantage of the uncavitated film is that if the journal eccentricity ratio should become very large, there is no rise in stiffness that could cause the system to become unstable or raise the critical speed above the operating speed. Figures (3-5) and (3-8) indicate that even at eccentricity ratios of 0.9 the damping value still remains acceptable. For the cavitated film at $\epsilon = .9$, the stiffness exceeds 2,000,000 lb/in and the system would be bordering on instability. For both films the maximum pressure exceeds 70000 psi. at $\epsilon = 0.9$ and this large a rotating pressure field could result in bearing failure.

If $Q = 100000$ lb/in, the bearing characteristic graphs reveal that for a cavitated film the clearance must be as small as possible because of the limitations on stiffness shown in Figure (3-4). With a 3.0 mil clearance, the stiffness is 250000 lb/in at $\epsilon = 0.23$ and this stiffness will produce system instability. For $Q = 100000$ lb/in it is desirable to study other bearing lengths and radii to obtain a cavitated bearing which pro-

SQUEEZE FILM DAMPER
OIL SUPPLY GROOVE AND SEALS
NO CAVITATION

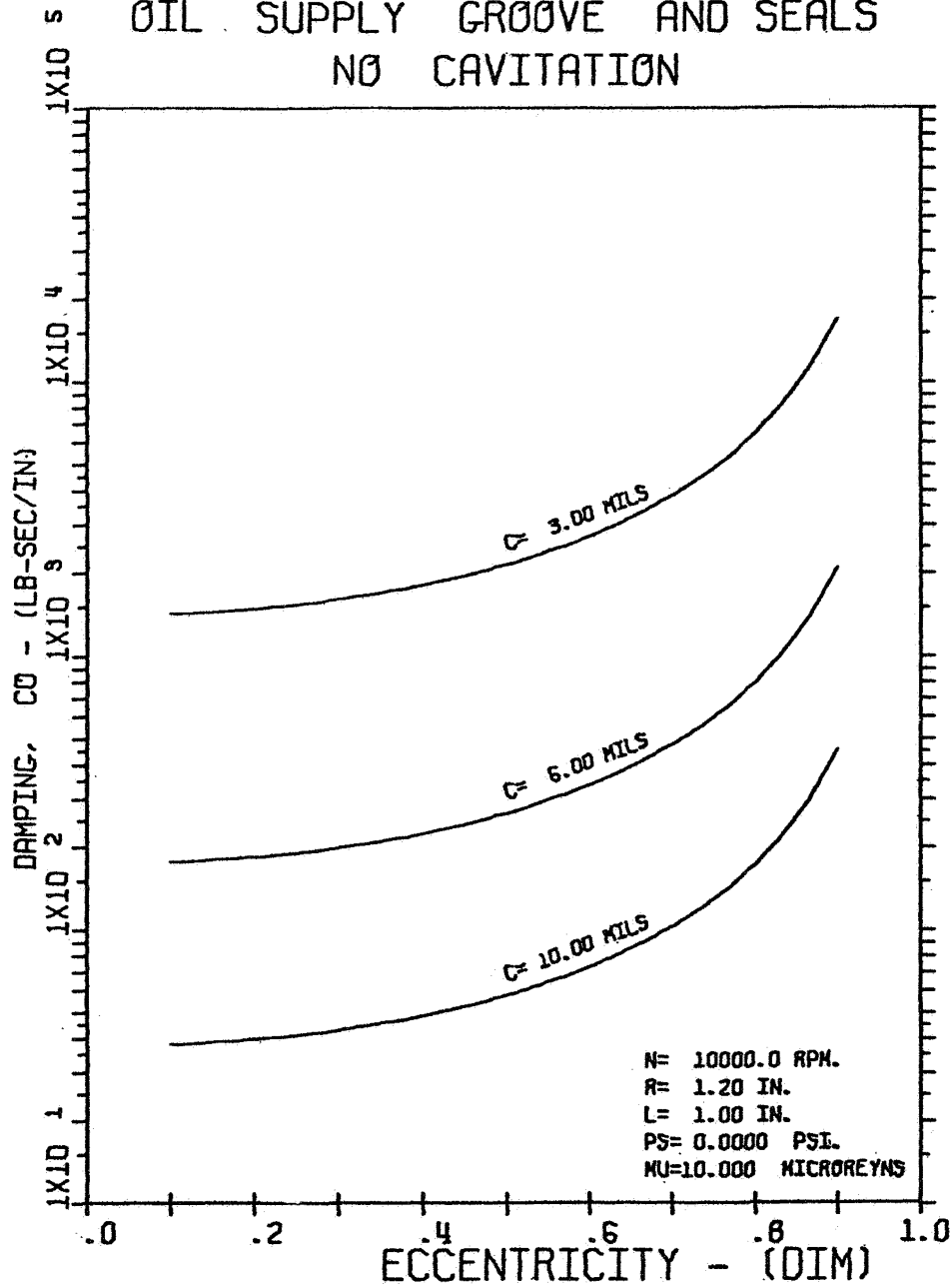


Figure 3-8. Damping Coefficient for Squeeze Film Bearing with Uncavitated Film - End Seals and Oil Supply Groove Included

SQUEEZE FILM DAMPER
OIL SUPPLY GROOVE AND SEALS
NO CAVITATION

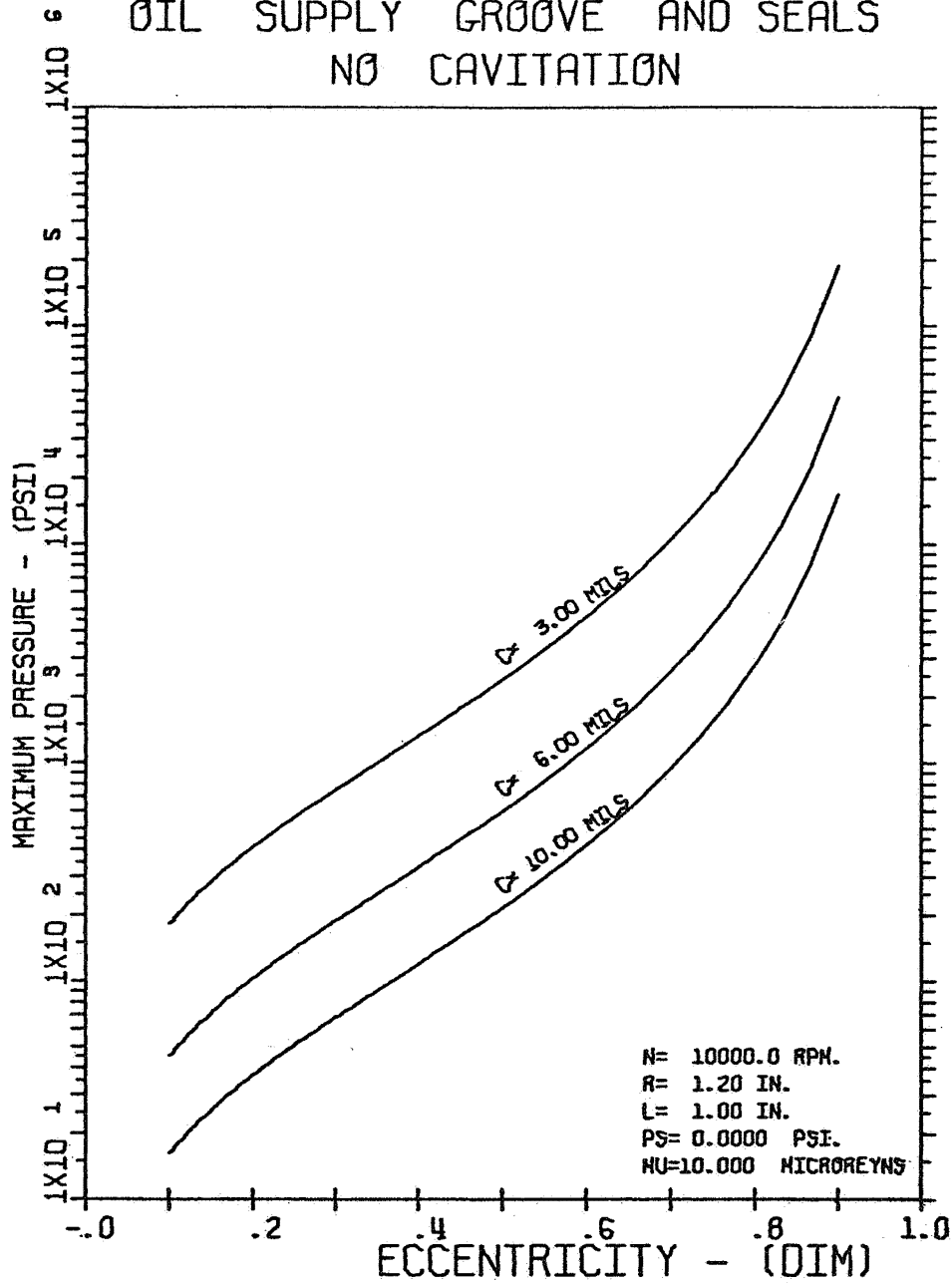


Figure 3-9. Maximum Pressure for Squeeze Film Bearing with Uncavitated Film - End Seals and Oil Supply Groove Included.

duces the required damping at low eccentricity ratios and also produces a stiffness of 100000 lb/in or less. For an uncavitated film a 3.0 mil clearance provides adequate damping.

The steady-state bearing characteristic equations used in conjunction with the stability analysis based on steady-state motion provide an excellent means of determining bearing configurations. Using the methods just described, good preliminary designs can be obtained which can be more thoroughly analyzed. The steady-state analysis described here and the transient analysis described in the next chapter provide bearing design criteria which will eliminate the experimental testing of unsuitable designs. The costs of the analysis more than offset the experimental losses when designs are tested that result in bearing or machine failure.

CHAPTER 4
TRANSIENT ANALYSIS

4.1 INTRODUCTION

There are a number of operating conditions in which the squeeze bearing journal does not orbit the bearing center in circular synchronous precession. These conditions can occur when there is a unidirectional load on the rotor or when there is a suddenly applied load such as the application of unbalance when blade loss occurs. Intermittent or cyclic forces transmitted to the machine from nearby equipment can also result in non-linear orbiting. Under these conditions the bearing stiffness and damping coefficients developed in Chapter 2 are no longer applicable and a time-transient analysis of the bearing is necessary to determine the squeeze bearing support's ability to restablize the system.

The equation for the squeeze film damper fluid film forces, in fixed coordinates, equation (2-19) provides a useful means of determining the time dependent transient behavior of a rotor bearing system. The force equations have been programmed on a digital computer and combined with the journal equations of motion. The resulting program, BRGTRAN [19] tracks the journal motion forward in time under the influence of the bearing forces, journal weight and unbalance. The program is capable of including the effects of retainer springs and cavitation.

Because both the bearing pressure equation and the journal

equations of motion must be integrated, the accuracy of the simulation depends upon the numerical integration method used. Two integration methods, Adam-Bashforth-Moulton Predictor-Corrector, and 4th Order Runge-Kutta, are provided as options in BRGTRAN. Although the 4th Order Runge-Kutta method is highly accurate, four functional evaluations of the pressure equation are required for each step in time. Even though the required time step size may be larger using the Runge-Kutta method, the total computer time required is still greater than other methods because of the many functional evaluations.

The Adams-Bashforth-Moulton method has been found to be sufficiently accurate for most cases run if the time step has been made sufficiently small, or about 0.01 cycles. At low eccentricities no problems are encountered in the integration process and the solutions are accurate for both methods. The changes in the bearing forces are relatively small from one time step to the next and even a very simple integration method such as the Modified Euler Method provides reasonable accuracy. However at high eccentricities the bearing forces change drastically with even a very small change in eccentricity. Even the more sophisticated integration schemes lose accuracy when the eccentricity is high unless the time step is made very small. The amount of computer time and core storage required for a small time step becomes prohibitive. This is especially true in light of the fact that at high eccentricities the validity of the short bearing approximation used in reducing the Reynolds equation is

doubtful. In using the short bearing approximation it was assumed that the pressure gradient in the tangential direction is small, and this assumption may be violated at high eccentricities.

It was also shown in Chapters 2 and 3 that at high eccentricities the bearing stiffness becomes very large. This can result in system instability as indicated in the stability maps, Figures (3-3) and (3-4), or in raising the system critical speed above the operating speed causing large forces to be transmitted to the machine structure. For these reasons the design criteria of $\epsilon < 0.4$ was established and it is unnecessary to use excessive computer time to obtain greater accuracy at higher eccentricities. The information provided at these eccentricities is very useful in showing trends in the ability of a bearing to perform adequately and should be used with this restriction kept in mind. Also recent transient analysis has been performed using hybrid computer simulation thereby avoiding the difficulties inherent in numerical integration. [20]

4.2 ANALYSIS

Using a time transient bearing program, a design engineer can make an analysis of the bearing effects without resorting to either a complete time-transient analysis of the entire rotor-bearing system or a costly experimental program during the preliminary design stage. During later design stages when the

bearing configuration has been tentatively fixed, a more complete theoretical and experimental analysis of the entire system may be performed. The bearing force calculations have also been incorporated as a subroutine in a computer program which analyzes the transient behavior of certain rotor-bearing models [21]. By using these programs to determine the bearing parameters experimental verification of the bearing effects can be performed with more assurance that the design is feasible, and costly and time consuming machine prototype failures can be reduced.

The computer program BRGTRAN was recently used as part of an analysis of an existing turbomachine which had suffered frequent bearing failures. The manufacturer had decided to use a squeeze film damper bearing to reduce the vibration amplitudes at the failing bearings. Without performing a complete analysis of the bearing effects, an experimental program was initiated where various bearing configurations were installed on a test machine. The damper bearings used did not dampen out the vibrations and much time and money was lost during the project.

The following discussion of the computer simulation of this system shows the effect of varying the rotor-bearing parameters including bearing length, unbalance, cavitation and retainer springs.

In this study of the problem, the analysis made using BRGTRAN showed why the bearings used were unable to reduce vibration amplitudes. Figure (4-1) shows the journal orbit in a cavitated

SQUEEZE FILM BEARING
CAVITATED FILM

HORIZONTAL

		CASE NO. ✓	325741
W =	73.7 LBS	N =	16800 RPM
L =	.450 IN	R =	2.550 IN
C =	4.00 MILS	MU =	.382 MICROREYNS
PS =	0.00 PSI	FMAX =	7405.4 LBS
WX =	0.00 LBS	WY =	0.00 LBS
FU =	1181.91 LBS	EMU =	.50
KRX =	0 LB/IN	KRY =	0 LB/IN
TRD =	6.27	PMAX =	13688.97 PSI

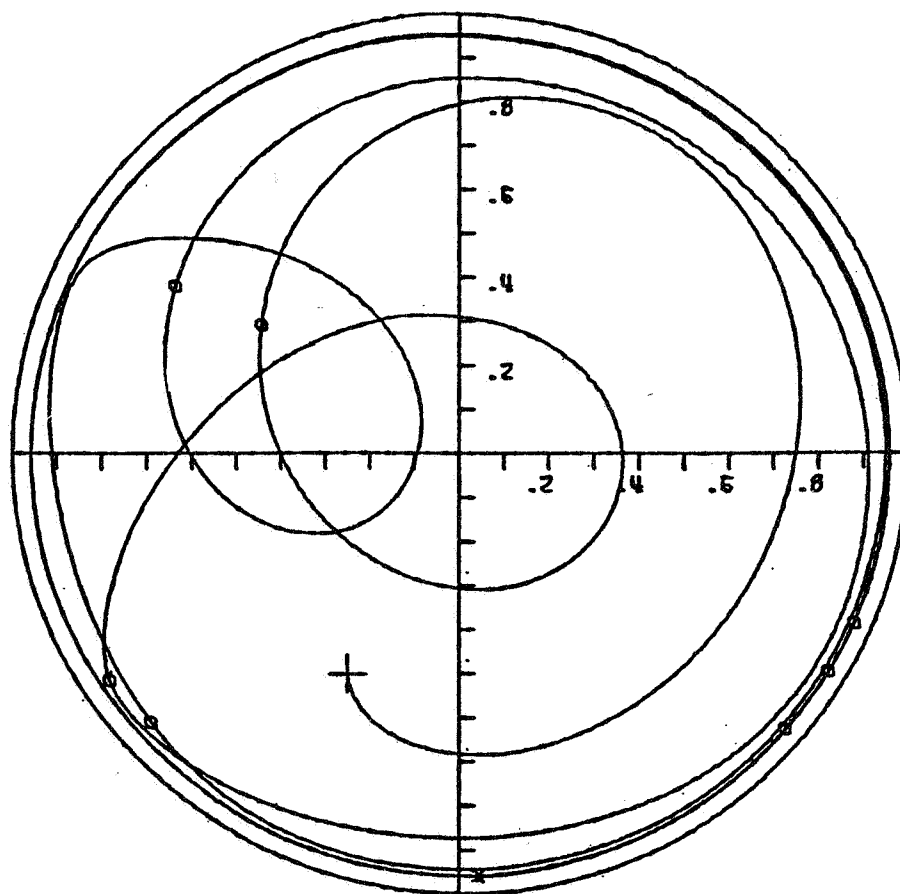


Figure 4-1. Unbalanced Rotor in Cavitated Squeeze Film Bearing - L = 0.45 IN. - Unbalance Eccentricity = 0.002 IN. - No Retainer Spring.

film during the first 10 cycles of transient motion. The bearing parameters are:

LENGTH	- 0.45 inches
RADIUS	- 2.55 inches
CLEARANCE	- 0.004 inches
FLUID VISCOSITY	- 0.38×10^{-6}
JOURNAL WEIGHT	- .74 lbs.
UNBALANCE ECCENTRICITY	- 0.002 inches
RETAINER SPRING RATE	
K _{xx}	- 0 lb/in
K _{yy}	- 0 lb/in
N	- 16800 RPM

In the transient orbit figures a standard right-hand coordinate system has been adopted with positive journal rotation in the counterclockwise direction. The asterisk on the orbit represents the point where the maximum force is generated. The small dots represent timing marks denoting one revolution of shaft motion. These marks can be used to determine the relative location of the unbalance with respect to the amplitude in the x-direction. The timing mark sensor is assumed to be located on the positive x-axis, and the phase angle is measured from the x-axis to the timing mark in the clockwise direction.

Returning to Figure (4-1), it is seen that the journal very quickly spirals out to an eccentricity ratio $\epsilon = 0.95$, where a limit cycle is formed due to the non-linearity of the bearing forces. The maximum force transmitted through the support

structure is 7405 lbs, which is over 6 times the rotating unbalance load of 1181 lbs. as shown by the parameter TRD Figure (4-1). This large rotating force will eventually lead to bearing failure and is therefore undesirable.

The phase angle between the maximum amplitude in the x direction and the timing mark is approximately 30° , and this indicates that the precession rate is less than the natural frequency of the bearing. This has been caused by the large stiffness developed in the bearing. Figure (4-2) shows that the stiffness is approximately 487,000 lb/in. The damping is given in Figure (4-3) as 71.5 lb-sec/in.

One possible design change considered was to increase the bearing length. Figure (4-4) shows the effect of increasing the bearing length of 0.90 inches, all other parameters remaining the same. The journal still spirals outward, however the limit cycle is produced at an eccentricity ratio, $\epsilon = 0.88$. This results in a reduction in the force transmitted to the support from 7405 to 3371 lbs., but it is still greater than the rotating unbalance load, and is undesirable since bearing failure will result. The phase angle has shifted from 30° to 60° and this would have been accompanied by an increase in the force transmitted except that the stiffness and damping values have also changed with the net effect being a reduction in the transmissibility. The stiffness and damping coefficients are shown in Figures (4-5) and (4-6) to be 880000 lb/in and 22 lb-

SQUEEZE FILM DAMPER
OIL SUPPLY GROOVE AND SEALS
CAVITATION

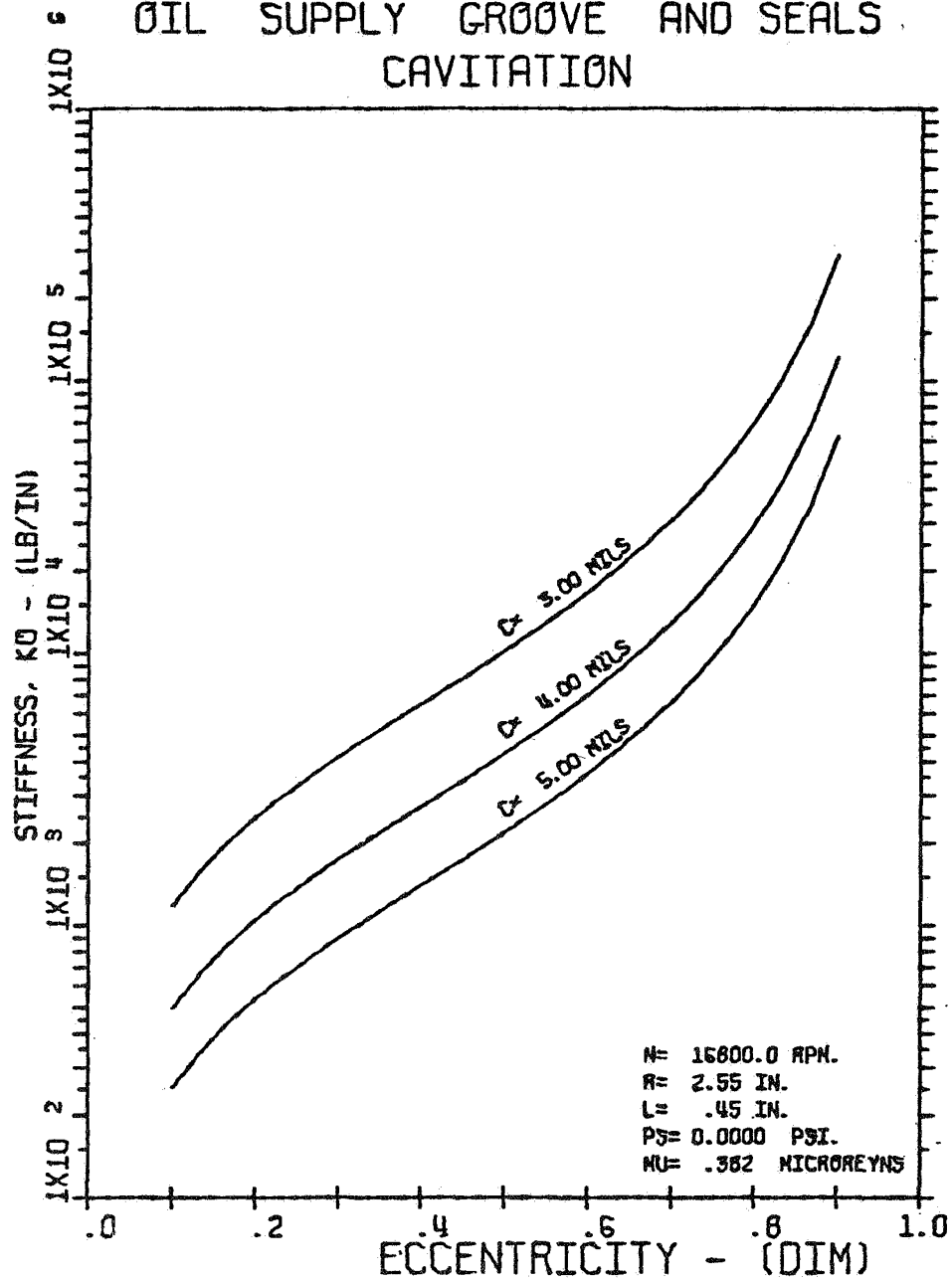


Figure 4-2. Stiffness Coefficient for Squeeze Film Bearing of Figure (4-1).

SQUEEZE FILM DAMPER
OIL SUPPLY GROOVE AND SEALS
CAVITATION

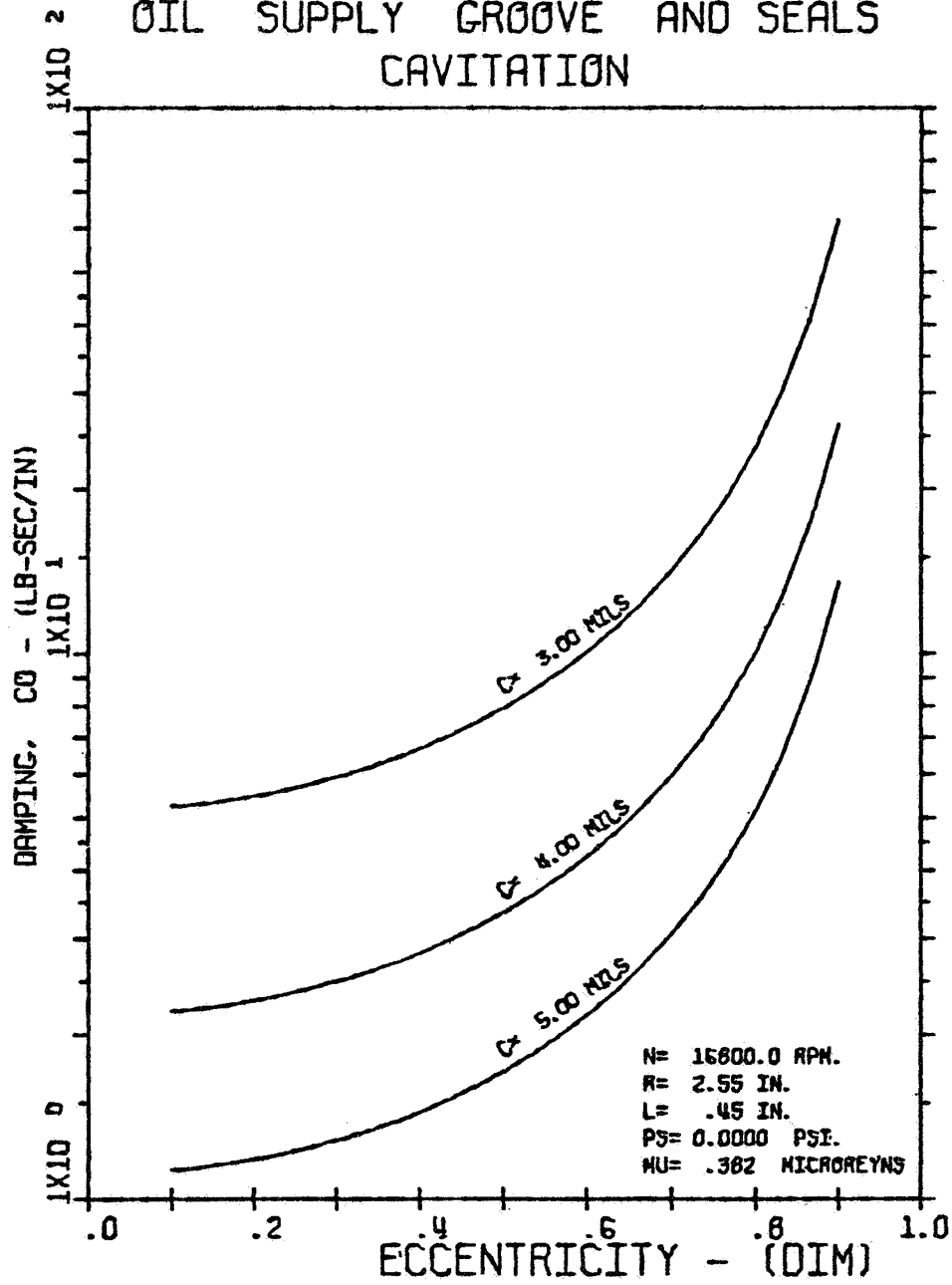


Figure 4-3. Damping Coefficient for Squeeze Film Bearing of Figure (4-1).

SQUEEZE FILM BEARING
CAVITATED FILM
HORIZONTAL

		CASE NO.	525712
W =	73.4 LBS	N =	16800 RPM
L =	.900 IN	R =	2.550 IN
C =	4.00 MILS	MU =	.382 MICROREYNS
PS =	0.00 PSI	FMAX =	3371.8 LBS
WX =	0.00 LBS	WY =	0.00 LBS
FU =	1177.10 LBS	EMU =	.50
KRX =	0 LB/IN	KRY =	0 LB/IN
TRD =	2.86	PMAX =	3828.76 PSI

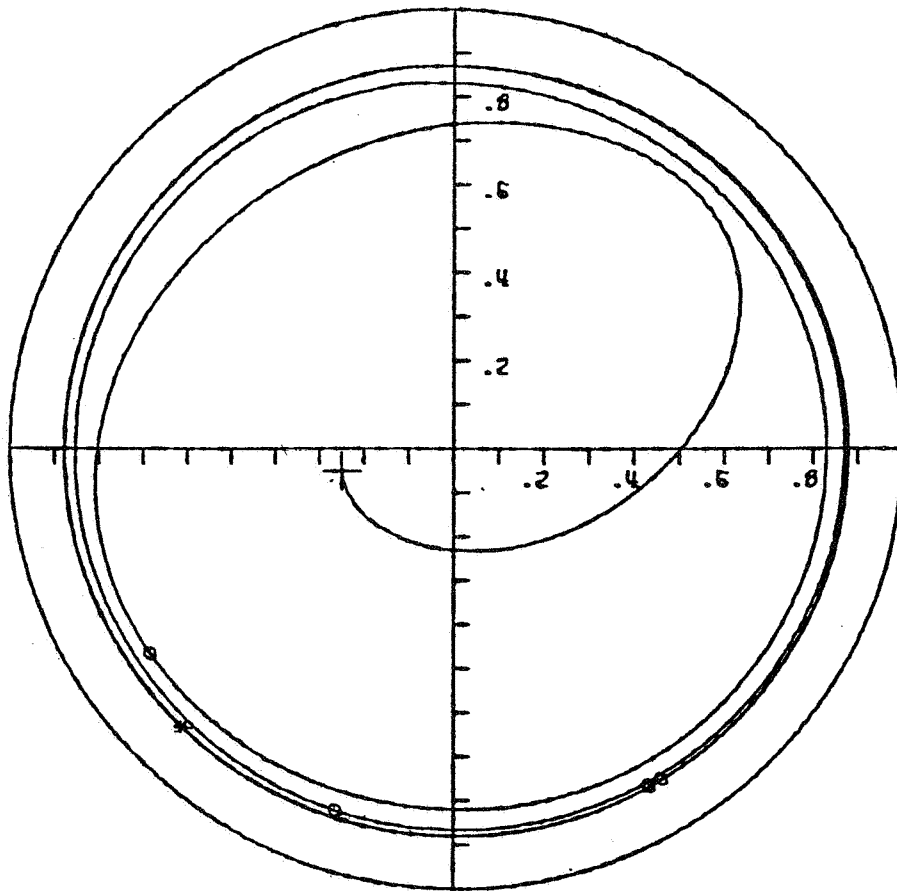


Figure 4-4. Unbalanced Rotor in Cavitated Squeeze Film Bearing L = 0.90 IN. - Unbalance Eccentricity = 0.002 IN. - No Retainer Spring.

SQUEEZE FILM DAMPER
OIL SUPPLY GROOVE AND SEALS
CAVITATION

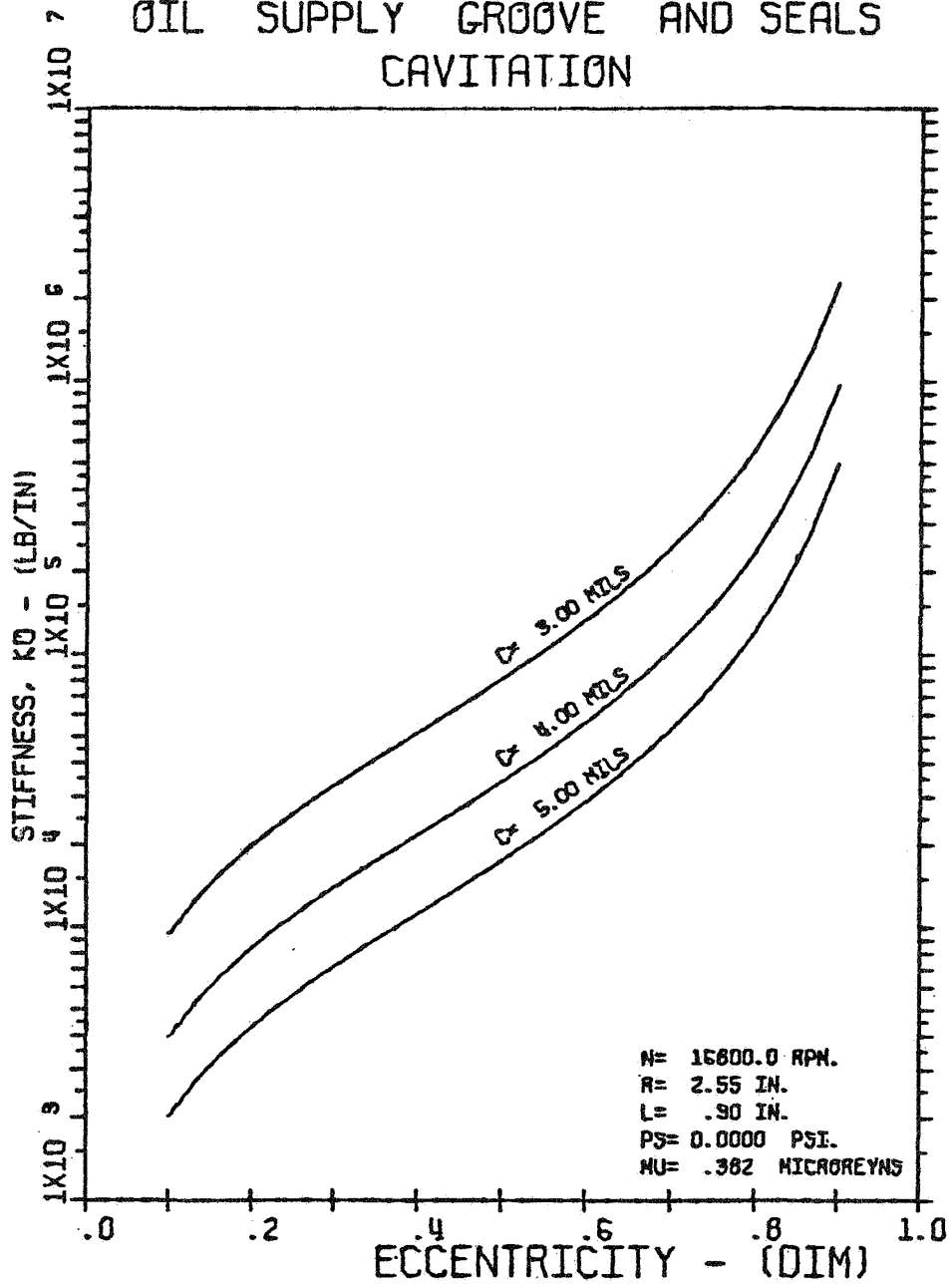


Figure 4-5. Stiffness Coefficient for Squeeze Film Bearing of Figure (4-4).

SQUEEZE FILM DAMPER
OIL SUPPLY GROOVE AND SEALS
CAVITATION

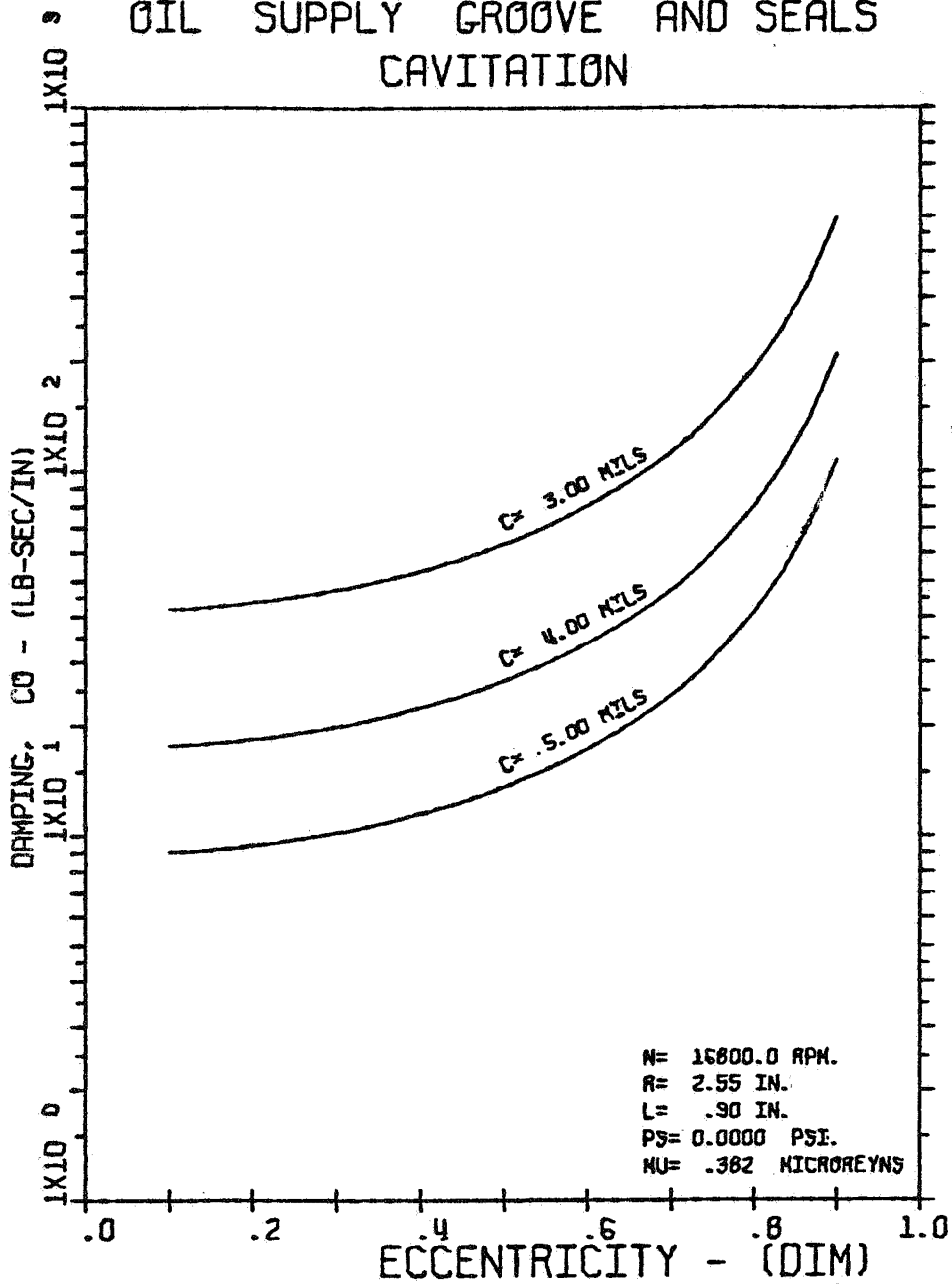


Figure 4-6. Damping Coefficient for Squeeze Film Bearing of Figure (4-4).

sec/in respectively.

Figure (4-7) shows the first 10 cycles of motion for the bearing configuration of Figure (4-1) with the addition of retainer springs with a stiffness of 123000 lb/in. Only a very slight improvement in force transmission results, and the bearing is still unacceptable.

The effect of changing the rotating unbalance load is shown in Figure (4-8). The bearing configuration is the same as Figure (4-4) except the unbalance has been reduced by one half. The journal orbit has been greatly reduced and the force transmitted to the support structure is reduced to only 80% of the unbalance load. The journal is now precessing about a point offset from the bearing center.

By adding retainer springs to the bearing of Figure (4-8) the motion in Figure (4-9) results. The retainer spring rate is 123,000 lb/in. The journal is orbiting about the center of the bearing at an eccentricity ratio of $\epsilon = 0.35$. The journal motion is stabilizing more quickly than without the retainer springs and the journal is precessing synchronously as indicated by the small dots on the orbit which represents one cycle of motion. The transmitted force has been further reduced to only 65% of the unbalance load. From the standpoint of producing a small amplitude orbit and attenuating the unbalance load such a bearing configuration is desirable.

If the unbalance eccentricity is again increased to 0.002 inches, the bearing configuration of Figure (4-9) is no longer

SQUEEZE FILM BEARING
CAVITATED FILM
HORIZONTAL

		CASE NO.	325743
W	= 73.7 LBS	N	= 16800 RPM
L	= .450 IN	R	= 2.550 IN
C	= 4.00 MILS	MU	= .382 MICROREYNS
PS	= 0.00 PSI	FMAX	= 7331.9 LBS
WX	= 0.00 LBS	WY	= 0.00 LBS
FU	= 1181.91 LBS	EMU	= .50
KRX	= 123000 LB/IN	KRY	= 123000 LB/IN
TRD	= 6.20	PMAX	= 12510.22 PSI

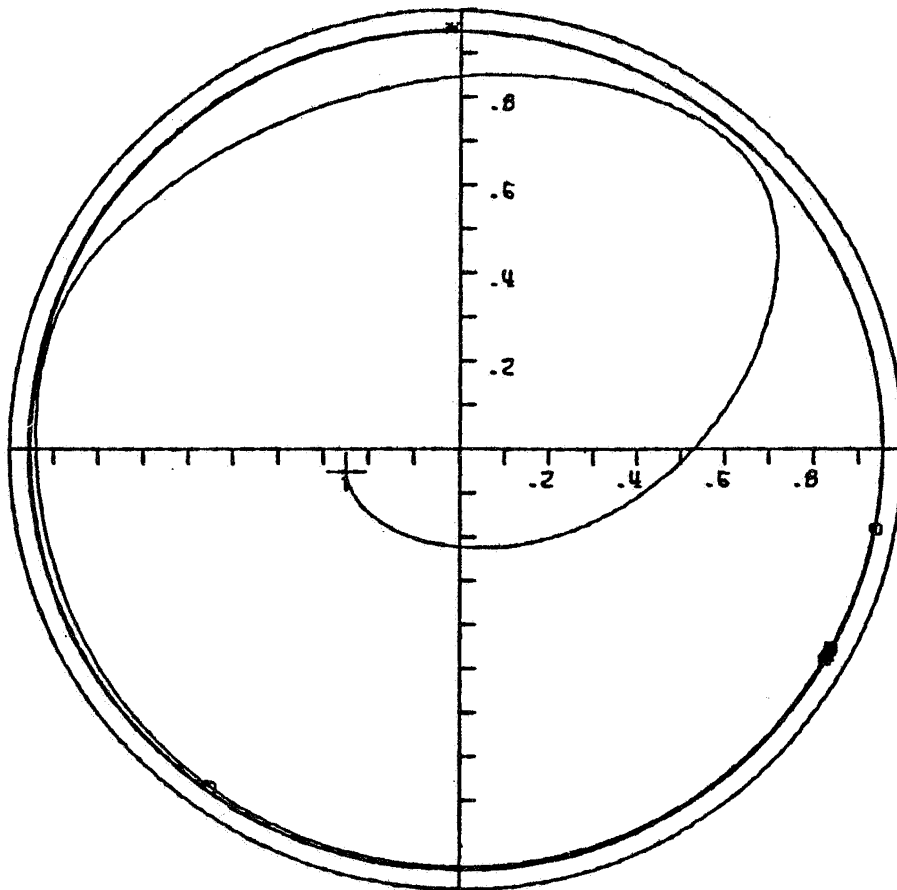


Figure 4-7. Unbalanced Rotor in Cavitated Squeeze Film Bearing - L = 0.45 IN. - Unbalance Eccentricity = 0.002 IN. - Retainer Spring Stiffness, KR = 123,000 LB/IN.

SQUEEZE FILM BEARING
CAVITATED FILM
HORIZONTAL

		CASE NO.	325744
W =	73.7 LBS	N =	16800 RPM
L =	.900 IN	R =	2.550 IN
C =	4.00 MILS	MU =	.382 MICROREYNS
PS =	0.00 PSI	FMAX=	470.0 LBS
WX =	0.00 LBS	WY =	0.00 LBS
FU =	590.96 LBS	EMU =	.25
KRX =	0 LB/IN	KRY =	0 LB/IN
TRD =	.80	PMAX=	52.28 PSI

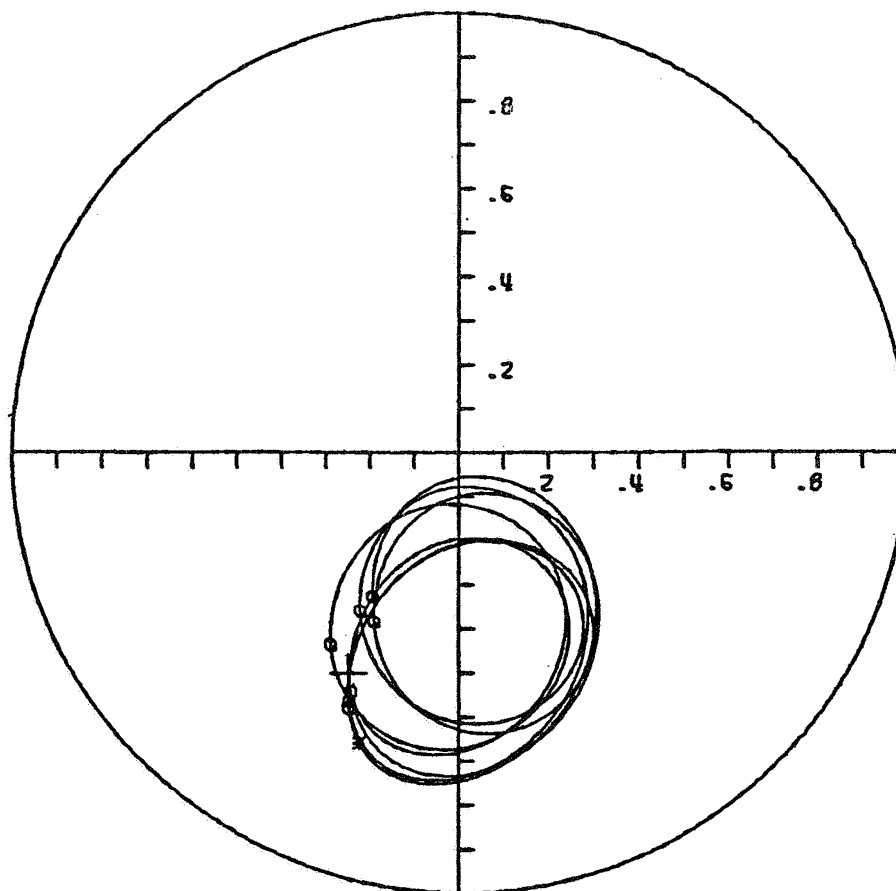


Figure 4-8. Unbalanced Rotor in Cavitating Squeeze Film Bearing - L = 0.90 IN. - Unbalance Eccentricity = 0.001 IN. - No Retainer Spring

SQUEEZE FILM BEARING
CAVITATED FILM
HORIZONTAL

		CASE NO.	325745
W =	73.7 LBS	N =	16800 RPM
L =	.900 IN	R =	2.550 IN
C =	4.00 MILS	MU =	.382 MICROREYNS
PS =	0.00 PSI	FMAX =	385.4 LBS
WX =	0.00 LBS	WY =	0.00 LBS
FU =	590.96 LBS	EMU =	.25
KRX =	123000 LB/IN	KRY =	123000 LB/IN
TRD =	.65	PMAX =	46.09 PSI

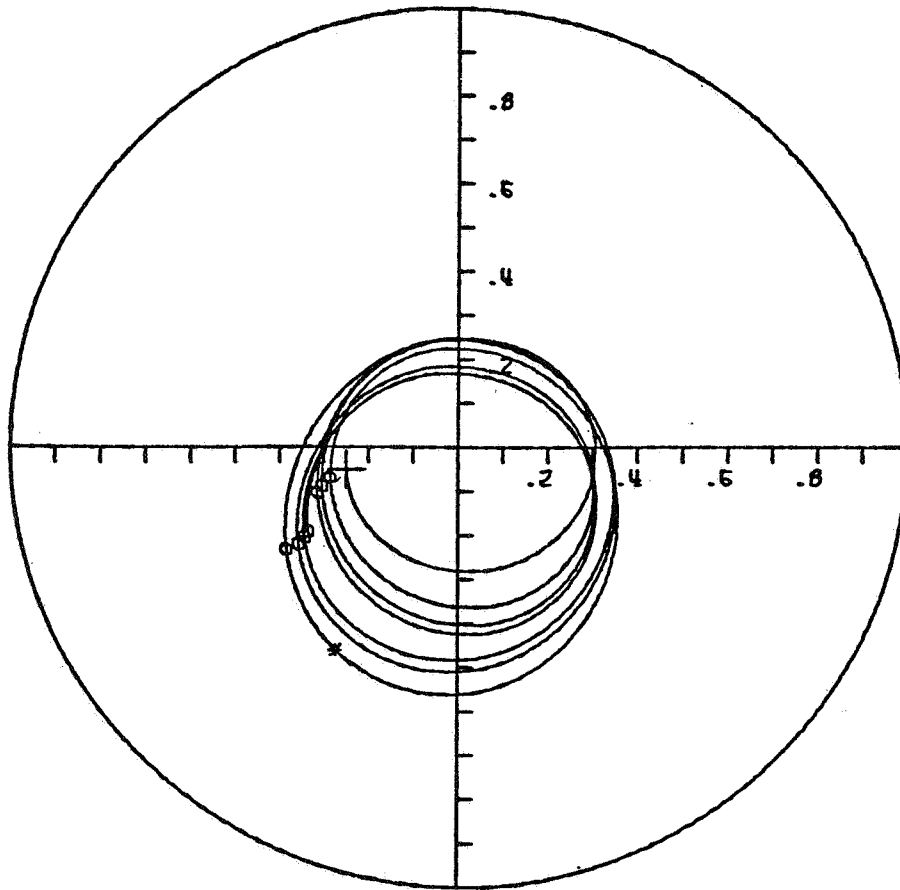


Figure 4-9. Unbalanced Rotor in Cavitated Squeeze Film Bearing - $L = 0.90$ IN - Unbalance Eccentricity = 0.001 IN. - Retainer Spring Stiffness, $KR = 123,000$ LB/IN.

acceptable. The resulting motion is shown in Figure (4-10) and a large amplitude limit cycle with large force transmission again occurs. However if the fluid film does not cavitate the bearing performance improves and is marginally acceptable as shown in Figure (4-11). The journal is orbiting at $\epsilon = 0.65$ and the transmitted force is only 5% less than the unbalance load.

Although this particular analysis includes only the journal weight and the unbalance loading, it shows the usefulness of this program in determining the bearing effects with different bearing parameters. The ability to perform the analysis without extensive preliminary experimental work provides a great savings in time and money. By systematically varying the bearing parameters design guidelines are established.

For instance Figures (4-12 - (4-15) shows the effect of varying the unbalance on a 675 lb. journal operating in a squeeze bearing with a 7 mil clearance. The unbalance eccentricity is increased from 1.75 to 3.5 mils with an accompanying increase in the journal amplitude and the force transmitted to the support structure. Although the exact unbalance may not be known precisely for a given rotor, a design estimate can be made based on the effect of a suddenly applied known unbalance due to blade loss or loss of chemical deposits from the blade surfaces. Prior to the sudden unbalance the rotor is assumed to be perfectly balanced. The ability of the bearing to reduce the amplitude to tolerable

SQUEEZE FILM BEARING
CAVITATED FILM

HORIZONTAL

	CASE NO.	32574C
W = 73.7 LBS	N = 16000 RPM	
L = .900 IN	R = 2.550 IN	
C = 4.00 MILS	MU = .382 MICROREYNS	
PS = 0.00 PSI	FMAX = 3641.9 LBS	
WX = 0.00 LBS	WY = 0.00 LBS	
FU = 1181.91 LBS	EMU = .50	
KRX = 123000 LB/IN	KRY = 123000 LB/IN	
TRO = 3.08	PMAX = 3334.52 PSI	

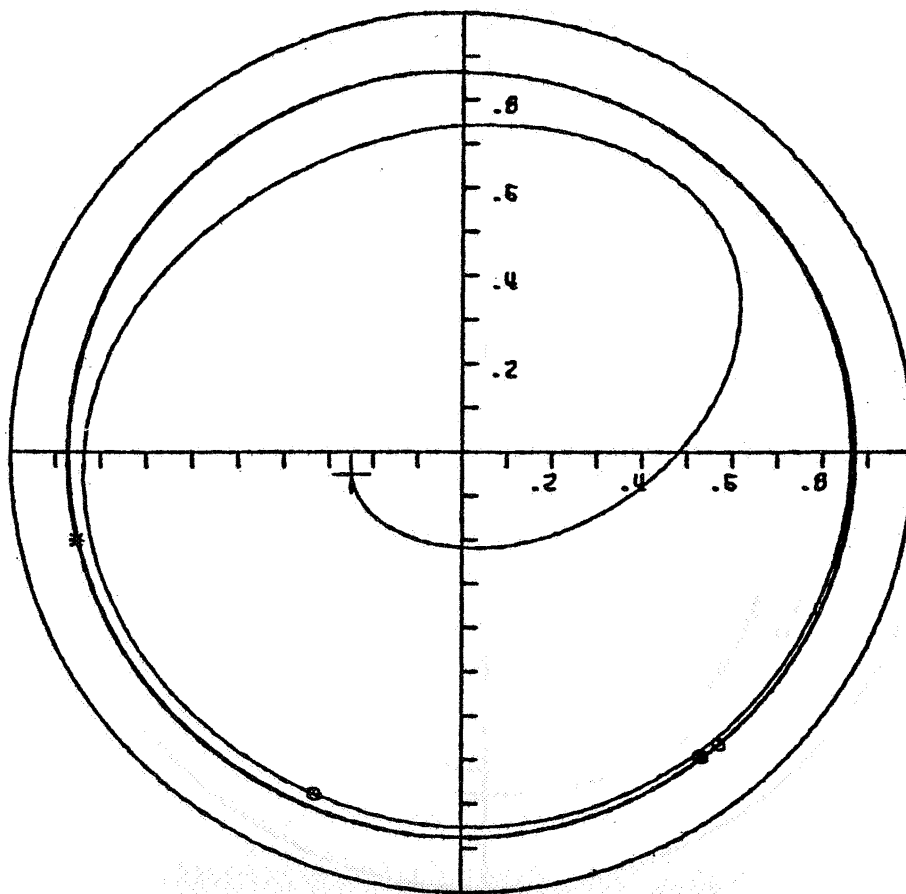


Figure 4-10. Unbalanced Rotor in Cavitated Squeeze Film Bearing - $L = 0.90$ IN. - Unbalance Eccentricity = 0.002 IN. - Retainer Spring Stiffness, $KR = 123,000$ LB/IN.

SQUEEZE FILM BEARING
UNCAVITATED FILM
HORIZONTAL

		CASE NO.	380745
W =	73.7 LBS	N =	16800 RPM
L =	.900 IN	R =	2.550 IN
C =	4.00 MILS	MU =	.382 MICROREYNS
PS =	4000.00 PSI	FMAX =	1123.5 LBS
WX =	0.00 LBS	WY =	0.00 LBS
FU =	1181.91 LBS	EMU =	.50
KRX =	123000 LB/IN	KRY =	123000 LB/IN
TRD =	.95	PMAX =	390.37 PSI

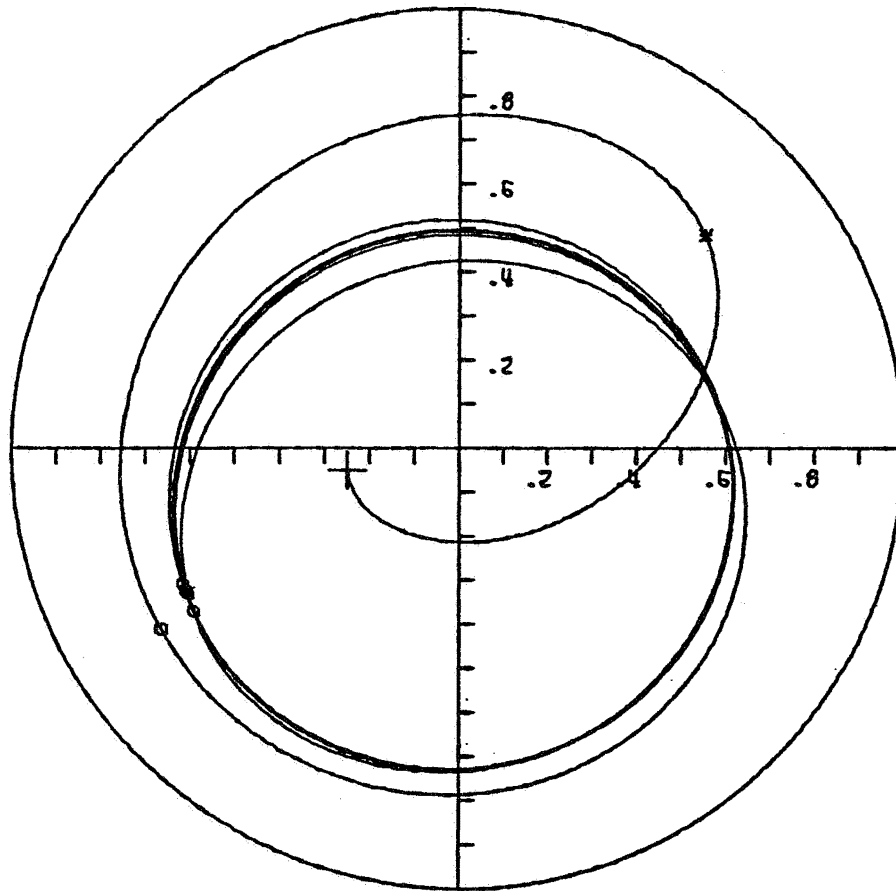


Figure 4-11. Unbalanced Rotor in Uncavitated Squeeze Film Bearing - $L = 0.90$ IN. - Unbalance Eccentricity = 0.002 IN. - Retainer Spring Stiffness, $KR = 123,000$ LB/IN.

SQUEEZE FILM BEARING
CAVITATED FILM
VERTICAL

		CASE NO.	330744
W =	675.0 LBS	N =	10500 RPM
L =	2.000 IN	R =	3.500 IN
C =	7.00 MILS	MU =	2.490 MICROREYNS
PS =	0.00 PSI	FMAX=	2725.1 LBS
WX =	0.00 LBS	WY =	0.00 LBS
FU =	3699.90 LBS	EMU =	.25
KRX =	50000 LB/IN	KRY =	50000 LB/IN
TRD =	.74	PMAX=	131.98 PSI

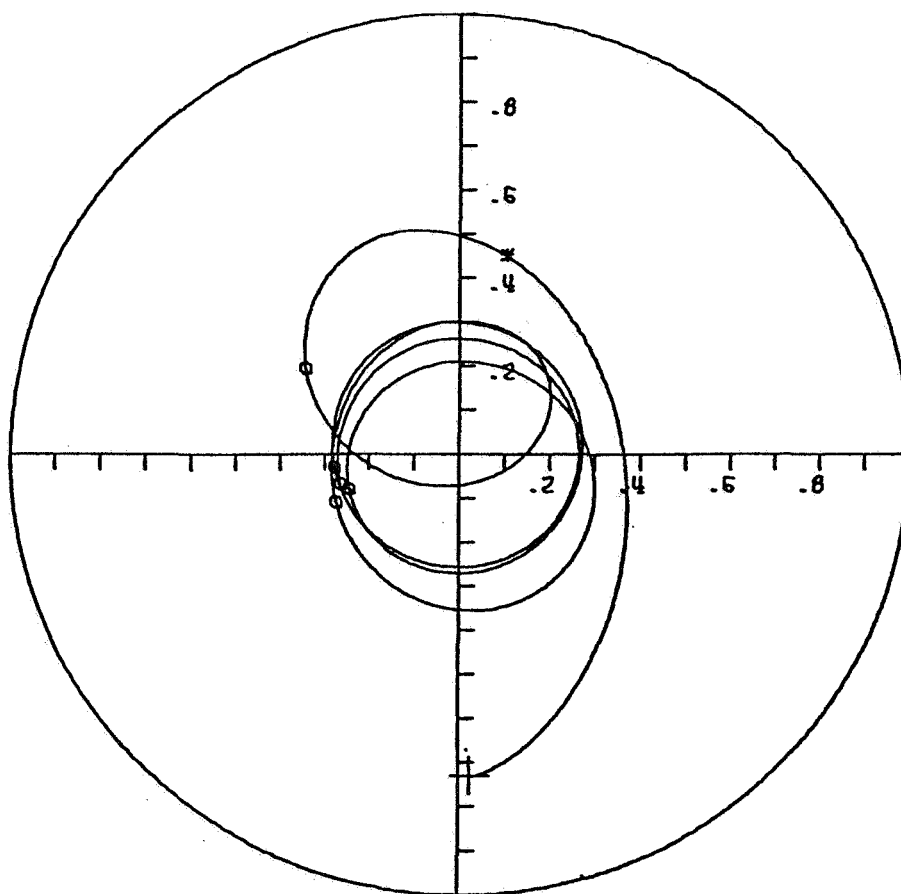


Figure 4-12. Vertical Unbalanced Rotor in Squeeze Film Bearing - Effect of Unbalance Magnitude - Unbalance Eccentricity = 1.75 Mils

SQUEEZE FILM BEARING
CAVITATED FILM
VERTICAL

		CASE NO.	390743
W =	675.0 LBS	N =	10500 RPM
L =	2.000 IN	R _y =	3.500 IN
C =	7.00 MILS	MU =	2.490 MICROREYNS
PS =	0.00 PSI	FMAX=	4368.2 LBS
WX =	0.00 LBS	WY =	0.00 LBS
FU =	4439.88 LBS	EMU =	.30
KRX =	50000 LB/IN	KRY =	50000 LB/IN
TRD =	98	PMAX=	181.61 PSI

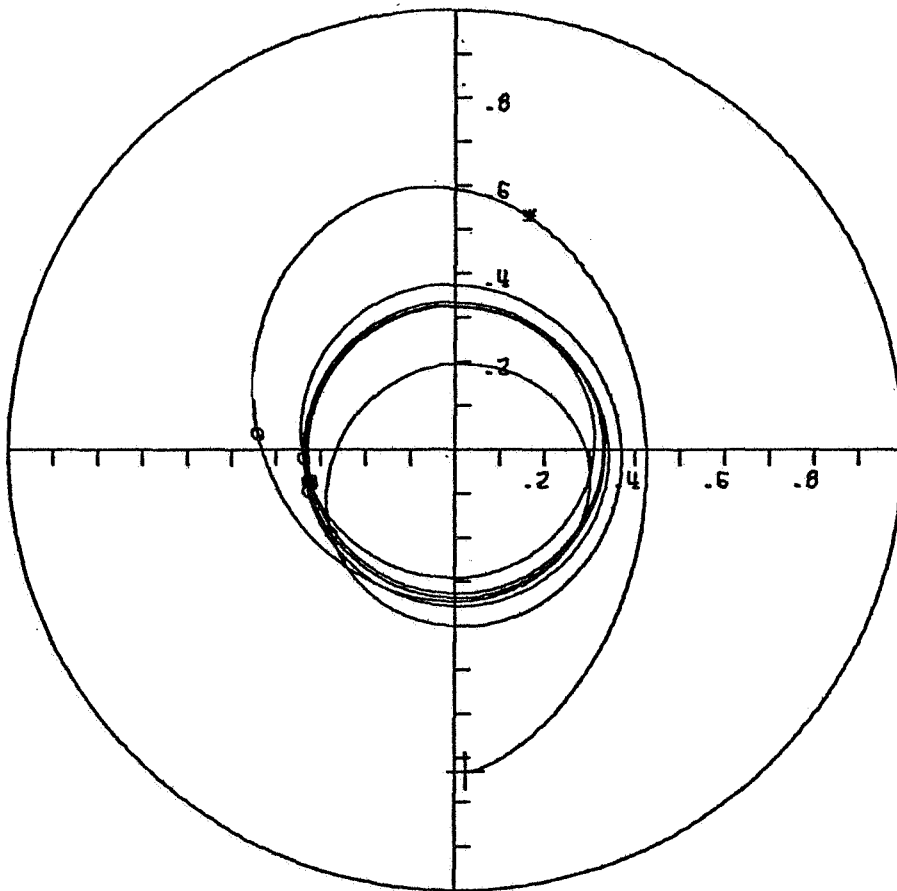


Figure 4-13. Vertical Unbalanced Rotor in Squeeze Film Bearing - Effect of Unbalance Magnitude - Unbalance Eccentricity = 2.10 Mils.

SQUEEZE FILM BEARING
 CAVITATED FILM

VERTICAL

CASE NO. 330702

W =	675.0 LBS	N =	10500 RPM
L =	2.000 IN	R =	3.500 IN
C =	7.00 MILS	MU =	2.490 MICROREYNS
PS =	0.00 PSI	FMAX=	6287.7 LBS
WX =	0.00 LBS	WY =	0.00 LBS
FU =	5179.86 LBS	EMU =	.35
KRX =	50000 LB/IN	KRY =	50000 LB/IN
TRD =	1.21	PMAX=	270.45 PSI

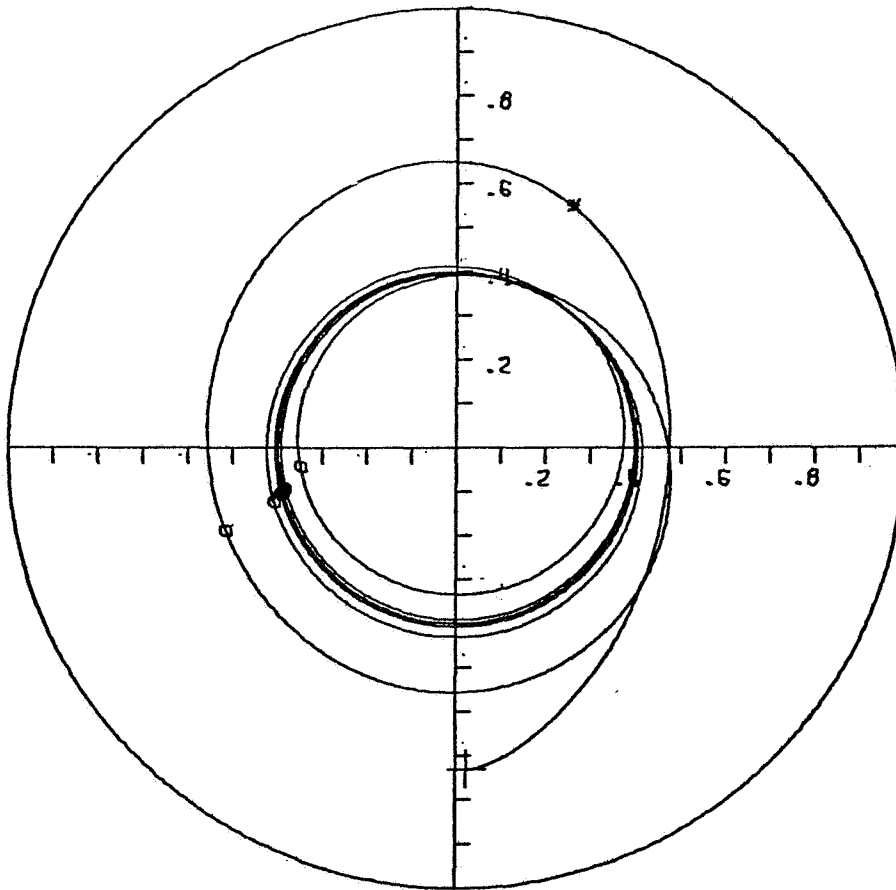


Figure 4-14. Vertical Unbalanced Rotor in Squeeze Film Bearing - Effect of Unbalance Magnitude - Unbalance Eccentricity = 2.45 Mils.

SQUEEZE FILM BEARING
CAVITATED FILM

HORIZONTAL

CASE NO.

3257411

W =	675.0 LBS	N =	10500 RPM
L =	2.000 IN	R =	3.500 IN
C =	7.00 MILS	MU =	2.490 MICROREYNS
PS =	0.00 PSI	FMAX =	15891.4 LBS
WX =	0.00 LBS	WY =	0.00 LBS
FU =	7399.81 LBS	EMU =	.50
KRX =	50000 LB/IN	KRY =	50000 LB/IN
TRD =	2.15	PMAX =	4699.92 PSI

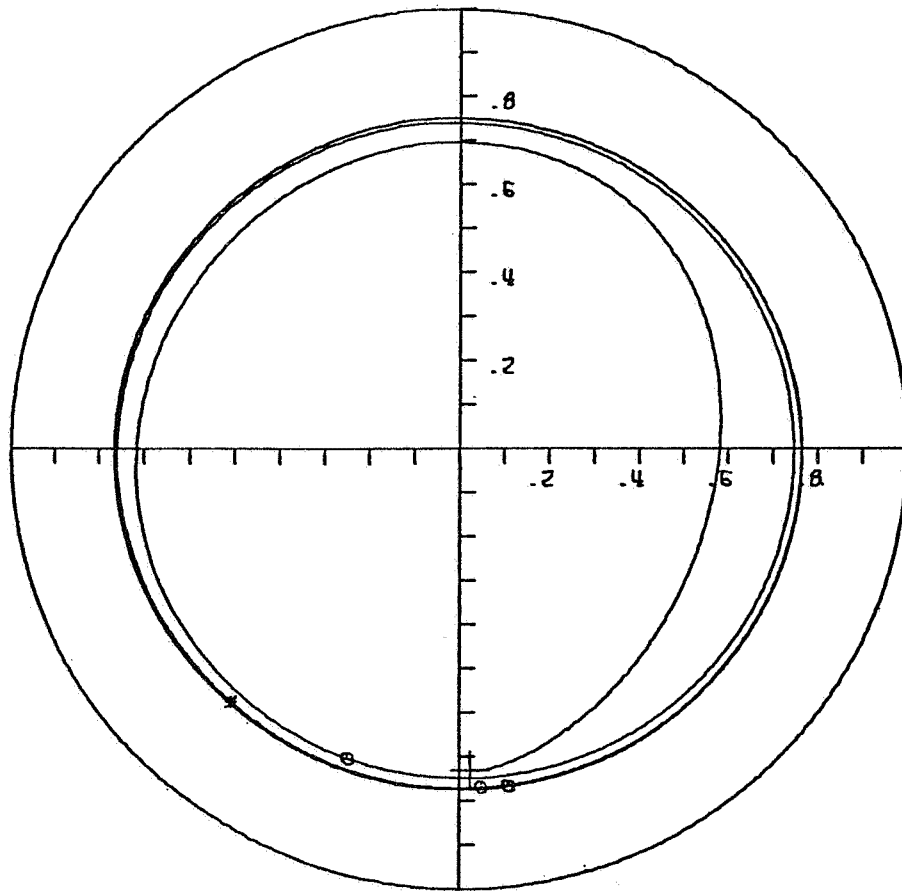


Figure 4-15. Vertical Unbalanced Rotor in Squeeze Film Bearing - Effect of Unbalance Magnitude - Unbalance Eccentricity = 3.50 Mils.

levels until the machine is shut down or its operating conditions changed can be determined. Note the shift in phase angle from 180° to 90° as the eccentricity increases.

It has been shown that retainer springs help center the journal and reduce the vibration amplitude. They may also be used to prevent oil leakage from the end of the bearing if they are of the O ring type. As noted in Chapter 2, the uncavitated film provides no equivalent stiffness when the journal is operating in synchronous precession about the bearing center. In this case the use of a retainer spring to provide a restoring force in the bearing is necessary. Although an increase in stiffness results in centering the journal in the bearing, (see Figures (4-16) (4-19) the magnitude of the transmitted force is minimized for some intermediate value of stiffness which depends on the bearing parameters and loading. Also the ability of the journal to quickly return to a stable, steady state operating condition is impaired with increasing stiffness. Both of these operating conditions were indicated by the stability maps in Chapter 3.

After the preliminary bearing design, a more thorough analytic study may be made by incorporating the damper bearing effects into a program which includes the dynamic effects of the entire system. Although such programs are not readily available for many complex systems, one has been developed for a three mass rotor in journal bearings on a squeeze film bearing support as noted earlier. The rotor bearing model is shown in Figure (3-1). This program may be used to calculate the ability of squeeze

SQUEEZE FILM BEARING
 CAVITATED FILM
 HORIZONTAL

CASE NO. 9257402

W =	675.0 LBS	N =	10500 RPM
L =	2.000 IN	R =	3.500 IN
C =	15.00 MILS	MU =	2.490 MICROREYNS
PS =	0.00 PSI	FMAX =	1867.2 LBS
WX =	0.00 LBS	WY =	0.00 LBS
FU =	951.40 LBS	EMU =	.03
KRX =	0 LB/IN	KRY =	0 LB/IN
TRD =	1.96	PMAX =	381.39 PSI

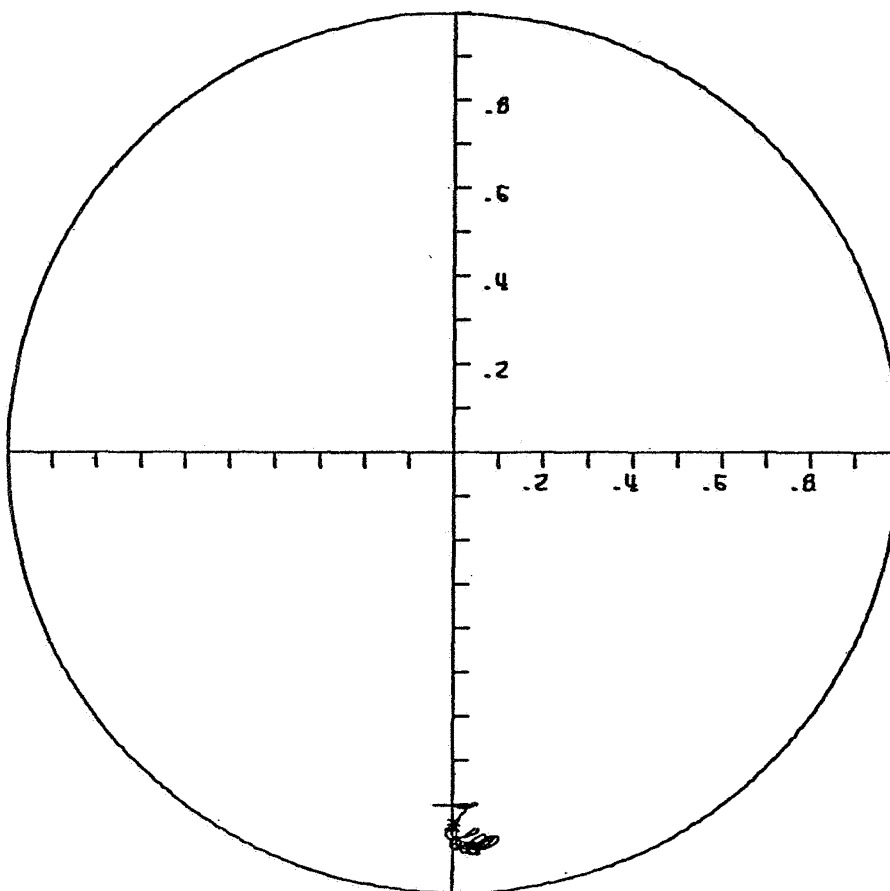


Figure 4-16. Horizontal Unbalanced Rotor in Squeeze Film Bearing - Effect of Retainer Springs - Retainer Spring Stiffness, KR = 0 LB/IN.

SQUEEZE FILM BEARING
CAVITATED FILM
HORIZONTAL

		CASE NO.	3257413
W	= 675.0 LBS	N	= 10500 RPM
L	= 2.000 IN	R	= 3.500 IN
C	= 15.00 MILS	MU	= 2.490 MICROREYNS
PS	= 0.00 PSI	FMAX	= 1054.1 LBS
WX	= 0.00 LBS	WY	= 0.00 LBS
FU	= 951.40 LBS	EMU	= .03
KRX	= 50000 LB/IN	KRY	= 50000 LB/IN
TRD	= 1.11	PMAX	= 99.41 PSI

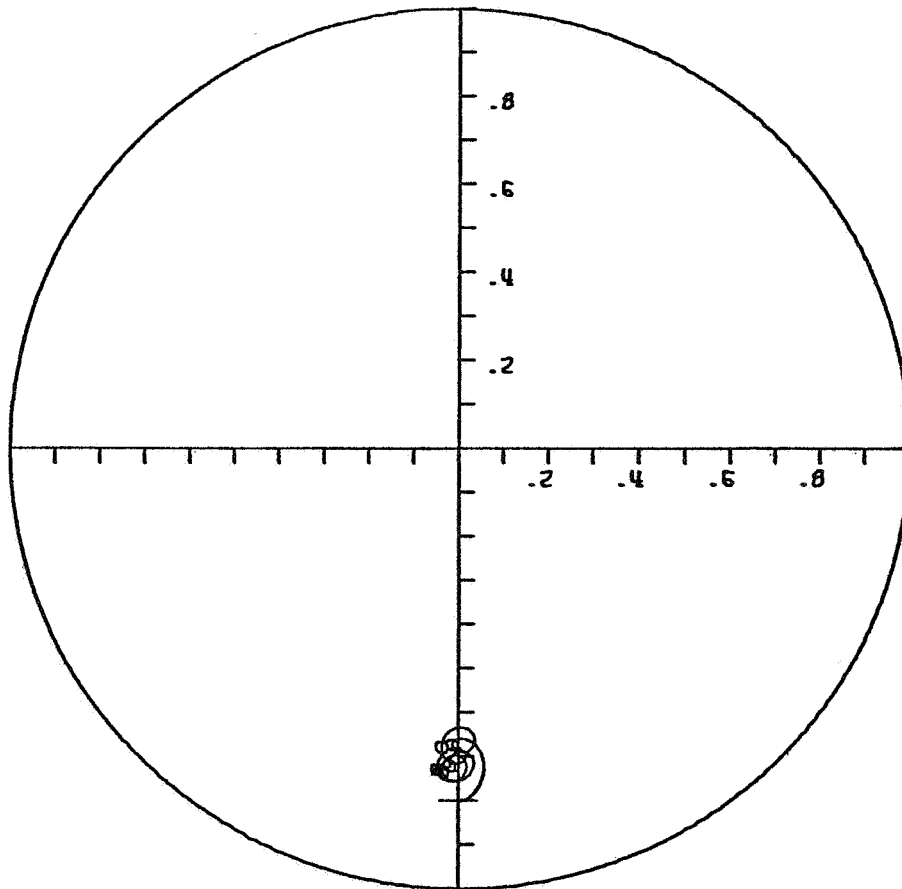


Figure 4-17. Horizontal Unbalanced Rotor in Squeeze Film Bearing - Effect of Retainer Springs - Retainer Spring Stiffness, $KR = 50,000$ LB/IN.

SQUEEZE FILM BEARING
CAVITATED FILM

HORIZONTAL

CASE NO.

3807A1

W =	675.0 LBS	N =	10500 RPM
L =	2.000 IN	R =	3.500 IN
C =	15.00 MILS	MU =	2.490 MICROREYNS
PS =	0.00 PSI	FMAX =	936.7 LBS
WX =	0.00 LBS	WY =	0.00 LBS
FU =	951.40 LBS	EMU =	.03
KRX =	100000 LB/IN	KRY =	100000 LB/IN
TRD =	.98	PMAX =	6.10 PSI

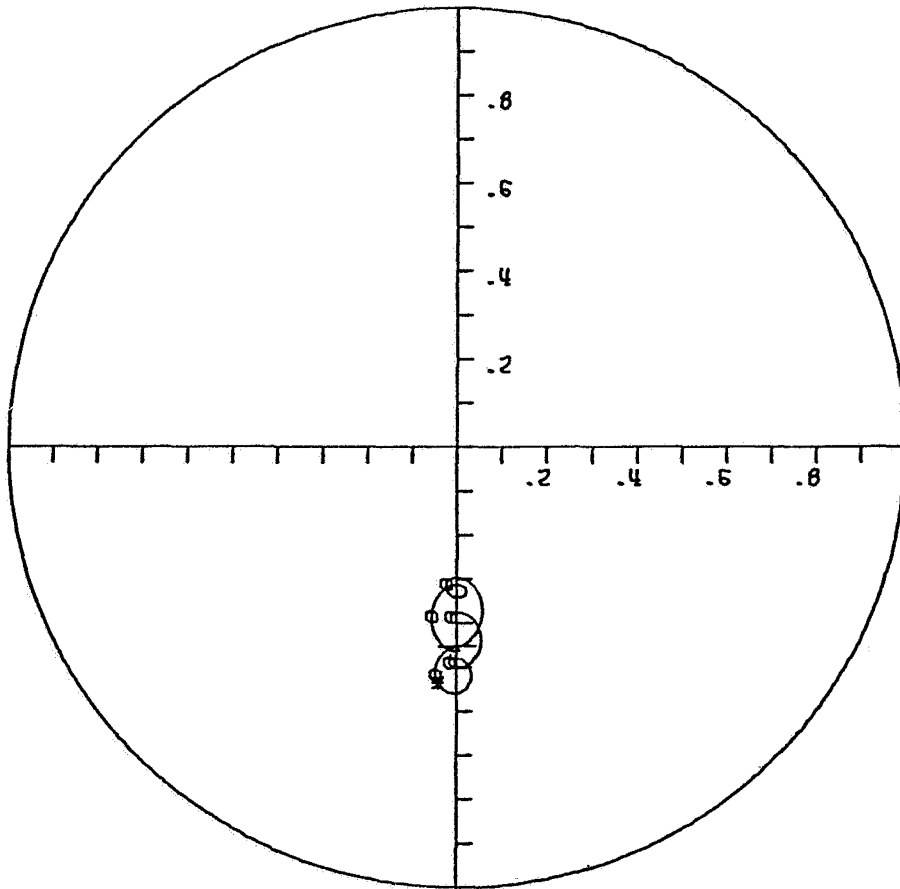


Figure 4-18. Horizontal Unbalanced Rotor in Squeeze Film Bearing - Effect of Retainer Springs - Retainer Spring Stiffness, $KR = 100,000$ LB/IN.

SQUEEZE FILM BEARING
 CAVITATED FILM
 HORIZONTAL

CASE NO. 32574115

W =	675.0 LBS	N =	10500 RPM
L =	2.000 IN	R =	3.500 IN
C =	15.00 MILS	MU =	2.490 MICROREYNS
PS =	0.00 PSI	FMAX=	1029.3 LBS
WX =	0.00 LBS	WY =	0.00 LBS
FU =	951.40 LBS	EMU =	.03
KRX =	200000 LB/IN	KRY =	200000 LB/IN
TRD =	1.08	PMAX=	9.18 PSI

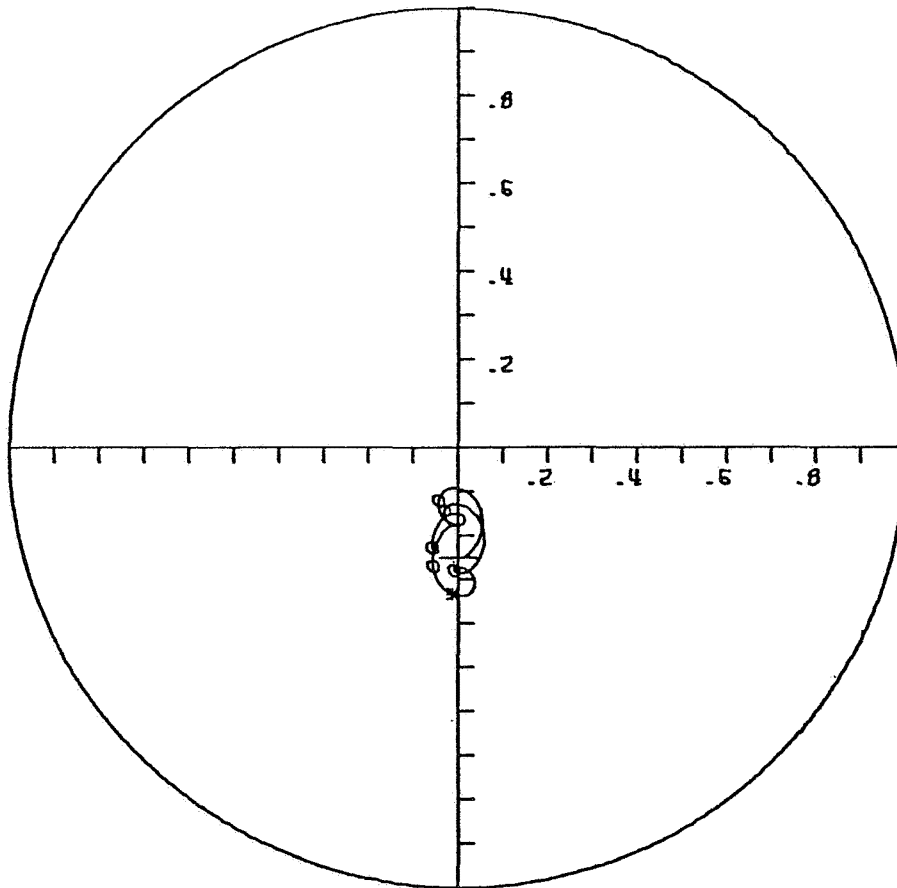


Figure 4-19. Horizontal Unbalanced Rotor in Squeeze Film Bearing - Effect of Retainer Springs - Retainer Spring Stiffness, KR = 200,000 LB/IN.

film bearings to stabilize a multi-mass rotor. In addition, information may be obtained to verify the stability maps obtained by other means (see Chapter 3). Because the bearing is initially designed using the criteria derived from a stability analysis such verification is useful in judging the overall worth and limitations of the analytical design process. Using these analytical methods leads to a more efficient testing program because unacceptable bearing designs are eliminated before testing begins.

CHAPTER 5

CONCLUSIONS AND RECOMMENDATIONS

The problem of rotor stability is of current importance because of the high speeds and complex dynamics of modern rotor bearing systems. Damped flexible supports have a great effect on the ability of a system to suppress unstable whirl. Therefore there is a need for methods of predicting rotor instability and obtaining bearing designs that provide the necessary support characteristics.

5.1 PREDICTING ROTOR INSTABILITY

Methods for determining the stability of rotor bearing systems include:

1. Using the rotor-bearing system equations of motion including the effects of aerodynamic forces, shaft damping and internal friction to obtain the system characteristic equation. The roots of this equation show the stability and natural frequencies of the system.
2. Using finite element and transfer matrix methods to obtain the system stability and natural frequencies.
3. Applying Routh stability criterion to the system characteristic equation.

The third method does not yield information on relative stability but only determines whether or not the system is absolutely

stable. The first two methods provide relative stability information that can be used to plot stability contours as functions of the support characteristics. The stability maps presented show that for a given value of support stiffness there is a range of damping values which will stabilize the system. If the support stiffness becomes too large, the system will be unstable for all values of support damping. The optimum stiffness and damping values for a particular system depend upon the rotor-bearing properties and the nature and magnitude of the forces acting on the system that produce instability.

5.2 DETERMINING THE STIFFNESS AND DAMPING COEFFICIENTS OF THE SQUEEZE FILM DAMPER BEARING

The assumption of steady state circular synchronous precession of the journal and the use of a rotating coordinate system allow the bearing forces to be equated to equivalent stiffness and damping forces. This establishes stiffness and damping coefficients for the bearing. These coefficients are functions of the bearing geometry, the use of end seals and cavitation of the fluid film. The coefficients obtained from the steady state bearing analysis are compared with the values from the stability maps to determine a bearing configuration that promotes system stability.

The stiffness and damping coefficients are non-linear functions of the journal eccentricity. However for $\epsilon < 0.4$ the coefficients do not change appreciably with changes in eccentricity.

For values of $\epsilon > 0.4$ a rapid increase in the coefficients occurs. The high stiffness developed can cause system instability or raise the system critical speed above the operating speed resulting in force transmissibilities greater than 1. For these reasons a design criteria of $\epsilon < 0.4$ has been established. If the fluid film does not cavitate a radial stiffness is not developed and must be supplied by retainer springs.

5.3 TRANSIENT ANALYSIS

The bearings designed using steady state analysis are further analyzed using transient response programs. The motion of a system under the influence of unbalance and other external forces is monitored. Effect of retainer springs to preload the bearing can be determined and the bearing design further refined.

The accuracy of transient response programs are dependent on the accuracy of the numerical integration methods employed. At high eccentricities very small integration step sizes are required to retain high accuracy in the solution because of the rapid variation in the bearing forces. The cost of obtaining high accuracy at high eccentricity does not justify using small time steps or complicated integration methods requiring many functional evaluations because optimum bearing design requires operation at low eccentricities. The information provided by simpler integration methods is sufficient to indicate trends in bearing operation at high eccentricities.

5.4 ADVANTAGES OF BEARING SIMULATION

The analytic simulation of the squeeze film damper bearing eliminates many bearing designs that would result in bearing or machine failure in a test installation. Because the cost of constructing and instrumenting a test rig is very high, preventing the failure of these machines is important. The time involved in manufacturing and testing bearings is also great and the elimination of unsuitable designs by analytic procedures results in a substantial savings in time and money.

A good test program is essential, however, to determine the actual rotor-bearing response under various conditions. The analytic simulation provides a means of interpreting the test data. Often the nature of the actual system excitation is unknown and the actual system response must be used to infer the nature of these excitations. Where it is possible to systematically vary the excitation the experimental results provide a check on the accuracy and limitations of the analytic simulation.

5.5 LIMITATIONS OF ANALYTICAL INVESTIGATIONS

In any analytical investigation it is very important to know the assumptions made in analyzing the problem. In deriving the bearing equations for this study several assumptions were made. To obtain the Reynolds equation from the Navier-Stokes equations it was assumed that:

1. The viscosity is constant
2. The flow is steady state
3. The fluid inertia terms are negligibly small

4. The density is constant
5. There is no flow in the radial direction
6. There is no pressure gradient in the radial direction

The Reynolds equation obtained was modified by using the short bearing approximation. The assumption made was that the pressure gradient in the tangential direction is small and when multiplied by h^3 it is very small in comparison to other terms containing only h . This assumption is valid only if the tangential pressure gradient is small, and at high eccentricity ratios this assumption may not be valid. For this reason the design criterion is that the eccentricity ratio be less than 0.4. In addition the short bearing approximation is valid for $\frac{L}{D} < 0.5$. For ratios greater than this the axial pressure gradient is not large compared to the tangential gradient. For $\frac{L}{D} > 0.5$ either the long bearing approximation or finite bearing techniques should be used.

The conditions under which cavitation occurs must be modified in light of the current experimental results. In this study cavitation conditions were assumed to be the same in squeeze bearings as in journal bearings.

5.6 RECOMMENDATIONS FOR FUTURE RESEARCH

1. Construct an experimental rotor with squeeze damper supports to provide data to verify the analytic squeeze bearing model.
2. Conduct analytic and experimental research into the conditions under which the squeeze bearing fluid film cavitates

and to determine how cavitation propagates through the film.

3. Investigate the heat transfer characteristics of the bearings and provide modifications to the bearing programs to account for variable viscosity of the lubricant.

BIBLIOGRAPHY

1. Kirk, R. G. and E. J. Gunter, "Transient Journal Bearing Analysis", NASA CR-1549, 1970.
2. Apfel, R. E., "The Tensile Strength of Liquids", Scientific American, December, 1972, p. 58.
3. White, D. C. "Squeeze Film Journal Bearings", Ph.D. Dissertation, Cambridge University, 1970.
4. Booker, J. F., "A Table of the Journal Bearing Integral", ASME, Jour. of Basic Engineering, June, 1965, p. 533.
5. Jeffcott, H. H., "The Lateral Vibrations of Loaded Shafts in the Neighborhood of a Whirling Speed — the Effect of Want of Balance", Phil. Mag. Series 6, Vol. 37, 1919, p. 304.
6. Newkirk, B.L., "Shaft Whipping", Gen. Elec. Rev., Vol 27, 1924, p. 169.
7. Kimball, A.L., "Internal Friction as a Cause of Shaft Whirling", Phil. Mag., Vol. 49, 1925, pp 724-727.
8. Newkirk, B.L. and H. D. Taylor, "Shaft Whipping Due to Oil Action in Journal Bearing", Gen. Elec. Rev., Vol. 28, 1925, pp. 559-568.
9. Robertson, D., "Whirling of a Journal in a Sleeve Bearing", Phil. Mag., Series 7, Vol. 15, 1933, pp. 113-130.
10. Poritsky, H., "Contribution to the Theory of Oil Whip", Trans. ASME, August 1953, pp. 1153-1161.
11. Pinkus, O., and B. Sternlicht, Theory of Hydrodynamic Lubrication, McGraw Hill, New York, 1961.
12. Alford, J. S., "Protecting Turbomachinery From Self-Excited Rotor Whirl", ASME Jour. of Engr. for Power, Vol. 87, October 1965, pp. 333-344.
13. Kirk, R. G. and E. J. Gunter, "The Influence of Damper Supports on the Dynamic Response of a Single Mass Flexible Rotor- Part I, Linear Systems", RLES, No. ME-4040-105-71U, March 1971, University of Virginia for NASA Lewis Research Center.
14. Gunter, E. J., "Dynamic Stability of Rotor-Bearing Systems", NASA SP-113, 1966.

15. Choudhury, P.De, "Dynamic Stability of Flexible Rotor-Bearing Systems", Ph.D. Dissertation, University of Virginia, June, 1971.
16. Kirk, R. G. and E. J. Gunter, "SDSTB", Computer program, University of Virginia.
17. Ruhl, R. L., "Dynamics of Distributed Parameter Rotor Systems: Transfer Matrix and Finite Element Techniques", Ph.D. Dissertation, Cornell University, 1970.
18. Bansal, P.N., "Application of Transfer Matrix Method for the Stability Analysis of Multi-Mass Flexible Rotors", University of Virginia.
19. Barrett, L. E. and E. J. Gunter, "BRGTRAN", Computer program University of Virginia.
20. Mohan, S. and E. Hahn, "Squeeze Film Bearing Simulation and Design Considerations", RLES REport No. ME-4040-107-720, University of Virginia, June 1972.
21. Kirk, R. G. and E. J. Gunter "TMASSNL", Computer Program, University of Virginia.

APPENDIX A

DESCRIPTION OF PROGRAM SQFDAMP

This program analyzes the stiffness, damping and pressure characteristics of the squeeze film damper bearing. Three bearing configurations may be analyzed:

1. Plain bearing without end seals or circumferential oil supply groove.
2. Bearing without end seals but with circumferential oil supply groove.
3. Bearing with both end seals and circumferential oil supply groove.

In addition the fluid film may be assumed to be cavitated or uncavitated. If cavitated the film extends from $\theta = \frac{\pi}{2}$ to $\theta = \frac{3\pi}{2}$. If uncavitated it extends from $\theta = 0$ to $\theta = 2\pi$. The θ is measured from the line of centers of the bearing in the direction of journal precession. The evaluation of the bearing characteristics assumes that the journal precesses synchronously about the bearing center in a circular orbit.

The following is a description of the program input data:

CARD 1 -80 column free-field comment card.

CARD 2 -80 column free-field comment card.

CARD 3 -Namelist/BRGTYPE/ TYP, CAV, PS

TYP - 0 for bearing type 1 (see above)

- 1 for bearing type 2 (see above)

- 2 for bearing type 3 (see above)

CAV - 0 for uncavitated film

- 1 for cavitated film

PS - oil supply pressure, psi.

CARD 4 Namelist/BEARING/ L,R, MU, N

L - Bearing length, in.

R - Bearing radius, in.

MU - Lubricant viscosity, microreyns

N - Rotor speed (journal precession rate), RPM

CARD 5 Namelist/ECRATIO/ES,EF

ES - initial journal eccentricity ratio ES>0

EF - final journal eccentricity ratio EF<1

CARD 6 Namelist/CLEARNC/ C(I), NC

C(I) - clearance

NC - Number of clearance values

CARD 7 Namelist/PLOTSEM/ CS, PC, PK, PP

CS - Plot control, .T. if plot desired, otherwise .F.

PC - .T. if damping plot desired, otherwise .F.

PK - .T. if stiffness plot desired, otherwise .F.
(if CAV=0, PK = .F.)

PP - .T. if pressure plot desired, otherwise .F.

Sample input data.

CARD	DATA
1	SAMPLE DATA FOR SQFDAMP
2	1 MARCH 1973
3	\$BRGTYP TYP = 0 , CAV = 1, PS = 0.0\$
4	\$BEARING L = 0.90, R = 2.55, MU = 0.382, N = 16800.0\$
5	\$ECRATIO ES = 0.1, EF = 0.9\$

```
6          $CLEARANC C(1) = .003, C(2) = .004, C(3) = .005  
          C(4) = .006, NC = 4$  
7          $PLOTSEM CS = .T., PC = .T., PK = .T., PP = .T.$
```

The following is a listing of the program and a sample output.

	PROGRAM SQFDAMP(INPUT,OUTPUT,TAPE5=INPUT,TAPE6=OUTPUT,TAPE1)	SQFD0100
C		SQFD0110
C	VERSION - 13 MARCH 1973	SQFD0120
C		SQFD0130
	REAL L,MU,KO,N	SQFD0140
	LOGICAL CRING,CS,PC,PK,PF	SQFD0150
	INTEGER COMENT1,COMENT2,JYP	SQFD0160
	INTEGER CAV	SQFD0170
	DIMENSION EO(135),CO(135),KO(135),PMAX(135),THETAM(135),C(5),	SQFD0180
	1COMENT1(8),CCMENT2(8)	SQFD0190
	NAMELIST/BRGTYPE/ JYP,CAV,FS	SQFD0200
	NAMELIST/BEARING/ L,R,MU,N	SQFD0210
	NAMELIST/EQRATIO/ ES,EF	SQFD0220
	NAMELIST/CLEARNC/ C,NC	SQFD0230
	NAMELIST/PLOTSEM/ CS,PC,PK,PP	SQFD0240
	COMMON NEO	SQFD0250
C		SQFD0260
C	READ DATA	SQFD0270
C		SQFD0280
	K=1	SQFD0290
900	READ(5,1) COMENT1	SQFD0300
1	FORMAT(8A10)	SQFD0310
	IF(EOF,5) 9999,2	SQFD0320
2	READ(5,1) COMENT2	SQFD0330
	READ(5,BRGTYPE)	SQFD0340
	READ(5,BEARING)	SQFD0350
	READ(5,EQRATIO)	SQFD0360
	READ(5,CLEARNC)	SQFD0370
	READ(5,PLOTSEM)	SQFD0380
	IF(.NOT. CS) GOTO 3	SQFD0390
	IF(K.EQ.0) GOTO 3	SQFD0400
	CALL CALCOMP(1)	SQFD0410
C		SQFD0420
C	SET UP NEW BLOCK AND MOVE ORIGIN	SQFD0430
	CALL PLOT(2.0,0.5,-3)	SQFD0440
C		SQFD0450
C	WRITE PROGRAM DESCRIPTION	SQFD0460
C		SQFD0470
3	WRITE(6,4)	SQFD0480
4	FORMAT(1H1,35X,27H***SQUEEZE FILM DAMPER***)	SQFD0490
	WRITE(6,5)	SQFD0500
5	FORMAT(1X,	SQFD0510
	158H THIS PROGRAM ANALYZES THE STIFFNESS, DAMPING AND PRESSURE /1X, SQFD0520	
	258H CHARACTERISTICS OF THE SQUEEZE FILM DAMPER BEARING. THREE /1X, SQFD0530	
	358H BEARING CONFIGURATIONS MAY BE ANALYZED- /1X, SQFD0540	
	458H 0 - PLAIN BEARING WITHOUT END LEAKAGE SEALS OR CIRCUM- /1X, SQFD0550	
	558H FERENTIAL OIL SUPPLY GROOVE /1X, SQFD0560	
	658H 1 - BEARING WITHOUT END LEAKAGE SEALS BUT WITH CIRCUM- /1X, SQFD0570	
	758H FERENTIAL OIL SUPPLY GROOVE /1X, SQFD0580	
	858H 2 - BEARING WITH BOTH END LEAKAGE SEALS AND CIRCUMFER- /1X, SQFD0590	
	958H ENTIAL OIL SUPPLY GROOVE /1X, SQFD0600	
	158H IN ADDITION, THE FILM MAY BE ASSUMED TO BE EITHER CAVI- /1X, SQFD0610	
	258H TATED OR UNCAVITATED. IF CAVITATED THE FILM IS ASSUMED /1X, SQFD0620	
	358H TO EXTEND FROM THETA=PI/2 TO THETA=3PI/2, WHERE THETA /1X, SQFD0630	
	458H IS MEASURED FROM THE LINE OF CENTERS IN THE DIRECTION OF /1X, SQFD0640	
	558H JOURNAL PRECESSION. THE EVALUATION OF THE BEARING CHARAC- /1X, SQFD0650	
	658H TERISTICS ASSUMES THAT THE JOURNAL PRECEDES SYNCHRONOUS- /1X, SQFD0660	

	758HLY ABOUT THE BEARING CENTER.	/1X,	SQFD0670
	858H THE FOLLOWING IS A DESCRIPTION OF THE INPUT PARAMETERS-	/1)	SQFD0680
	WRITE(6,6)		SQFD0690
6	FORMAT(1X,		SQFD0700
	158H CARD 1. -80 COLUMN FREE-FIELD COMMENT CARD	/1X,	SQFD0710
	258H CARD 2. -80 COLUMN FREE-FIELD COMMENT CARD	/1X,	SQFD0720
	358H CARD 3. -NAMELIST/BRGTYPE/ TYP,CAV,PS	/1X,	SQFD0730
	458H TYP - 0 FOR BEARING TYPE 0 (SEE ABOVE)	/1X,	SQFD0740
	558H 1 FOR BEARING TYPE 1 (SEE ABOVE)	/1X,	SQFD0750
	658H 2 FOR BEARING TYPE 2 (SEE ABOVE))	SQFD0760
	WRITE(6,8)		SQFD0770
8	FORMAT(1X,		SQFD0780
	158H CAV - 0 FOR UNCAVITATED FILM	/1X,	SQFD0790
	258H 1 FOR CAVITATED FILM	/1X,	SQFD0800
	358H IF CAV=0 PK=.F. (SEE CARD 7)	/1X,	SQFD0810
	458H PS - OIL SUPPLY PRESSURE, PSI	/1X,	SQFD0820
	758H CARD 4. -NAMELIST/BEARING/ L,R,MU,N	/1X,	SQFD0830
	858H L - BEARING LENGTH, IN.	/1X,	SQFD0840
	958H R - BEARING RADIUS, IN.	/1X,	SQFD0850
	158H MU - LUBRICANT VISCOSITY, MICROREYNS	/1X,	SQFD0860
	258H N - ROTOR SPEED (JOURNAL PRECESSION RATE,RPM)	/1X,	SQFD0870
	358H CARD 5. -NAMELIST/ECRATIO/ ES,EF	/1X,	SQFD0880
	458H ES - INITIAL JOURNAL ECCENTRICITY RATIO, ES>0.	/1X,	SQFD0890
	558H EF - FINAL JOURNAL ECCENTRICITY RATIO, EF<1.0	/1X,	SQFD0900
	658H CARD 6. -NAMELIST/CLEARNC/ C(I),NC	/1X,	SQFD0910
	758H C(I) - CLEARANCE VALUES, IN. 0<I<=5	/1X,	SQFD0920
	858H NC - NUMBER OF CLEARANCE VALUES)	SQFD0930
	WRITE(6,7)		SQFD0940
7	FORMAT(1X,		SQFD0950
	158H CARD 7. -NAMELIST/FLOTSEM/ CS,PC,PK,PP	/1X,	SQFD0960
	258H CS - PLOT CONTROL, .T. IF PLOT DESIRED,	/1X,	SQFD0970
	358H OTHERWISE .F.	/1X,	SQFD0980
	458H PC - .T. IF DAMP FLOT DESIRED, OTHERWISE .F.	/1X,	SQFD0990
	558H PK - .T. IF STIFF. FLOT DESIRED, OTHERWISE .F.	/1X,	SQFD1000
	658H PP - .T. IF PRESS PLOT DESIRED, OTHERWISE .F.	/1X,	SQFD1010
	758H SAMPLE DATA	/1X,	SQFD1020
	858H COMMENT CARD 1	/1X,	SQFD1030
	958H COMMENT CARD 2	/1X,	SQFD1040
	158H \$BRGTYPE TYP=0,CAV=1,PS=0.0\$	/1X,	SQFD1050
	258H \$BEARING L=0.90,R=2.55,MU=0.382,N=16800\$	/1X,	SQFD1060
	358H \$ECRATIO ES=0.1,EF=0.9\$	/1X,	SQFD1070
	458H \$CLEARNC C(1)=.003,C(2)=.004,C(3)=.005,C(4)=.006,NC=4\$	/1X,	SQFD1080
	558H \$PLOTSEM CS=.T.,PC=.T.,PK=.T.,PP=.T.\$)	SQFD1090
C			SQFD1100
C	WRITE OUT INPUT DATA		SQFD1110
C			SQFD1120
	WRITE(6,25) COMMENT1,COMMENT2		SQFD1130
25	FORMAT(1H1,1X,2(8A10/1X))		SQFD1140
	IF(TYP.EQ.0) WRITE(6,27)		SQFD1150
	IF(TYP.EQ.1) WRITE(6,28)		SQFD1160
	IF(TYP.EQ.2) WRITE(6,29)		SQFD1170
	IF(CAV.EQ.0) WRITE(6,31)		SQFD1180
	IF(CAV.EQ.1) WRITE(6,32)		SQFD1190
27	FORMAT(/1X,		SQFD1200
	158H PLAIN BEARING, NO END SEALS OR OIL SUPPLY GROOVE	/1)	SQFD1210
28	FORMAT(/1X,		SQFD1220
	158H BEARING WITH NO END SEALS BUT WITH OIL SUPPLY GROOVE	/1)	SQFD1230
29	FORMAT(/1X,		SQFD1240

	158HBEARING WITH ENC SEALS AND OIL SUPPLY GROOVE	SQFD1250
31	FORMAT(1X,16HUNCAVITATED FILM/)	SQFD1260
32	FORMAT(1X,14HCAVITATED FILM/)	SQFD1270
	WRITE(6,10) L,R,N,PL,PS,ES,EF,NC	SQFD1280
10	FORMAT(////1X,15HBEARING LENGTH=,F8.2,	SQFD1290
	120H INCHES BEARING RADIUS=,F8.2,12H INCHES	SQFD1300
	21X,15HN= ,F8.1,	SQFD1310
	320H RPM MU ,F8.3,12H MICROREYNS/	SQFD1320
	41X,15HPS= ,F8.1,	SQFD1330
	520H PSI ES= ,F8.3/	SQFD1340
	61X,15HEF= ,F8.3,	SQFD1350
	720H NC= ,I8//)	SQFD1360
	WRITE(6,11) (C(J),J=1,NC)	SQFD1370
11	FORMAT(50X,19HCLEARANCES - INCHES//5(64X,F7.5)////)	SQFD1380
C		SQFD1390
C	INITIALIZE CONSTANTS	SQFD1400
C		SQFD1410
	NEO=25	SQFD1420
	DELE=(EF-ES)/(NEO-1)	SQFD1430
	PI=3.55/1.13	SQFD1440
	W=N*0.10472	SQFD1450
	MU=MU*1.0E-6	SQFD1460
C		SQFD1470
C	OUTER LOOP FOR CLEARANCE VALUES	SQFD1480
C		SQFD1490
	DO 100 II=1,NC	SQFD1500
	WRITE(6,12) C(II)	SQFD1510
12	FORMAT(1H1,13X,6H C= ,F10.4,4H IN.//	SQFD1520
	11X,94H EO CO KO	SQFD1530
	2 PMAX THETA/	SQFD1540
	31X,97H (DIM) LB-SEC/IN LB/IN	SQFD1550
	4 LB/IN**2 DEGREES)	SQFD1560
C		SQFD1570
C	INNER LOOP FOR ECCENTRICITY RANGE	SQFD1580
C		SQFD1590
C		SQFD1600
	DO 20 I=1,NEO	SQFD1610
	KK=I+(I-1)*(NC-1)+II-1	SQFD1620
	EO(KK)=(I-1)*DELE + ES	SQFD1630
	IF(CAV.EC.0) GOTO 26	SQFD1640
	CO(KK)=(MU*(L**3)*R/(2.*(C(II)**3)))	SQFD1650
	CO(KK)=CO(KK)*(PI/((1.-EO(KK)**2)**(3./2.)))	SQFD1660
	KO(KK)=(2.*MU*W*R*((L/C(II))**3)*EO(KK))	SQFD1670
	KO(KK)=KO(KK)/((1.-EO(KK)**2)**(2.))	SQFD1680
26	THETAM(KK)=270.443 - 191.831*EO(KK) + 218.223*(EO(KK)**2)	SQFD1690
	THETA(KK)=THETAM(KK) - 114.803*(EO(KK)**3)	SQFD1700
	THETA=THETA(KK)/57.29577751	SQFD1710
	PMAX(KK)=-1.5*((L/C(II))**2)*MU*W*EO(KK)*SIN(THETA)	SQFD1720
	PMAX(KK)=PMAX(KK)/((1.+EO(KK)*COS(THETA))**3)	SQFD1730
	IF(CAV.EC.1) GOTO 40	SQFD1740
	KO(KK)=0.0	SQFD1750
	CO(KK)=PL*((L/C(II))**3)*R*PI	SQFD1760
	CO(KK)=CO(KK)/((1.-EO(KK)**2)**(3./2.))	SQFD1770
40	IF(TYP.NE.1) GOTO 20	SQFD1780
	PMAX(KK)=PMAX(KK)/2.	SQFD1790
	CO(KK)=CO(KK)/4.	SQFD1800
	KO(KK)=KO(KK)/4.	SQFD1810
20	CONTINUE	SQFD1820

300	NN=NEO*NC	SQFD1830
	DD_30_III=II,NN,NC	SQFD1840
	I=III	SQFD1850
	WRITE(6,13) E0(I),CG(I),KO(I),PMAx(I),THETAN(I)	SQFD1860
13	FORMAT(5(5X,F12.3,5X))	SQFD1870
30	CONTINUE	SQFD1880
100	CONTINUE	SQFD1890
	IF(.NOT. CS) GOTO 1000	SQFD1900
	NP1=NC*NEO+1	SQFD1910
	NP2=NC*NEO+NC	SQFD1920
	DO 400 I=NP1,NP2	SQFD1930
400	E0(I)=0.0	SQFD1940
	NP1=NP1+NC	SQFD1950
	NP2=NP2+NC	SQFD1960
	DO 500 I=NP1,NP2	SQFD1970
500	E0(I)=0.16667	SQFD1980
	NP=NC*NEO	SQFD1990
	CALL PLCIER(NP,L,R,MU,N,PS,ORING,COMENT1,COMENT2,NC,C,	SQFD2000
	1EO,CO,KO,PMAx,PC,PK,PP,TYP,CAV)	SQFD2010
	K=0	SQFD2020
1000	GOTO 900	SQFD2030
9999	STOP	SQFD2040
	END	SQFD2050

	SUBROUTINE PLOTTER(NP,L,R,MU,N,PS,ORING,COMENT1,COMENT2,NC,C, 1EO,CO,KO,PMAX,PC,PK,PP,TYP,CAV)	SQFD2060
		SQFD2070
C		SQFD2080
C	THIS SUBROUTINE PLCTS CO,KO,AND PMAX AS FUNCTIONS OF EO	SCFD2090
C	EACH SET OF CLEARANCE VALUES REQUIRES ONE BLOCK	SQFD2100
C		SQFD2110
	DIMENSION C(5),COMENT1(8),COMENT2(8),CLABEL(2)	SQFD2120
	INTEGER COMENT1,COMENT2,CLABEL,TYP	SQFD2130
	INTEGER CAV	SQFD2140
	REAL L,MU,N,KO,MU1	SQFD2150
	LOGICAL CRING,PC,PK,PP	SQFD2160
	DIMENSION EO(135),CO(135),KO(135),PMAX(135)	SQFD2170
	COMMON NEO	SQED2180
	DATA CLABEL(1),CLABEL(2)/	SQFD2190
	110HC= M,10HILS /	SQFD2200
C		SQFD2210
	NNF=NP/NC	SQFD2220
	DELE=(EC(NP)-EO(1))/NNP	SQFD2230
	NEQ=NNP	SQFD2240
	MU1=MU*1.0E6	SQFD2250
	IF(.NOT. PC) GOTO 101	SQFD2260
C		SQFD2270
C	PLOT CO	SQFD2280
C		SQFD2290
	JAXIS=1	SQED2300
	CALL GRID(L,R,N,MU1,PS,COMENT1,COMENT2,JAXIS,EO,CO,KO,PMAX, 1NP,TYP,CAV)	SQFD2310
	NP1=NC*NEQ+1	SQFD2320
	NP2=NC*NEQ+NC	SQFD2330
	DO 400 I=NP1,NP2	SQFD2340
400	CO(I)=0.0	SQFD2350
	NP1=NP1+NC	SQFD2360
	NP2=NP2+NC	SQFD2370
	DO 500 I=NP1,NP2	SQFD2380
500	CO(I)=1.0	SQFD2390
	DO 30 I=1,NC	SQFD2400
	CALL LINE(EO(I),CO(I),NNF,NC,0,0)	SQFD2410
		SQED2420
C		SQFD2430
C	DECIDE WHETHER LABELING SHOULD BE OVER CURVE OR	SQED2440
C	AT END OF CURVE. IF MAXIMUM ECCENTRICITY [0.7	SQFD2450
C	PLACE LABELING OVER CURVE, OTHERWISE AT END	SQFD2460
C		SQFD2470
	IF(EC(NE) .GE. 0.7) GOTO 60	SQFD2480
C		SQFD2490
C	DETERMINE THE X AND Y COORDINATES OF THE LOWER	SQFD2500
C	LEFT HAND CORNER OF THE LABELING AND THE ANGLE	SQFD2510
C	IT MAKES WITH THE X-AXIS	SQFD2520
C		SQFD2530
	XX=(EO(NE)/0.16667) + 0.1	SQFD2540
	III=NP-NC+1	SQFD2550
	YY=CO(III) + 0.1	SQFD2560
	THETA=ATAN((CO(III)-CO(III-10*NC))/((EO(III)-EO(III-10*NC))*6.0))	SQFD2570
	THETA1=THETA*57.2958	SQFD2580
	CALL SYMBOL(XX,YY,0.1,CLABEL,THETA1,13)	SQFD2590
C		SQED2600
C	DETERMINE THE X AND Y COORDINATES OF THE LOWER	SQFD2610
C	LEFT HAND CORNER OF THE CLEARANCE VALUE TO BE	SQFD2620

C	PLOTTED	SQFD2630
C		SQFD2640
	XX=XX+0.26*COS(THETA)	SQFD2650
	YY=YY+0.26*SIN(THETA)	SQFD2660
	CV=1000.0*C(I)	SQFD2670
	CALL NUMEER(XX,YY,0.1,CV,THETA1,4HF5.2)	SQFD2680
	GOTO 30	SQFD2690
C		SQFD2700
C	DETERMINE THE X AND Y COORDINATES OF THE LOWER	SQFD2710
C	LEFT HAND CORNER OF THE LABELING AND THE ANGLE	SQFD2720
C	IT MAKES WITH THE X-AXIS	SQFD2730
C		SQFD2740
60	XX=EC(NC*((NEO-1)/2)+1)*6.0	SQFD2750
	III=((NEC-1)/2)*NC+I	SQFD2760
	YY=CO(III) + 0.1	SQFD2770
	IP=(IFIX(0,13129/DELE))*NC + III	SQFD2780
	THETA=ATAN((CO(IP)-CO(III))/(EO(IP)-EO(III))*6.0)	SQFD2790
	THETA1=THETA*57.2958	SQFD2800
	CALL SYMBOL(XX,YY,0.1,CLABEL,THETA1,13)	SQFD2810
C		SQFD2820
C	DETERMINE THE X AND Y COORDINATES OF THE LOWER	SQFD2830
C	LEFT HAND CORNER OF THE CLEARANCE VALUE TO BE	SQFD2840
C	PLOTTED	SQFD2850
C		SQFD2860
	XX=XX+ 0.26*COS(THETA)	SQFD2870
	YY=YY + 0.26*SIN(THETA)	SQFD2880
	CV=1000.0*C(I)	SQFD2890
	CALL NUMBER(XX,YY,0.1,CV,THETA1,4HF5.2)	SQFD2900
30	CONTINUE	SQFD2910
	CALL PLCT(15.0,0.0,-6)	SQFD2920
101	IF(.NOT. PK) GOTO 201	SQFD2930
	JAXIS=2	SQFD2940
	CALL GRID(L,R,N,MU1,PS,COMMENT1,COMMENT2,JAXIS,EO,CO,KO,PMAX,	SQFD2950
	1NP,IYP,CAV)	SQFD2960
	NP1=NC*NEO+1	SQFD2970
	NP2=NC*NEO+NC	SQFD2980
	DO 401 I=NP1,NP2	SQFD2990
401	KO(I)=0.0	SQFD3000
	NP1=NP1+NC	SQFD3010
	NP2=NP2+NC	SQFD3020
	DO 501 I=NP1,NP2	SQFD3030
501	KO(I)=1.0	SQFD3040
	DO 40 I=1,NC	SQFD3050
	CALL LINE(EQ(I),KO(I),NMF,NC,0,0)	SQFD3060
	IF(EO(NP) .GE. 0.7) GOTO 70	SQFD3070
	XX=EC(NP)*6.0 +0.1	SQFD3080
	III=NP-NC+I	SQFD3090
	YY=KO(III) + 0.1	SQFD3100
	THETA=ATAN((KO(III)-KO(III-10*NC))/(EO(III)-EO(III-10*NC))*6.0)	SQFD3110
	THETA1=THETA*57.2958	SQFD3120
	CALL SYMBOL(XX,YY,0.1,CLABEL,THETA1,13)	SQFD3130
	XX=XX+ 0.26*COS(THETA)	SQFD3140
	YY=YY + 0.26*SIN(THETA)	SQFD3150
	CV=1000.0*C(I)	SQFD3160
	CALL NUMEER(XX,YY,0.1,CV,THETA1,4HF5.2)	SQFD3170
	GOTO 40	SQFD3180
70	XX=EC(NC*((NEO-1)/2)+1)*6.0	SQFD3190
	III=((NEC-1)/2)*NC+I	SQFD3200

	IP=(IFIX(0.13129/DELE))*NC +III	SQFD3210
	YY=KO(III)+0.1	SQFD3220
	THETA=ATAN((KO(IP)-KO(III))/((EO(IP)-EO(III))*6.0))	SQFD3230
	THEIA1=THEIA*57.2958	SQFD3240
	CALL SYMBOL (XX,YY,0.1,CLABEL,THEIA1,13)	SQFD3250
	XX=XX+0.26*COS(THETA)	SQFD3260
	YY=YY+0.26*SIN(THETA)	SQFD3270
	CV=1000.0*C(I)	SQFD3280
	CALL NUMBER (XX,YY,0.1,CV,THEIA1,4HF5.2)	SQFD3290
40	CONTINUE	SQFD3300
	CALL PLCT(15.0,0.0,-6)	SQFD3310
201	IF(.NOT. PP) RETURN	SQFD3320
	JAXIS=3	SQFD3330
	CALL GRID(L,R,N,MU1,PS,COMMENT1,COMMENT2,JAXIS,EO,CO,KD,PMAX,	SQFD3340
	INP,TYP,CAV)	SQFD3350
	NP1=NC*NEO+1	SQFD3360
	NP2=NC*NEO+NC	SQFD3370
	DO 402 I=NP1,NP2	SQFD3380
402	PMAX(I)=0.0	SQFD3390
	NP1=NP1+NC	SQFD3400
	NP2=NP2+NC	SQFD3410
	DO 502 I=NP1,NP2	SQFD3420
502	PMAX(I)=1.0	SQFD3430
	DO 50 I=1,NC	SQFD3440
	CALL LINE(EO(I),PMAX(I),NNF,NC,0,0)	SQFD3450
	IF(EO(NP).GE.0.7) GOTO 80	SQFD3460
	XX=EC(NP)*6.0 +0.1	SQFD3470
	III=NP-NC + I	SQFD3480
	YY=PMAX(III) + 0.1	SQFD3490
	THETA=ATAN((PMAX(III)-PMAX(III-10*NC))/	SQFD3500
	1((EO(III)-EO(III-10*NC))*6.0))	SQFD3510
	THEIA1=THEIA*57.2958	SQFD3520
	CALL SYMBOL (XX,YY,0.1,CLABEL,THEIA1,13)	SQFD3530
	XX=XX+0.26*COS(THETA)	SQFD3540
	YY=YY+0.26*SIN(THETA)	SQFD3550
	CV=1000.0*C(I)	SQFD3560
	CALL NUMBER (XX,YY,0.1,CV,THEIA1,4HF5.2)	SQFD3570
	GOTO 50	SQFD3580
80	XX=EO(NC*((NEO-1)/2)+1)*6.0	SQFD3590
	III=((NEC-1)/2)*NC+I	SQFD3600
	YY=PMAX(III)+0.1	SQFD3610
	IP=(IFIX(0.13129/DELE))*NC +III	SQFD3620
	THETA=ATAN((PMAX(IP)-PMAX(III))/((EO(IP)-EO(III))*6.0))	SQFD3630
	THEIA1=THEIA*57.2958	SQFD3640
	CALL SYMBOL (XX,YY,0.1,CLABEL,THEIA1,13)	SQFD3650
	XX=XX+0.26*COS(THETA)	SQFD3660
	YY=YY+0.26*SIN(THETA)	SQFD3670
	CV=1000.0*C(I)	SQFD3680
	CALL NUMBER (XX,YY,0.1,CV,THEIA1,4HF5.2)	SQFD3690
50	CONTINUE	SQFD3700
	CALL PLCT(15.0,0.0,-6)	SQFD3710
	RETURN	SQFD3720
	END	SQFD3730

```

SUBROUTINE GRID(L,R,N,MU1,PS,COMENT1,CCMENT2,JAXIS,EO,CO,KO,PHAX, SQFD3740
1NP,TYP,CAV) SQFD3750
C SQFD3760
C THIS SUBROUTINE PLCTS THE GRID AND LABELS THE PLOTS SQFD3770
C SQFD3780
DIKENSICA COMENT1(8),COMENT2(8),EO(135),CO(135),KC(135), SQFD3790
1PMAX(135),LEGEND1(2),LEGEND2(2),LEGEND3(2),LEGEND4(2),LEGEND5(3), SQFD3800
2HEADER1(2),HEADER2(3),XLABEL(2),YLABEL1(3),YLABEL2(3), SQFD3810
3YLABEL3(3) SQFD3820
REAL L,N,MU1,KO SQFD3830
INTEGER CAV SQFD3840
INTEGER TYP,HEADER3(3),HEADER4(3),HEADERS5(2),HEADER6(2) SQFD3850
INTEGER COMENT1,CCMENT2,LEGEND1,LEGEND2,LEGEND3,LEGEND4, SQFD3860
1LEGEND5,HEADER1,HEADER2,XLABEL,YLAEE1,YLABEL2,YLABEL3 SQFD3870
COMMON AEO SQFD3880
DATA LEGEND1(1),LEGEND1(2),LEGENC2(1),LEGEND2(2), SQFD3890
1LEGEND3(1),LEGEND3(2),LEGEND4(1),LEGEND4(2),LEGEND5(1), SQFD3900
2LEGEND5(2),LEGEND5(3),HEADER1(1),HEADER1(2), SQFD3910
3HEADER2(1),HEADER2(2),HEADER2(3),XLABEL(1),XLABEL(2), SQFD3920
4 YLABEL1(1),YLABEL1(2),YLABEL1(3),YLABEL2(1), SQFD3930
5YLABEL2(2),YLABEL2(3),YLABEL3(1),YLABEL3(2),YLABEL3(3)/ SQFD3940
610HN= ,10H RPM. ,10HR= I,10HN. , SQFD3950
710HL= I,10HN. ,10HPS= ,10H PSI. , SQFD3960
810HMU= ,10H MICROREYN,10HS ,10HSQUEEZE FI, SQFD3970
910HLM_DAMPER ,10HNC_SEALS_C,10HR_OIL_SUPP,10HLY_GROOVE, SQFD3980
110HECCENTRICI,10HTY - (DIM),10HDAMPING, ,10HCO - (LB-S, SQFD3990
210HEC/IN) , ,10HSTIFFNESS,,10H KO - (LE/,10HIN) , SQFD4000
310HMAXIMUM FR,10HESSURE - (,10HPSI) / SQFD4010
DATA HEADER3(1),HEADER3(2),HEADER3(3),HEADER4(1), SQFD4020
1HEADER4(2),HEADER4(3),HEADERS5(1),HEADERS5(2), SQFD4030
2HEADER6(1),HEADER6(2)/ SQFD4040
310HOIL SUPPLY,10H GROOVE -,10H NO SEALS,10HOIL SUPPL, SQFD4050
410HY GROOVE ,10H AND SEALS,10H NO CAV,10HITATION , SQFD4060
510H CAVIT,10HATION / SQFD4070
ICYCLES=0 SQFD4080
LOEXP=0 SQFD4090
GO TO (100,200,300),JAXIS SQFD4100
100 CALL LOGSCAL(CO,NP,1,8.0,LCEXP,ICYCLES,NP+2) SQFD4110
GOTO 150 SQFD4120
200 CALL LOGSCAL(KO,NP,1,8.0,LCEXP,ICYCLES,NP+2) SQFD4130
GOTO 150 SQFD4140
300 CALL LOGSCAL(PMAX,NP,1,8.0,LOEXP,ICYCLES,NP+2) SQFD4150
150 CONTINUE SQFD4160
NNC=(NP/AEO)+1 SQFD4170
CALL AXIS1(0.0,0.0,XLABEL,-20,6.0,0.0,EO(NP+1),EO(NP+NNC),16.667) SQFD4180
GO TO(101,201,301),JAXIS SQFD4190
101 CALL LOGAXIS(0.0,0.0,YLABEL1,26,+8.0,90.0,LOEXP,ICYCLES) SQFD4200
GOTO 160 SQFD4210
201 CALL LOGAXIS(0.0,0.0,YLABEL2,23,+8.0,90.0,LOEXP,ICYCLES) SQFD4220
GOTO 160 SQFD4230
301 CALL LOGAXIS(0.0,0.0,YLABEL3,24,+8.0,90.0,LOEXP,ICYCLES) SQFD4240
160 CALL PLCT(0.0,8.0,3) SQFD4250
CALL PLCT(6.0,8.0,2) SQFD4260
CALL LOGAXIS(6.0,0.0,2H ,0,+8.0,-90.0,LOEXP,ICYCLES) SQFD4270
C SQFD4280
C PLOT LEGENDS AND HEADINGS SQFD4290
C SQFD4300

```



```
CALL SYMBOL (1.29,8.96,0.21,HEADER1,0.0,19) SQFD4310
IF (TYP.EQ.0) CALL SYMBOL (0.30,8.57,0.21,HEADER2,0.0,30) SQFD4320
IF (TYP.EQ.1) CALL SYMBOL (0.30,8.57,0.21,HEADER3,0.0,30) SQFD4330
IF (TYP.EQ.2) CALL SYMBOL (0.30,8.57,0.21,HEADER4,0.0,30) SQFD4340
IF (CAV.EQ.0) CALL SYMBOL (1.20,8.18,0.21,HEADER5,0.0,20) SQFD4350
IF (CAV.EQ.1) CALL SYMBOL (1.20,8.18,0.21,HEADER6,0.0,20) SQFD4360
CALL SYMBOL (4.0,1.0,0.10,LEGEND1,0.0,16) SQFD4370
CALL SYMBOL (4.0,0.8,0.10,LEGEND2,0.0,12) SQFD4380
CALL SYMBOL (4.0,0.6,0.10,LEGEND3,0.0,12) SQFD4390
CALL SYMBOL (4.0,0.4,0.10,LEGEND4,0.0,16) SCFD4400
CALL SYMBOL (4.0,0.2,0.10,LEGEND5,0.0,21) SQFD4410
CALL NUMEER (4.26,1.0,0.10,K,0.0,4HF8.1) SQFD4420
CALL NUMBER (4.26,0.8,0.10,R,0.0,4HF5.2) SQFD4430
CALL NUMBER (4.26,0.6,0.10,L,0.0,4HF5.2) SQFD4440
CALL NUMBER (4.26,0.4,0.10,PS,0.0,4HF7.4) SQFD4450
CALL NUMEER (4.26,0.2,0.10,MU1,0.0,4HF6.3) SQFD4460
CALL SYMBOL (-0.43,-0.75,0.10,COSENT1,0.0,80) SQFD4470
CALL SYMBOL (-0.43,-0.90,0.10,COSENT2,0.0,80) SQFD4480
RETURN SQFD4490
END SCFD4500
```

	SUBROUTINE LOGSCAL(Y,N,K,S,LO,CYCLES,NN)	SQFD4510
C		SQFD4520
C	THIS SUBROUTINE TAKES AN ARRAY OF DATA *Y* AND SCALES ITS VALUES FOR	SQFD4530
C	A LOGARITHMIC PLOT. THERE ARE TWO ENTRIES---	SQFD4540
C	LOGSCAL IS USED IF THE RANGE OF DATA VALUES ARE UNKNOWN	SQFD4550
C		SQFD4560
C	LOGCYC IS USED IF THE RANGE OF DATA ARE KNOWN AND CAN BE PROVIDED	SQFD4570
C		SQFD4580
C	INPUT PARAMETERS FOR BOTH ROUTINES*****	SQFD4590
C	Y= THE ARRAY IN WHICH THE DATA TO BE SCALED IS STORED	SQFD4600
C	N=THE NUMBER OF THE POINTS IN THE ARRAY	SQFD4610
C	S= THE LENGTH OF THE AXIS IN INCHES	SQFD4620
C	K=A REPETITION FACTOR FOR ACCESSING DATA IN Y	SQFD4630
C	INPUT PARAMETERS FOR LOGCYC BUT OUTPUT PARAMETERS OF LOGSCAL	SQFD4640
C	CYCLES =THE NUMBER OF CYCLES OF REPETITIONS OF THE GRAPH	SQFD4650
C	LO=THE LOWEST EXPONENT OF OF THE DATA	SQFD4660
C	IT IS AN OUTPUT PARAMETER OF LOGSCAL ***INPUT FOR LOGCYC	SQFD4670
C	IE THE DIFFERENCE BETWEEN HIGHEST AND LOWEST EXPONENTS + ONE	SQFD4680
C	IE. IF Y(I) IS GREATER THAN 1.0*10**4 THEN LO =4	SQFD4690
C	INTERNAL VARIABLES	SQFD4700
C	HI =THE MAXIMUM VALUE OF THE DATA	SQFD4710
C	AHI AND ALO ARE REAL VALUES FOR INTEGER HI AND LO	SQFD4720
C	CL =A SCALE FACTOR	SQFD4730
C	*****	SQFD4740
	INTEGER HI, CYCLES	SQFD4750
	DIMENSION Y(NN)	SQFD4760
	AHI=-10.**321	SQFD4770
	ALO=10.**321	SQFD4780
C		SQFD4790
C	FIND THE MAXIMUM OF THE DATA	SQFD4800
C		SQFD4810
5	DO 10 I=1,N,K	SQFD4820
	AHI=AMAX1(AHI, Y(I))	SQFD4830
	ALO=AMIN1(ALO, Y(I))	SQFD4840
10	CONTINUE	SQFD4850
C		SQFD4860
C	COMPUTE LOG HI AND CYCLES	SQFD4870
C		SQFD4880
	ALO=ALOG10(ALO)	SQFD4890
	AHI=ALOG10(AHI)	SQFD4900
	LO=IFIX(ALO)	SQFD4910
	IF(ALO.LT.0.0) LO=LO-1	SQFD4920
	HI=IFIX(AHI)+1	SQFD4930
	CYCLES=HI-LO	SQFD4940
	GO TO 11	SQFD4950
C		SQFD4960
C	THIS ENTRY POINT IS USED WHEN LO AND CYCLES ARE KNOWN	SQFD4970
C		SQFD4980
	ENTRY LOGCYC	SQFD4990
11	CL=S/CYCLES	SQFD5000
	DO 20 I=1, N, K	SQFD5010
C		SQFD5020
C	GET LOG 10 OF THE DATA AND ADJUST TO SCALE	SQFD5030
C		SQFD5040
	IF(Y(I).LE.0.) PRINT 30	SQFD5050
30	FORMAT(1X,*NEGATIVE OR 0 VALUES HAVE BEEN ACCESSED BY THE SCALING	SQFD5060
	1SUBROUTINE***** THE ABSOLUTE VALUE OF THE VALUE HAS BEEN USED	SQFD5070

1ED FOR PLOTTING PURPOSES)	SQFD5080
Y(I)=ALOG10 (ABS (Y(I)))	SCFD5090
20 Y(I)=(Y(I)-LC)*CL	SQFD5100
Y(N+1)=0.0	SQFD5110
Y(N+2)=1.0	SQFD5120
RETURN	SCFD5130
END	SQFD5140

```

SUBROUTINE LOGAXIS(X, Y, IBCD, NCH, SZ, THTA, LOEXP, ICYCLES) SQFD5150
C THIS ROUTINE CREATES A LOGARITHMIC AXIS WHICH MAY BE HORIZONTAL SQFD5160
C (ALONG THE LENGTH OF THE PAPER, OR THTA=0.0) OR VERTICAL SQFD5170
C (ACROSS THE WIDTH OF THE PAPER OR THTA=90.0), OR AT ANY SQFD5180
C OTHER ANGLE. FURTHER THE AXIS CAN BE DRAWN WITH DESIRED LABELS SQFD5190
C PRINTED SQFD5200
C VARIABLES ***** SQFD5210
C INPUT PARAMETERS SQFD5220
C X, Y - THE COORDINATES OF THE BEGINNING POINT OF THE AXIS SQFD5230
C IBCD = AN ARRAY OF HOLLRITH CHARACTERS PRINTED AS LABELING SQFD5240
C NCHAR = NUMBER OF CHARACTERS IN IBCD TO PLOT SQFD5250
C SIZE = THE LENGTH OF THE AXIS IN INCHES SQFD5260
C THETA = THE ANGLE AT WHICH THE AXIS IS DRAWN SQFD5270
C LOEXP = MINIMUM EXPONENT (POWER OF TEN) OF ANY VALUE TO BE PLOTTED SQFD5280
C ICYCLES = NUMBER OF REPEATITIONS OF THE AXIS TO BE PLOTTED SQFD5290
C INTERNAL VARIABLES SQFD5300
C FINE DETERMINES FINE OR COARSE TICK MARKS SQFD5310
C HGT - CONTAINS THE HEIGHTS OF THE TICK MARKS SQFD5320
C COORD - CONTAINS LOGS USED TO MOVE THE PEN THE CORRECT LENGTH SQFD5330
C WHILE THE GRAPH IS BEING DRAWN SQFD5340
C ***** SQFD5350
DIMENSION COORD(65), HGT(65), IBCD(8) SQFD5360
LOGICAL FINE SQFD5370
C SQFD5380
C NOTE WE NEED THE ABSOLUTE VALUES OF SIZE, THETA, NCHAR SQFD5390
C SQFD5400
SIZE = SZ SQFD5410
NCHAR = NCH SQFD5420
THETA = THTA SQFD5430
Z = COORD(1) SQFD5440
ZZ = ALOG(FLQAI(11)/10.) SQFD5450
IF(Z.EQ.ZZ) GO TO 1 SQFD5460
C SQFD5470
C THIS PROCEDURE FILLS THE ARRAYS WITH NEEDED INFORMATION SQFD5480
C SQFD5490
ITEN = 6H 1X10 SQFD5500
K = 10 SQFD5510
INCR = 1 SQFD5520
DO 5 I = 1, 65 SQFD5530
K = K + INCR SQFD5540
A = FLQAI(K)/10. SQFD5550
COORD(I) = ALOG10(A) SQFD5560
HGT(I) = .04 SQFD5570
J = K - (K/5)*5 SQFD5580
IF(J.EQ.0) HGT(I) = .06 SQFD5590
J = K - (K/10)*10 SQFD5600
IF(J.EQ.0) HGT(I) = .100 SQFD5610
IF(K.EQ.50) INCR = 2 SQFD5620
5 CONTINUE SQFD5630
C SQFD5640
C THIS SECTION SETS THE VALUES FOR THE DIFFERENT OPTIONS IN TICK SQFD5650
C MARKS LABELING ETC. SQFD5660
C SQFD5670
1 DIRECT = 1. SQFD5680
IF(NCHAR.LT.0) DIRECT = (-1.) SQFD5690
TICK = DIRECT SQFD5700
IF(THETA.LT.0.) TICK = (-TICK) SQFD5710

```

	FINE=.FALSE.	SQFD5720
	IF(SIZE.LT.0.) FINE=.TRUE.	SQFD5730
	THETA=ABS(THETA)	SQFD5740
	NCHAR=IABS(NCHAR)	SQFD5750
	SIZE=ABS(SIZE)	SQFD5760
	CSTHETA=COS(THETA*.017455)	SQFD5770
	SNTHETA=SIN(THETA*.017455)	SQFD5780
C		SQFD5790
C	THIS DRAWS THE AXIS AT THE PROPER ANGLE AND LENGTH	SQFD5800
C	IT USES CCORD ARRAY FOR GIVING THE RIGHT LENGTH FOR TH AXIS AND TICS	SQFD5810
C	MARKS TICK, DIRECT AND FINE SET THE DIRECTION OF TICK MARKS,	SQFD5820
C	DIRECTION OF THE LABELING AND OF THE NUMBER OF TICK MARKS	SQFD5830
C		SQFD5840
	CYCLESZ=SIZE/FLOAT(ICYCLES)	SQFD5850
	V=.10*(-TICK)*SNTHETA+X	SQFD5860
	W=TICK*.10*CSTHETA+Y	SQFD5870
	CALL PLCT(V, W, 3)	SQFD5880
	CALL PLCT(X, Y, 2)	SQFD5890
	K=5	SQFD5900
	IF(FINE)K=1	SQFD5910
	DO 20 I=1,ICYCLES	SQFD5920
	J=0	SQFD5930
	CALL WHERE(C, I, IDUMMY)	SQFD5940
10	J=J+K	SQFD5950
	A=COORD(J)*CSTHETA*CYCLESZ+C	SQFD5960
	B=COORD(J)*SNTHETA*CYCLESZ+D	SQFD5970
	CALL PLOT(A, B, 2)	SQFD5980
	V=HGT(J)*(-TICK)*SNTHETA+A	SQFD5990
	W=TICK*HGT(J)*CSTHETA+B	SQFD6000
	CALL PLOT(V,W,1)	SQFD6010
	CALL PLOT(A, B, 1)	SQFD6020
	IF(J.LT.65) GO TO 10	SQFD6030
20	CONTINUE	SQFD6040
	IF(NCHAR.EQ.0) GO TO 820	SQFD6050
C		SQFD6060
C	THIS ROUTINE PROVIDES LABELING IN THE PROPER DIRECTION,	SQFD6070
C	FOR THE IDENTIFICATION OF THE TICK MARKS	SQFD6080
C		SQFD6090
	IQ=5	SQFD6100
	IUL=40	SQFD6110
310	BB=.07*TICK+.21*DIRECT-.07-((TICK+DIRECT)*.03	SQFD6120
	DX=CSTHETA*(-.28)-BB*SNTHETA	SQFD6130
	DY=SNTHETA*(-.28)+BB*CSTHETA	SQFD6140
	XA=SIZE*CSTHETA+X+DX	SQFD6150
	YA=SIZE*SNTHETA+Y+DY	SQFD6160
	CALL SYMBOL(XA, YA, .14, ITEN, THETA, 6)	SQFD6170
	I1=ICYCLES+LOEXP	SQFD6180
	XA=CSTHETA*.72-SNTHETA*.05+XA	SQFD6190
	YA=SNTHETA*.72+CSTHETA*.05+YA	SQFD6200
	POWER=2HI3	SQFD6210
	CALL NUMEER(XA, YA, .10, I1, THETA, POWER)	SQFD6220
	II=ICYCLES	SQFD6230
C		SQFD6240
C	THIS MOVES THE PEN DOWN THE AXIS PUTTING THE TICK MARK LABELING	SQFD6250
C	AT THE CORRECT POSITION	SQFD6260
C		SQFD6270
320	K=IQ	SQFD6280
	II=II-1	SQFD6290

	INCR=-5	SQFD6300
	I=IUL	SQFD6310
330	QA= (COORD(I)+ FLOAT(II))*CYCLESZ +.25	SQFD6320
	XA=QA*CSTHETA+X+DX	SQFD6330
	YA=QA*SNTHETA+Y+DY	SQFD6340
	K=K-1	SQFD6350
	IF(I.EQ.40) INCR=-10	SQFD6360
	I=I+INCR	SQFD6370
	IF(I.GT.0) GO TO330	SQFD6380
	QA=FLOAT(II)*CYCLESZ	SQFD6390
	XA=QA*CSTHETA+X+DX	SQFD6400
	YA=QA*SNTHETA+Y+DY	SQFD6410
	CALL SYMBOL(XA, YA, .14, ITEXT, THETA, 6)	SQFD6420
	I1=II+LOEXP	SQFD6430
	XA=CSTHETA*.72-SNTHETA*.05+XA	SQFD6440
	YA=SNTHETA*.72+CSITHEJA*.05+YA	SQFD6450
	POWER=2HI3	SQFD6460
	CALL NUMBER(XA, YA, .10, I1, THETA, POWER)	SQFD6470
	IF(II.GT.0) GO TO320	SQFD6480
C		SQFD6490
C	THIS PRINTS THE DESIRED ALPHA NUMERIC INFORMATION ABOVE OR BELOW	SQFD6500
C	THE AXIS AS IS NEEDED TO IDENTIFY THE AXIS	SQFD6510
C		SQFD6520
	BA=.5*SIZE-FLOAT(NCHAR) *.06	SQFD6530
	BB =TICK*.05 +DIRECT*.40-.07	SQFD6540
	XA=BA*CSTHETA-BB*SNTHETA+X	SQFD6550
	YA =BA*SNTHETA+BB*CSTHETA+Y	SQFD6560
	CALL SYMBOL(XA, YA, .14, IBCD, THETA, NCHAR)	SQFD6570
820	RETURN	SQFD6580
	END	SQFD6590

SQUEEZE FILM DAMPER

THIS PROGRAM ANALYZES THE STIFFNESS, DAMPING AND PRESSURE CHARACTERISTICS OF THE SQUEEZE FILM DAMPER BEARING. THREE BEARING CONFIGURATIONS MAY BE ANALYZED-

- 0 - FLAIN BEARING WITHOUT END LEAKAGE SEALS OR CIRCUMFERENTIAL OIL SUPPLY GROOVE
- 1 - BEARING WITHOUT END LEAKAGE SEALS BUT WITH CIRCUMFERENTIAL OIL SUPPLY GROOVE
- 2 - BEARING WITH BOTH END LEAKAGE SEALS AND CIRCUMFERENTIAL OIL SUPPLY GROOVE

IN ADDITION, THE FILM MAY BE ASSUMED TO BE EITHER CAVITATED OR UNCAVITATED. IF CAVITATED THE FILM IS ASSUMED TO EXTEND FROM $\theta = \pi/2$ TO $\theta = 3\pi/2$, WHERE θ IS MEASURED FROM THE LINE OF CENTERS IN THE DIRECTION OF JOURNAL PRECESSION. THE EVALUATION OF THE BEARING CHARACTERISTICS ASSUMES THAT THE JOURNAL PRECEDES SYNCHRONOUSLY ABOUT THE BEARING CENTER.

THE FOLLOWING IS A DESCRIPTION OF THE INPUT PARAMETERS-

CARD 1. -80 COLUMN FREE-FIELD COMMENT CARD

CARD 2. -80 COLUMN FREE-FIELD COMMENT CARD

CARD 3. -NAMELIST/BRGTYPE/ TYP,CAV,PS

- TYP - 0 FOR BEARING TYPE 0 (SEE ABOVE)
- 1 FOR BEARING TYPE 1 (SEE ABOVE)
- 2 FOR BEARING TYPE 2 (SEE ABOVE)

- CAV - 0 FOR UNCAVITATED FILM
- 1 FOR CAVITATED FILM
- IF CAV=0 PK=.F. (SEE CARD 7)

PS - OIL SUPPLY PRESSURE, PSI

CARD 4. -NAMELIST/BEARING/ L,R,MU,N

- L - BEARING LENGTH, IN.
- R - BEARING RADIUS, IN.
- MU - LUBRICANT VISCOSITY, MICRCREYNS
- N - ROTOR SPEED (J649E13 7IEC589C5 I1CE,RPM)

CARD 5. -NAMELIST/ECCRATIO/ ES,EF

- ES - INITIAL JOURNAL ECCENTRICITY RATIO, ES>0.
- EF - FINAL JOURNAL ECCENTRICITY RATIO, EF<1.0

CARD 6. -NAMELIST/CLEARNC/ C(I),NC

- C(I)- CLEARANCE VALUES, IN. 0<I<5
- NC - NUMBER OF CLEARANCE VALLES

CARD 7. -NAMELIST/PLOTSEM/ CS,PC,PK,PF

- CS - PLOT CONTRCL, .T. IF PLOT DESIRED, OTHERWISE .F.
- PC - .T. IF DAMP PLOT DESIRED, OTHERWISE .F.
- PK - .T. IF STIFF. PLOT DESIRED, OTHERWISE .F.
- PF - .T. IF PRESS PLOT DESIRED, OTHERWISE .F.

SAMPLE DATA

COMMENT CARD 1

COMMENT CARD 2

```
$BRGTYPE TYP=0,CAV=1,PS=0.0$
$BEARING L=0.90,R=2.55,MU=0.382,N=16800$
$ECCRATIO ES=0.1,EF=0.9$
$CLEARNC C(1)=.003,C(2)=.004,C(3)=.005,C(4)=.006,NC=4$
$PLOTSEM CS=.T.,PC=.T.,PK=.T.,PF=.T.$
```

BEARING WITH END SEALS AND OIL SUPPLY GROOVE

UNCAVITATED FILM

BEARING LENGTH= .31 INCHES BEARING RADIUS= .31 INCHES
N= 7000.0 RPM MU 1.600 MICRONS
FS= 0.0 PSI ES= .100
EF= .900 AC= 3

CLEARANCES = INCHES

.00300
.00500
.01000

C= .0030 IN.

EC (DIM)	CO LB-SEC/IN	KO LB/IN	PMAX LB/IN**2	THETA DEGREES
.100	1.802	0.000	1.996	253.327
.133	1.824	0.000	2.752	248.473
.167	1.852	0.000	3.590	244.001
.200	1.888	0.000	4.536	239.887
.233	1.931	0.000	5.617	236.105
.267	1.983	0.000	6.871	232.629
.300	2.045	0.000	8.343	229.434
.333	2.119	0.000	10.089	226.494
.367	2.205	0.000	12.184	223.784
.400	2.306	0.000	14.725	221.279
.433	2.425	0.000	17.844	218.952
.467	2.566	0.000	21.719	216.779
.500	2.733	0.000	26.601	214.733
.533	2.933	0.000	32.844	212.789
.567	3.174	0.000	40.964	210.923
.600	3.468	0.000	51.735	209.107
.633	3.831	0.000	66.349	207.317
.667	4.288	0.000	86.720	205.528
.700	4.875	0.000	116.049	203.713
.733	5.650	0.000	159.976	201.848
.767	6.708	0.000	229.101	199.906
.800	8.220	0.000	345.612	197.862
.833	10.512	0.000	556.595	195.691
.867	14.299	0.000	991.914	193.367
.900	21.438	0.000	2067.593	190.864

86

C= .0060 IN.

EC (DIP)	CO LB-SEC/IN	KO LB/IN	FMAX LB/IN**2	THETA DEGREES
.100	.225	0.000	.499	253.327
.133	.228	0.000	.688	248.473
.167	.232	0.000	.898	244.001
.200	.236	0.000	1.134	239.887
.233	.241	0.000	1.404	236.105
.267	.248	0.000	1.718	232.629
.300	.256	0.000	2.086	229.434
.333	.265	0.000	2.522	226.494
.367	.276	0.000	3.046	223.784
.400	.288	0.000	3.681	221.279
.433	.303	0.000	4.461	218.952
.467	.321	0.000	5.430	216.779
.500	.342	0.000	6.650	214.733
.533	.367	0.000	8.211	212.789
.567	.397	0.000	10.241	210.923
.600	.433	0.000	12.934	209.107
.633	.479	0.000	16.537	207.317
.667	.536	0.000	21.680	205.528
.700	.609	0.000	29.012	203.713
.733	.706	0.000	39.994	201.848
.767	.839	0.000	57.275	199.906
.800	1.027	0.000	86.253	197.862
.833	1.314	0.000	139.149	195.691
.867	1.787	0.000	247.979	193.367
.900	2.680	0.000	516.898	190.864

C= .0100 IN.

EO (DIP)	CO LB-SEC/IN	RO LE/IN	FMAX LB/IN**2	THETA DEGREES
.100	.049	0.000	.180	253.327
.133	.049	0.000	.248	248.473
.167	.050	0.000	.323	244.061
.200	.051	0.000	.402	239.887
.233	.052	0.000	.506	236.105
.267	.054	0.000	.618	232.629
.300	.055	0.000	.751	229.434
.333	.057	0.000	.908	226.494
.367	.060	0.000	1.097	223.784
.400	.062	0.000	1.325	221.279
.433	.065	0.000	1.606	218.952
.467	.069	0.000	1.955	216.779
.500	.074	0.000	2.394	214.733
.533	.079	0.000	2.956	212.789
.567	.086	0.000	3.687	210.923
.600	.094	0.000	4.659	209.167
.633	.103	0.000	5.971	207.317
.667	.116	0.000	7.805	205.528
.700	.132	0.000	10.444	203.713
.733	.153	0.000	14.398	201.848
.767	.181	0.000	20.619	199.906
.800	.222	0.000	31.051	197.862
.833	.284	0.000	50.094	195.691
.867	.386	0.000	89.272	193.367
.900	.579	0.000	186.083	190.864

100